AMERICAN UNIVERSITY OF BEIRUT

THE ANTITUMOR EFFECT OF THE ATYPICAL RETINOID ST1926 IN HUMAN GLIOBLASTOMA

By

ZEINAB MOHAMMAD KAWTHARANI

A thesis
submitted in partial fulfillment of the requirements
for the degree of Master of Science
to the Department of Biochemistry and Molecular Genetics
of the Faculty of Medicine
at the American University of Beirut

Beirut, Lebanon
September 2020

AMERICAN UNIVERSITY OF BEIRUT

THE ANTITUMOR EFFECT OF THE ATYPICAL RETINOID ST1926 IN HUMAN GLIOBLASTOMA

By

ZEINAB MOHAMMAD KAWTHARANI

Approved by:

Dr. Nadine Darwiche, Professor
Department of Biochemistry and Molecular Genetics
Advisor

Dr. Marwan EL-Sabban, Professor
Department of Anatomy, Cell Biology, and Physiology
Member of Committee

Dr. Firas Kobeissy, Associate Professor
Department of Biochemistry and Molecular Genetics
Member of Committee

Date of thesis defense: September 01, 2020

AMERICAN UNIVERSITY OF BEIRUT

THESIS, DISSERTATION, PROJECT RELEASE FORM

Student Name: Kawtharani_____Zeinab_____Mohammad_____
Last First Middle

☑ Master's Thesis ☐ Master's Project ☐ Doctoral Dissertation

☑ I authorize the American University of Beirut to: (a) reproduce hard or electronic copies of my thesis, dissertation, or project; (b) include such copies in the archives and digital repositories of the University; and (c) make freely available such copies to third parties for research or educational purposes.

☐ I authorize the American University of Beirut, to: (a) reproduce hard or electronic copies of it; (b) include such copies in the archives and digital repositories of the University; and (c) make freely available such copies to third parties for research or educational purposes

after : **One ---- year from the date of submission of my thesis, dissertation, or project.**

Two----years from the date of submission of my thesis, dissertation, or project.

Three----years from the date of submission of my thesis, dissertation, or project.

_____Zeinab_Kawtharani_____06_September_2020_____
Signature Date

ACKNOWLEDGEMENTS

All my praise and thanks to the merciful GOD who has blessed me to accomplish this project, surrounded by a precious project team and lab mates, loving family and friends.

First and foremost, my sincere thanks and gratitude, respect and appreciation to Dr. Nadine Darwiche, for giving me the opportunity to join her laboratory, and for always surrounding me with her sympathy and kindness, encouragement and guidance, and for igniting my curiosity to follow my dreams and to take my first steps as a cancer researcher, and as they say "The dream begins with a teacher who believes in you, who tugs and pushes and leads you to the next plateau".

I also want to extend my appreciation to my committee members: Dr. Marwan El-Sabban and Dr. Firas Kobeissy. Thank you for taking the time to correct my thesis. Your lectures have been inspirational and widened my thinking towards research. Dr. El-Sabban thank you for your constructive instructions regarding the biomimetic BBB model. Dr. Firas Kobeissy thank you for providing us with the GBM cell lines and helping us with the proteomics experiment.

I would like to extend my thanks and gratitude to Dr. Chirine El Baba , for accepting the supervision on my master thesis, for your patience and kindness, all the time, learning me different lab techniques, answering my questions and tolerating my mistakes.

Special thanks to Berthe Hayar, for your gentelness, guidance, for explaining every single step behind different lab techniques and helping me face my fear of animals. Thanks for your endless trust and encouragement.

My thanks extend to our collaborator, Dr. Claudio Pisano, for generously providing us with the drug.

To my dear colleagues in the Blue Lab: Fatima, Noor, Sahar, Botheina and Khaled; I had the pleasure to work with amazing people like you. I wish you all the best in research and in your private life. Special thanks to Fatima Ghamloushe, for always encouraging me to excel, particularly during my tough days.

My love and appreciation to all my friends, pharmacists from university of Gothenburg "GU girls" Sara, Hasna and Shaima; You know that you mean a lot for me and I am very grateful to have you in my life. You have been more than sisters, always supportive and caring, despite the long distances between us.

My love and gratitude also extends to the girls from the department of biochemisty at AUB, especially Nawara and Mariam that have been with me through thick and thin throughout my journey at AUB. Special thanks go to a special friend whom shoulder and comfort were present especially during my last days at AUB. Thank you Haifa for the unforgettable moments, I wish we had the opportunity to spend much more time

from the beginning of our journey at AUB, but still, I´m very delighted to have you in my life.

To my beloved family, my parents who made me who I am; my mother that has always been caring and patient, and my father; my inspirational idol, thank you for always encouraging me to never give up and to keep chasing my dreams.

To my brothers and sisters, my second family, my father, mother, brothers and sisters in law. I cannot thank you enough for all the things you've done for me. Your love and support gave me the strength to be who I am today.

To my kids, Douaa, Mohammad and Ali. You are the hope that brightens my life. No words in the world are enough to express my feelings. I´m sorry for all the times that I´ve been busy with my studies, but I want you to know that you are the reason for what I´m doing. I want you to be proud of me, and I hope that I´ll be a good idol you´ll look up to one day.

Finally, but mostly, to the love of my life, my best friend and my everything, my husband Talal. No words can describe my deep gratitude and appreciation, for always being there for me, during my tough and happy days, for always believing in my capabilities and for being proud of me. Without you, I wouldn´t achieve anything in my life. A "thank you" for your endless love, patience and support, can never give you justice, but I want you to know that I stand here today because of you.

I love you all, and I hope I´ll always make you proud.

AN ABSTRACT OF THE THESIS

Zeinab Mohammad Kawtharani for Master of Science
Major: Biochemistry

Title: The antitumor effect of the atypical retinoid ST1926 in human glioblastoma

Abstract

Background: Glioblastoma Multiforme (GBM) is the most aggressive form of malignant brain tumors. It accounts for 70% of newly diagnosed malignant primary brain tumors in adults. The current standard therapy comprises surgical resection with adjuvant radiotherapy, followed by the administration of Temozolomide, an alkylating chemotherapeutic agent. Despite the available therapies, the median survival rate does not exceed two years, since patients tend to relapse and eventually develop resistance. Tumor heterogeneity and the restrictive nature of the blood-brain barrier (BBB) are major obstacles faced in GBM management. Therefore, there is an eminent need to develop more adapted and efficient treatments. Natural and synthetic retinoids have been investigated in several cancer types and showed promising antitumor effects through the regulation of proliferation, differentiation, and apoptosis. Synthetic retinoids offered an enhanced specificity and reduced the toxicity of their natural counterparts. The atypical adamantyl synthetic retinoid ST1926 induces apoptosis and growth inhibition in different cancer types at sub-micromolar concentrations independently of retinoid receptor signaling pathway. We have recently found that ST1926 is an inhibitor of the catalytic subunit of DNA polymerase alpha (POLA1) which is involved in DNA synthesis initiation. Our *in silico* analysis revealed elevated levels of POLA1 expression in glioblastoma tumor tissues *versus* normal counterparts. This suggests POLA1 as a relevant and attractive target for ST1926 in GBM.

Aims: We investigated the antitumor activities and the mechanism of action of ST1926 on a panel of human GBM cell lines. In addition, we tested the therapeutic properties of ST1926 using a mouse GBM xenograft model.

Methods: Experiments were conducted both *in vitro* and *in vivo* to explore the efficacy of ST1926 as a potential therapeutic agent against human GBM. Several human GBM cell lines of different p53 status were used in this study namely U87MG (WT *p53*), U251 (mutated *p53*), U118 (mutated *p53*), and A172 (WT *p53*) cells. We measured cell viability assays by MTT and SRB, flow cytometry by propidium iodide staining of DNA, and apoptosis by TUNEL assay. Western blot were performed to study the mechanism of action of ST1926 on GBM cell extract. We finally investigated the effect of ST1926 in a xenografted mouse model of human glioblastoma cells.

Results: ST1926 reduced cell viability in all tested human GBM cell lines with IC_{50} values at sub-micromolar levels. ST1926 induced early DNA damage and reduction of POLA1 protein levels. Flow cytometry results of ST1926-treated GBM cells showed that ST1926 exhibited G1 phase cell cycle arrest and sub-G_1 cell accumulation. ST1926 induced apoptosis was further confirmed by PARP cleavage and TUNEL. ST1926 reduced tumor volume in a GBM xenograft model. Experiments are still in progress to

optimize the therapeutic properties of ST1926 in a xenograft model and to elucidate its mechanism of action by proteomic analysis of treated GBM cell extracts.

Conclusion: ST1926 showed favorable preclinical efficacy and thus is worth to be tested in GBM orthotopic animal models.

CONTENTS

Page

IV. RESULTS

V. DISCUSSION

ILLUSTRATIONS

Figure Page

TABLES

Table Page

ABBREVIATIONS

μM	micromolar
2-HG	2-hydroxyglutarate
5-hmc	5-hydroxymethyl cytosine
9c-RA	9-*cis* retinoic acid
APL	Acute promyelocytic leukemia
ATRA	all-*trans* retinoic acid
BBB	Blood Brain Barrier
CD437	6-[3-(1-adamantyl)-4-hydroxyphenyl] -2-naphthalene carboxylic acid
CDKN2A	Cyclin- dependent kinase inhibitor A
CNS	Central Nervous System
CRC	Colorectal cancer
CSF	Cerebospinal fluid
DMSO	dimethylsulfoxide
DNA	deoxyribonucleic acid
DSB	double-strand break
EDTA	ethylene-diamineteraacetic acid
EGFR	Epidermal growth factor receptor
FBS	fetal bovine serum
FLAIR	Fluid-attenuated inversion recovery
GAPDH	glyceraldehyde-3-phosphate dehydrogenase
GBM	Glioblastoma Multoforme

G-CIMP	Glioma- CpG island methylator phenotype
h	hour
H&E	Hematoxylin and Eosin
HIF-1α	Hypoxia inducible factor
HPR	N-(4-hydroxyphenyl) retinamide
IDH	Isocitrate dehydrogenase
LOH	Loss of heterozygosity
MAP	mitogen-activated protein
MGMT	O-6-methyl guanine DNA methyl transferase
MRI	Magnetic resonance imaging
NADPH	Nicotinamide adenine dinucleotide phosphate
OD	optical density
PAGE	polyacrylamide gel electrophoresis
PARP	Poly (ADP-ribose) polymerase
PBS	phosphate-buffered saline
PDGFRA	Platelet- derived growth factor alpha
PI	propidium iodide
PML	Promyelocytic leukemia
POLA1	DNA Polymerase alpha
PTEN	Phosphatase and tensin homolog
RA	Retinoic acid
RAR	retinoic acid receptor
RAR	Retinoic acid receptor
RARE	retinoic acid response element

RNR	Retinoic nuclear receptor
RTK	Receptor tyrosine kinase
RXR	retinoic X receptor
RXR	retinoid X receptor
SD	standard deviation
SDS	sodium dodecyl sulfate
SEM	standard error of the mean
ST1926	E-4-(4’-hydroxy-3’-adamantyl biphenyl-4-yl) acrylic acid
TCGA	The Cancer Genome Atlas
TMZ	Temozolomide
TUNEL	dUTP nick end labeling
VEGF	Vascular endothelial growth factor
WHO	World Health Organization
α-KG	α-ketoglutarate

CHAPTER I

INTRODUCTION

A. Cancer

Cancer is one of the most spreading diseases and the second leading cause of morbidity and mortality after cardiovascular diseases worldwide (WHO 2018). Alarmingly increasing incidence in the 21st century is probably due to changing lifestyle, habits, increased life expectancy and constant exposure to cancer causing agents so called carcinogens. All cancer types share a common phenotype: abnormal cell growth. It all starts by a genome alteration that may occur at multiple sites, either as point mutations or as changes in chromosome complement (Kinzler 1996). Accumulation of mutations in proto-oncogenes and tumor-suppressor genes (McCormick 1999) override the normal mechanisms for cellular proliferation leading to progressive conversion from normalcy into malignancy (Hahn 1999). Another force shaping the cancer genome is the evolutionary selection whereby one group of cells within the tumor overgrows the other cells. These selected cells have phenotypic traits that give advantage for the growth of the tumor. For example, cells with low metabolic demand grow faster than cells with high metabolic demand in a nutrient-poor microenvironment (Graham 2017). Mutations in these favored cells are more frequent in the tumor population, leading to creation of mass of cells that eventually form the primary tumor (Pozo 2007). Most solid cancers have to reach 1 cm in size or comprise 1 million cells in order to be detected as mass of cells or tumor, unless it is detected accidently earlier by a laboratory test or radiological routine test (Roy P 2016). Beside gene mutations, epigenetic alterations including DNA methylation, histone

modifications, chromatin structure, and non-coding RNAs are other causes of deregulated gene expression leading to cancer progression (Regine Schneider-Stock 2012).

Cancer acquires six core biological capabilities during its multistep development (Figure 1). These hallmarks described by Hanahan (Hanahan 2000) include sustaining proliferative signaling, evading growth suppressors, resisting cell death, inducing angiogenesis, enabling replicative immortality as well as activating invasion and metastasis to the rest of the body.

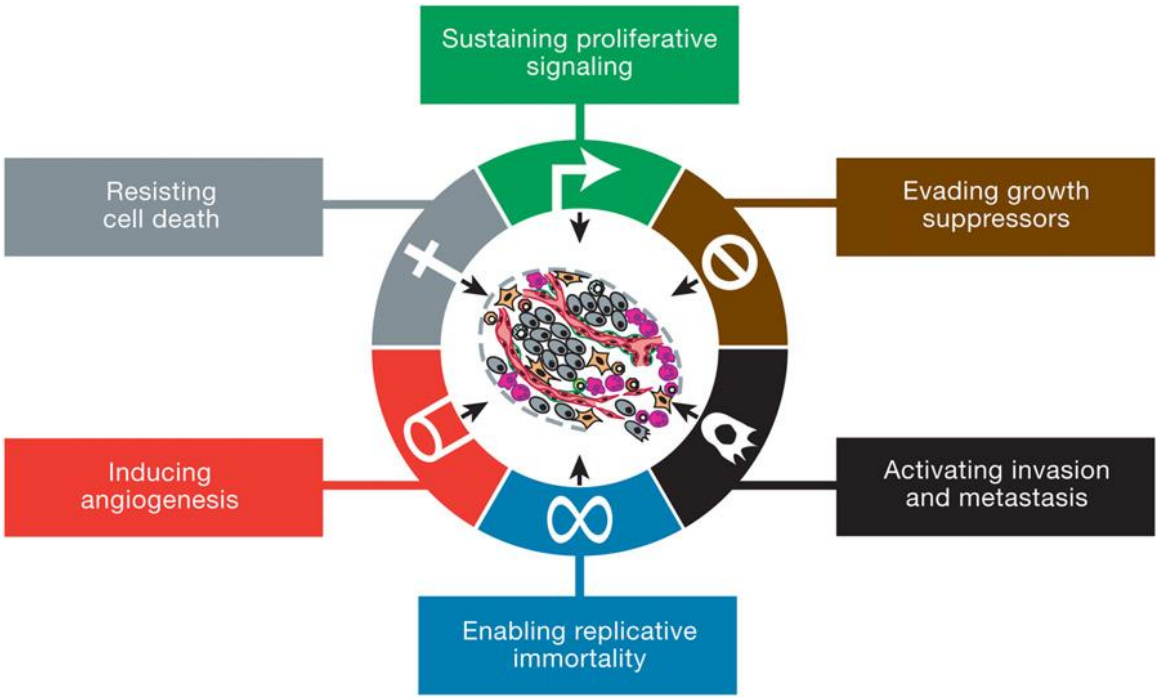

Figure 1. The hallmarks of cancer, originally described by (Hanahan 2000). Illustration adopted from (Hanahan 2011).

An increasing body of research in cancer allowed two additional emerging hallmarks to be involved in the pathogenesis of probably most cancers: the capability of regulating cellular metabolism and deregulating cellular energetics in order to effectively support neoplastic proliferation, and the ability to avoid immunological destruction mainly by T and B lymphocytes, macrophages, and natural killer cells (Figure 2). Both core and emerging hallmarks facilitate two additional consequential characteristics: the genomic instability and altering the innate immunity. Genomic instability indicates mutability, allowing genetic alterations in cancer cells that drive tumor progression. Altering innate immunity is achieved by turning the innate immune cells that normally fight infections and heal wounds to instead inadvertent support the multiple hallmark capabilities, thereby both characteristics promote tumor growth (Hanahan 2011).

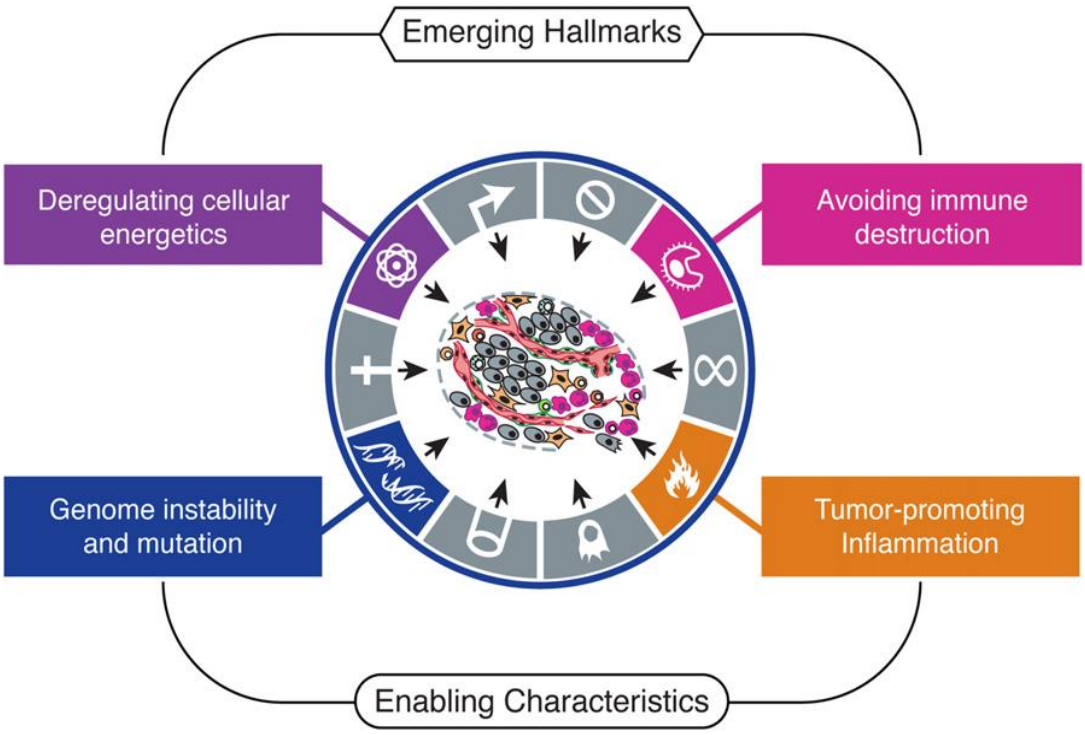

Figure 2. Emerging hallmarks and enabling characteristics (Hanahan 2011)

B. Brain

B.1. Anatomy of the Brain:

The brain is the most important and complex organ in the human body located in the head. It is a mass of nerve tissues containing over 100 billion nerve cells that communicate together through synapses. Together with the spinal cord, the brain constitutes the central nervous system (CNS).

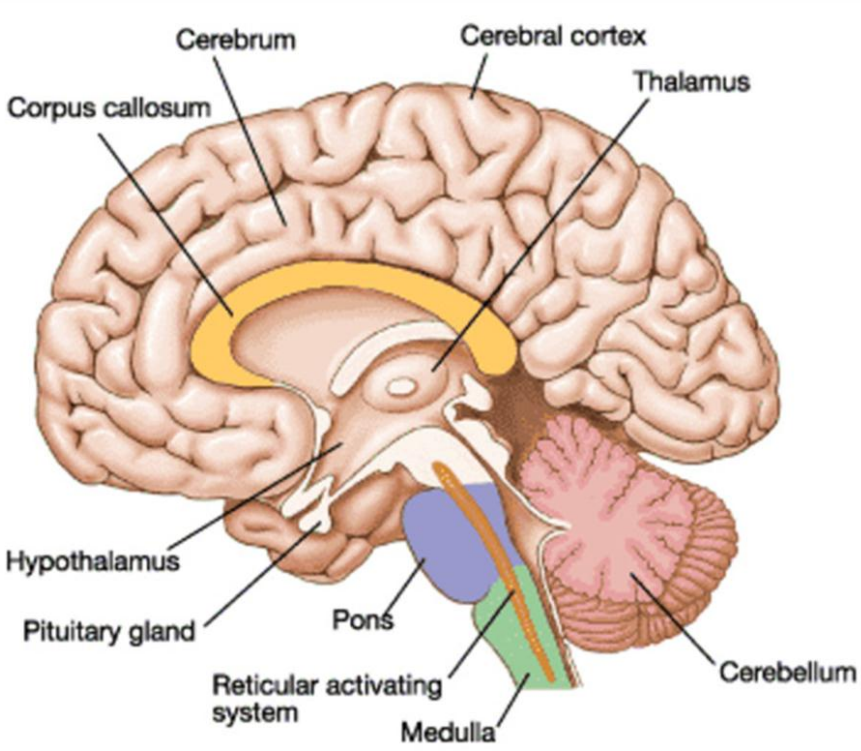

Figure 3. Illustration of the brain structures by (Oscar-Berman 1997).

The brain is composed of three major parts, the cerebrum, cerebellum, and brainstem (Tonya Hines 2018) (Figure 3). The cerebellum is located under the cerebrum at the base of the brain. It is responsible for maintaining posture, balance, and coordination of muscle movements. The brainstem connects the brain to the spinal cord. It controls involuntary functions such as heart rate, body temperature, sleep cycle, digestion, and breathing.

The largest component of the brain is the cerebrum which is divided into two hemispheres, left and right, also called left and right brain, connected through a bundle of fibers called corpus callosum. Each hemisphere controls functions on the opposite side of the body. These hemispheres control higher functions like emotions, learning, vision, hearing, interpreting touch, as well as speech, reasoning, and fine control of movement. The cerebrum contains 70 billion neurons. It has distinct fissures that divide the brain into several lobes: frontal, temporal, parietal, and occipital. Each lobe is further divided into areas that serve very specific functions. These functions are result of complex relationships between the different lobes of the brain and the right and left hemispheres:

- The frontal lobe is responsible for body movement, personality including behavior and emotions, speech (Broca´s area), as well as intelligence counting concentration, judgement and problem solving (Figure 4).
- The temporal lobe manages memory, hearing, sequencing, organization and understanding language (Wernicke's area) (Figure 4).
- The parietal lobe serves for sensation of touch, pain and temperature. It manages interpretation of words, signals from sensory inputs (vision and hearing), as well as memory (Figure 4).

- The occipital lobe contains brain´s visual processing system for interpretation of light, color, and movement (Figure 4).

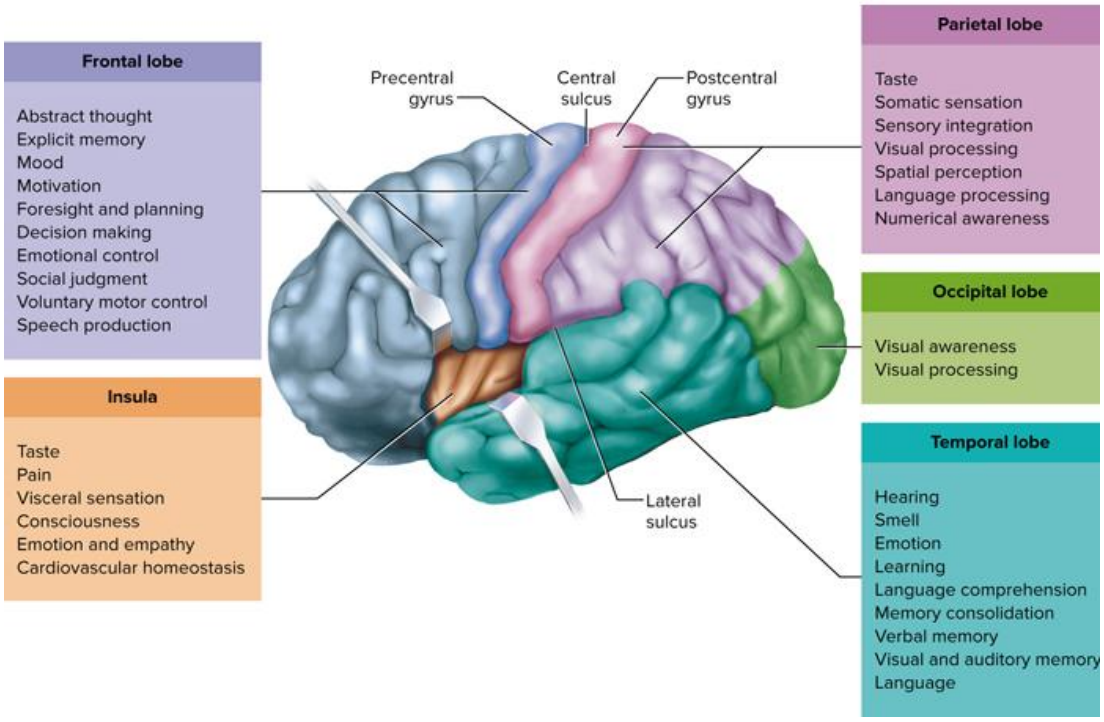

Figure 4. Lobes of the brain with different functions adopted from "Anatomy & physiology: the unity of form and function." 9th edition (2020), chapter 14, figure 13 (Saladin 2020).

The outer layer of the cerebrum is called the cortex. It has folds that appear as hills and valleys called gyri and sulci, respectively. These foldings allow more neurons to fit inside the skull and enable higher functions. The cortex contains around 16 billion neurons referred to as the grey matter interconnected to other brain areas by long nerve axon fibers called white matter. This organization allows the cortex to be considered as the origin of thinking and voluntary movements (Rea 2016).

B.2. Types of brain cells

The CNS is made up of mainly two basic cell types; the neurons and the neuroglia (Rea 2016). Neurons, key players in the CNS, consist of three basic parts: the cell body, the axon and the dendrite (Figure 5). The nucleus is found within the cell body and contains the cell´s genetic material, therefore, it controls all cell activities. The neurons are electrically excitable and thus act as information messengers. Using electrical impulses and chemical signals called neurotransmitters, the neurons transmit information from one neuron to another connecting the brain with the complete nervous system. Transmission occurs along protoplasmic fibers that form a long tail extending from the cell body to the terminal bud called the axon. These neurotransmitters are then released across the synapse, a tiny space between the axons and dendrites of adjacent neurons. The dendrites that look like branches of a tree forming extensive networks around the cell body are responsible for receiving afferent messages from connecting neurons.

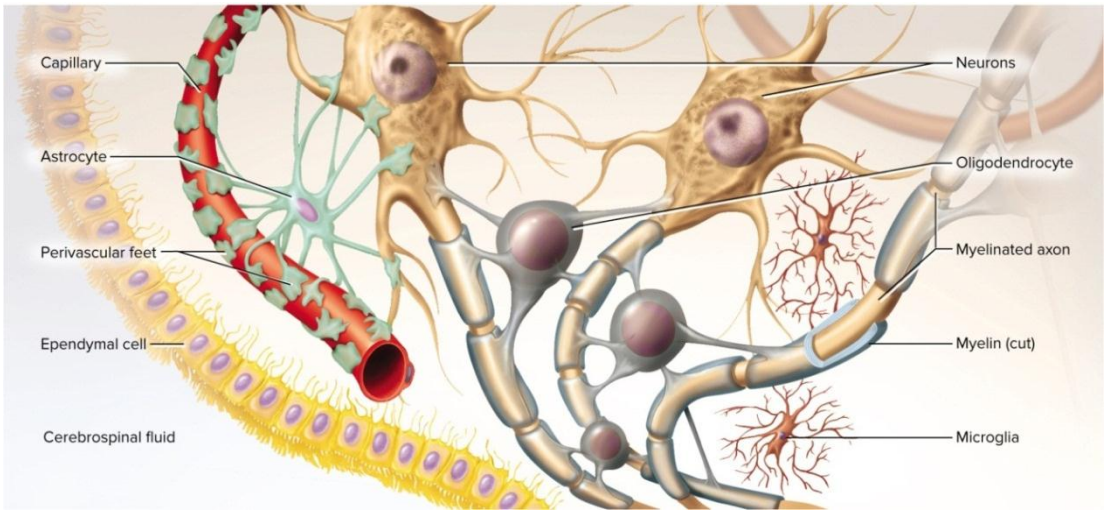

Figure 5. Neurons and other brain cells adopted from "Anatomy & physiology: the unity of form and function." 9th edition (2020), chapter 14, figure 13 (Saladin, 2020)

Neuroglia, also called glia or glial cells, are the most abundant cell type in the CNS. They perform essential functions including structural support, metabolic and nutrient support, maintenance of homeostasis, insulation, and guidance of development for the neurons. Neuroglia is subdivided into two broad classifications: microglia and macroglia. Microglias are found throughout the CNS and have a defense role as phagocytic cells. They are capable of altering their shapes in order to engulf particulate material and thus protect the CNS (Figure 5). On the other hand, the macroglias are subdivided into several types including astrocytes, oligodendrocytes, ependymal cells, Schwann cells, radial glial, enteric glia, and satellite cells, where each have a special role (Figure 5). These cells serve in the CNS and the peripheral nervous system (PNS), with different roles to maintain functional and proper signal transmission within different brain parts and between the brain and the whole body. The most abundant glial cells in the brain are the astrocytes. They account for 25% of the total brain volume (Guillamón-Vivancos 2015). Astrocytes are distinguished by their star-like shape and known to provide structural integrity by filling the spaces between the neurons (Rea 2016). These cells surround the cerebral capillaries through astrocytic end feet. Through this close apposition to the blood vessels, astrocytes control metabolic exchange between the neurons and the vasculature.

B.3. Blood-Brain-Barrier

The brain is protected by different elements that provide defense against physical injury: a 7 mm thick skull, a protective fluid called cerebrospinal fluid (CSF) that surrounds the brain and spine, and a protective membrane called the meninges. To accomplish proper neuronal function, blood vessels are critical to deliver oxygen and nutrients to the brain as well as to all tissues and organs throughout the body (Daneman 2015). However, these may also bring a serious threat to the brain. Thus, blood vessels that vascularize the CNS possess unique properties, providing protecting element against disease-causing pathogens and toxins that may be present in the blood. Endothelial cells that line the microvessels in the brain are interconnected by highly extensive tight junctions and adherent junctions, thus exhibiting highly regulated movement of ions, molecules, and cells between the blood and the brain (Figure 6).

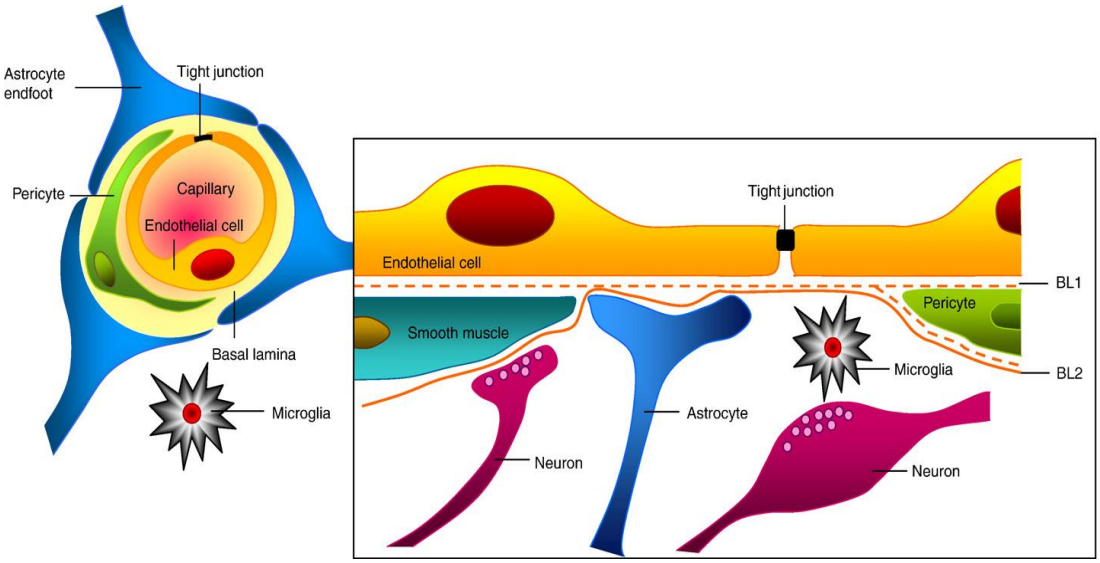

Figure 6. A schematic diagram of the cerebral endothelial cells together with tight junctions form the restricted blood-brain-barrier and their association with brain cells (Abbott 2010).

This configuration decreases endocytosis and transcytosis activities when compared to peripheral endothelial cells (Shi 2016). This barrier is called the blood-brain barrier (BBB) and provides a highly controlled microenvironment required for

neuronal signaling (Abbott 2010). BBB restricts most water-soluble molecules from crossing into the brain. Only small gaseous molecules such as O_2 and CO_2 and few small lipid-soluble agents, such as ethanol, which are smaller than 400 Da and/or contain less than eight pairs of hydrogen bonds, can passively diffuse through the regulated lipophilic membranes (Abbott 2006). Specific transport routes offer transport of nutrients and other compounds (Figure 7). Therefore, in case of any drug discovery either to target or to avoid the CNS, the special features of the BBB must be considered.

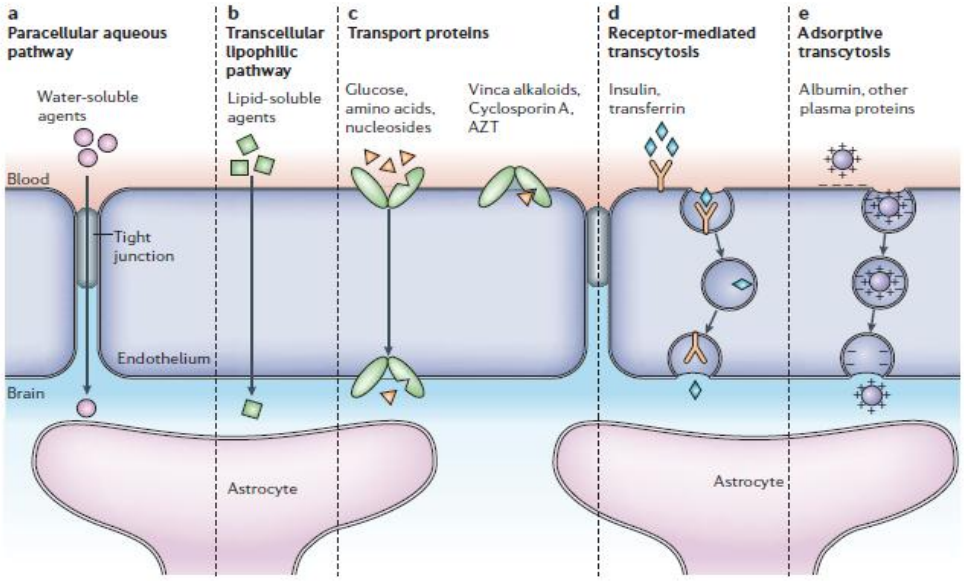

Figure 7. The restrictive nature of the BBB allows passage of some molecular compounds through specific routes of transport. (Abbott 2006)

C. Brain Cancers

A brain tumor, known also as intracranial tumor, is an abnormal growth of cells forming a mass of tissues in the brain or central spine that can disrupt proper brain function. WHO classified brain tumor based on the origin and the behavior of the identified cells. The location and the growth rate of the tumor determine its impact on the function of the nervous system. According to the National Brain Tumor Society, there are over 120 types of tumors in the brain and the CNS arranged from the least (benign) to the most (malignant) aggressive. There are mainly categorized into four types; benign, malignant, primary, and secondary or metastatic.

Benign tumor is the least aggressive and initiates from non-cancerous cells within or surrounding the brain. These tumors are characterized by their slow growth with clear borders without spreading to the adjacent tissues. Depending on their size and location, they can cause pressure on brain structures in the nearby which results in significant neurological symptoms. They can also grow asymptomatically and can be removed without recurrence. Unluckily, some benign tumors may progress into malignancy (Deanna Glass-Macenka 2013). On the other hand, malignant brain tumors contain cancer cells with rapid and invasive growth to adjacent areas of the brain and the spine. Thus, these tumors do not have borders, have to be surgically resected and need to be treated with radio- and/or chemotherapy. Unfortunately, these tumors often recur after treatment.

Primary brain tumors are tumors that originated in the cells of the brain. These tumors are among the top ten causes of cancer-related death in the US (Mawson 2012). The World Health Organization (WHO) classified primary brain tumors based on their histopathologic criteria and immunohistochemical data (Allen Perkins 2016). They are

mainly categorized after the type of cell they originate from or where they first develop in the brain. Astrocytoma, for example, is formed from astrocytes. Primary tumors are subdivided into two groups: glial tumors and non-glial tumors. Glial tumors are composed of glial cells and consist of one-third of all primary brain tumors (National Brain Tumor Society). About 80% of malignant brain tumors are gliomas that develop from glial cells (Goodenberger 2012). Gliomas tend to be fast growing, diffusely invasive, poorly understood, and highly resistant to treatment. Thus gliomas are the most deadly type of primary brain tumors (Wion 2018). To this group belong ependymomas, astrocytomas of which glioblastoma multiforme (GBM) is the most common, oligodendrogliomas, and mixed gliomas, such as oligoastrocytomas that contain cells from different types of glia (Mawson 2012). Gliomas are further categorized according to their grade: low-grade gliomas (WHO grade II) are non-anaplastic and well differentiated, and high-grade gliomas (WHO grade III–IV), which are anaplastic, undifferentiated, and have poor prognosis.

The other group of primary brain tumors is non-glial tumors that developed from nerves, blood vessels or glands. About 50% of primary brain tumors are benign lesions that can be treated and have relatively good prognosis (Laws 1993). However, primary brain tumors may spread to other areas in the CNS, but rarely to other organs.

Secondary or metastatic brain tumors are tumors that start in other parts of the body and metastasize to the brain. These tumors are named and treated after the location in which they originated. Melanoma, lung, and breast cancers are responsible for three-quarters of brain metastasis. Secondary tumors are more common than primary brain tumors (Jaime Gállego Pérez-Larraya 2014).

D. Glioblastoma

Among gliomas, glioblastoma or glioblastoma multiforme (GBM) is the most frequent and aggressive form of malignant brain tumors. GBM comprises about 45.2% of malignant primary brain and CNS tumors, 54% of all gliomas and 16% of all primary brain tumors (Thakkar 2014, Davis 2016). According to the WHO, GBM is classified as Grade IV Glioma, or also called Grade IV Astrocytoma (Louis 2007). Biologically, GBM originates from astrocytes. It occurs most often in the cerebral hemispheres mainly in the frontal and temporal lobes of the brain (Figure 8). It is fast-growing and invasive tumor that grows along white matter tracts into the healthy brain parenchyma. Single tumor cells can be traced in other areas of the brain far away from the radiologically visible tumor mass (Giese 2003), giving rise to regular tumor relapses after therapy. GBM is distinguished from other gliomas by several histological features, such as the presence of necrotic cells and increase of abnormal growth of blood vessels around the tumor (Niederhuber 2020).

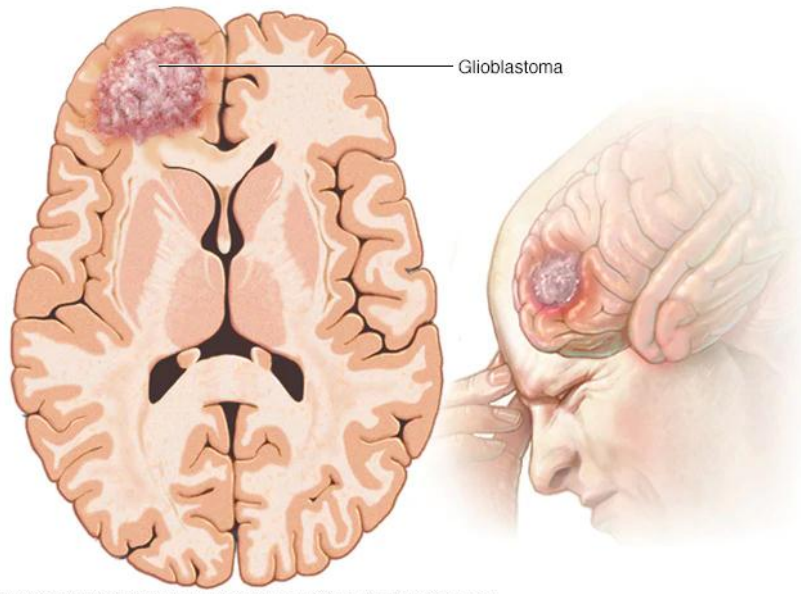

Figure 8. Glioblatoma, adopted from MAYO foundation for medical education and Research.

In 80% to 90% of cases, GBM arise *de novo* as grade IV glioma, without any traces of lower grade precursors (Ohgaki 2007). This type is called primary GBM and often occurs in elderly patients with a mean age of 62 years. It can also evolve as secondary GBM from lower grade gliomas such as astrocytomas or oligodendrogliomas and occur in younger patients with a mean age of 45 years (Thakkar 2014). Although they are histologically indistinguishable, primary GBM is more aggressive while secondary GBM is associated with better prognosis.

Glioblastoma is 1.6 times more common in men than women, and slightly higher in Caucasians relative to other ethnicities (Ellor 2014, Brem 2017). The incidence of glioblastoma increases with age, the lowest incidence being among people from 0 to 19 years old and the highest among those older than 75 years old (Brem 2017).

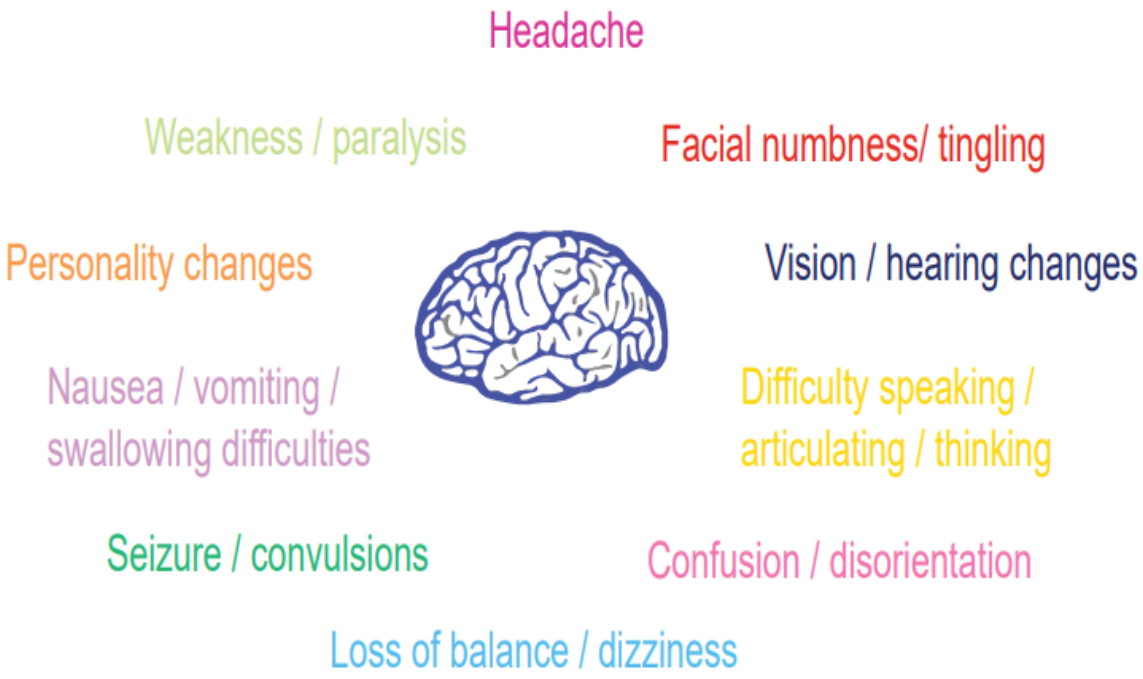

Figure 9. Symptoms of glioblastoma.

D.1. Symptoms, Diagnosis and Treatment:

General symptoms associated with glioblastoma are the same as for different brain tumors. However, specific symptoms depend on the location and the size of the tumor in the brain. These include severe headaches that get worse in the morning and may awaken the patient at night. In addition, patients may suffer from seizures or convulsions, difficulty in thinking, speaking or articulating, personality changes, weakness or paralysis in one side of the body, loss of balance or dizziness, facial numbness or tingling, vision and hearing changes, confusion and disorientation, nausea or vomiting, and swallowing difficulties (Figure 9).

Persistent headaches, vomiting, swelling or protrusion of the blind spot at the back of the eye that may be caused by increased pressure inside the skull, or signs of mental dysfunction and seizures, all are neurological signs that need to be evaluated by a neurologist. Examinations may include magnetic resonance imaging (MRI) scan,

Fluid-attenuated inversion recovery (FLAIR), computed tomography (CT) scan to detect the presence of tumor inside the brain or the spine. A chest X-ray may also be used to determine if there is any sign of a tumor metastasis. Other symptoms that may affect vision or hearing may require specialized tests to be done. Examination of CSF may be performed if results of other tests are not conclusive. Recently, several artificial intelligence methods have been applied in glioma diagnosis. Computer-assisted diagnosis (CAD) is a procedure that digitizes the tumor and directs the attention of the physician to a change in volume, using several MRI scans and segmentation FLAIR sequence to follow up the progress of a glioma (De Nunzio 2019). All these configurations are used to examine brain tumors in order to early detect the tumor and improve the outcomes.

Many challenges face glioblastoma treatments due to several characteristics such as localization of the tumor in the brain, limited response to therapy, inherent resistance to conventional therapy and neurotoxicity resulted by treatments. In addition, migration of malignant cells into adjacent brain areas due to tumor capillary leakage, resulted in an accumulation of fluid around the tumor and disrupted tumor blood supply thus inhibited effective drug delivery. All that beside the limited capacity of the brain to repair itself, result in limited response to treatment and deteriorate the survival chances.

Glioblastoma has one of the poorest survival rates of all other malignant brain tumors and contributes to mortality and morbidity. Patients with glioblastoma invariably relapse despite multimodal standard therapy that combine maximal safe surgical resection, adjuvant radiochemotherapy, followed by monochemotherapy with the alkylating agent temozolomide (TMZ) (Kratzsch 2018). The survival period after diagnosis and treatment ranges between one and five years with a median survival rate

around 15 months (Chen 2020). This rate varies significantly by age at diagnosis where younger patients tend to have the best overall survival (Brem 2017). New therapy approaches aim to prolong survival and overcome therapy resistance. Immunotherapy has recently been applied to treat glioblastoma, by altering the functional immune response to attack the tumor and extend survival in patients, as this modality has demonstrated remarkable improvements in the management of several solid tumors. Such treatments include programmed cell death receptor-1 (PD-1) inhibitors (Zhao 2019) and anti-cytotoxic T-lymphocyte-associated protein 4 (CTLA-4). Immunotherapy has been tried as single therapy and in combination by using immune checkpoint therapies and vaccine therapy such as chimeric antigen receptor T cells (CAR T) (Medikonda 2020).

D.2. Molecular Genetics of Glioblastoma:

GBM is an extremely heterogeneous tumor characterized by high degree of inter- and intra-tumoral heterogeneity and thus can be composed of different cell lines and genetic subsets. This means that the two types of glioblastoma, primary and secondary GBM, differ at the genetic and epigenetic level. The National Cancer Institute and the National Human Genome Research Institute in the United States of America launched a comprehensive project in 2005 called The Cancer Genome Atlas (TCGA). This project aimed to improve the understanding of the molecular basis of cancer by mapping the major cancer-causing somatic alterations in large cohorts of human tumors through integrated multi-dimensional genomic sequence, transcriptome, and epigenome analyses. The first cancer type studied by the TCGA was glioblastoma. TCGA GBM Analysis Working Group (AWG) constructed a detailed somatic

landscape of GBM through a series of comprehensive genomic, epigenomic, transcriptomic, and proteomic analysis to distinguish between different types of GBM. Further sequencing projects revealed more about somatic changes in well-known GBM genes.

Such distinguishable features are mainly mutations in isocitrate dehydrogenase (*IDH*), loss of heterozygosity (LOH) 10q, receptor tyrosine kinase (*RTK*), epidermal growth factor receptor (*EGFR)* amplification, O-6 methylguanine DNA methyltransferase *MGMT* status, cyclin-dependent kinase inhibitor 2A (*CDKN2A*), glioma-CpG island methylator phenotype (G-CIMP), phosphatase and tensin homolog (*PTEN*), platelet-derived growth factor receptor alpha (PDGFRA), tumor suppressor gene *p16* and *p53*, and tumor suppressor gene transcription factor (*TP53*) (Figure 10).

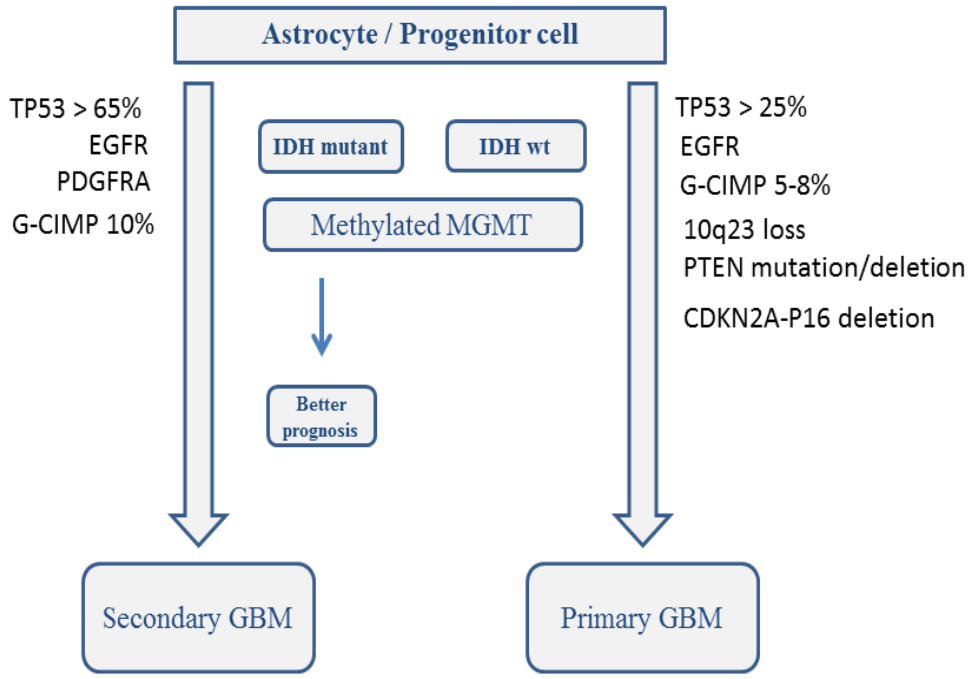

Figure 10. Summary of detected genetic alterations that contribute to GBM. Some of these mutations are found in one type of GBM more than the other.

Because of the heterogeneity of glioblastoma, there is a persistent need to identify these mutations and their affected downstream pathways in order to design specific drugs. In addition, suggesting combination therapies targeting multiple pathways may be a key for more efficient treatments for glioblastoma. This has created hopes of personalizing therapies for glioblastoma patients (Lau 2014).

D.2.a. Isocitrate Dehydrogenase Family

Isocitrate dehydrogenase (IDH) family consists of three self-regulating enzymes (IDH1, IDH2, and IDH3). IDH1 is primarily found in the cytoplasm and in peroxisomes, whereas IDH2 in the mitochondrial matrix. IDHs catalyze the conversion of isocitrate into α-ketoglutarate (α-KG), a metabolite with oncogenic activity via

epigenetic mechanism. This reaction also leads to production of reduced nicotinamide adenine dinucleotide phosphate NADPH from NADP+ (Figure 11.A). The physiologic function of the NADP-dependent IDH1/2 enzymes has not been well characterized yet, but they are thought to play roles in the metabolism of glucose, fatty acids, and glutamine. They are also functional in protecting cells from harmful reactive oxygen species (ROS) and contributing to the maintenance of normal cellular redox status. IDH1 and IDH2 are highly homologous to each other. However IDH1/IDH2 are structurally, functionally, and evolutionarily distinct from heterotrimeric IDH3 that functions in the tricarboxylic acid (TCA) cycle to produce the NADH required for oxidative phosphorylation (Reitman 2010, Cairns 2013, Upadhyay 2017).

Mutations of IDH1 and IDH2 were first reported in 2008 to be found in different human cancers, most commonly in gliomas. The mutation is frequently found in arginine residue in the catalytic pocket of the enzyme. In IDH1, the mutated arginine at codon 132 is often substituted into R132H, R132C, R132L, R132, S and R132G. Mutation in IDH2 affects the arginine at codon 172 and 140 (Clark 2016). Mutant IDH loses its normal enzymatic activity and gains a new ability in producing the oncometabolite 2- hydroxyglutarate (2-HG). 2-HG is a competitive inhibitor of several α-KG-dependent dioxygenases that occupies the same space in the active site of the enzyme. These enzymes include histone demethylases and the Ten-eleven translocation (TET) family of 5-methlycytosine (5mC) hydroxylase that play crucial roles in gene regulation and tissue homeostasis. IDH1 mutations and the subsequent 2-HG accumulation are associated with important epigenetic alterations such as increased histone methylation and decreased hydroxylation of methyl groups on DNA cytosines (5-hydroxylmethylcytosine (5hmC)). This leads to decreased expression of key

differentiating enzymes and thus impaired cellular differentiation and promoted tumor progression (Xu 2011). Elevated levels of 2-HG results in increased levels of hypoxia-inducible factor subunit (HIF-1α), a transcription factor that facilitates tumor growth in low oxygen environment and whose stability is regulated by α-KG. Levels of HIF-1α were found to be elevated in human gliomas harboring mutant IDH1 than in tumors without the mutation (Zhao 2009, Madala 2018). Consequently, HIF-1α controls genes promoting cell adaptation to hypoxia, i.e., vascular endothelial growth factor (VEGF) which is a key mediator of angiogenesis that act through VEGFR2 receptor for the formation of new blood vessels needed for the growth of the tumor (Figure 11.B). Clinical reports have noted that GBM has very high HIF-1α expression in 15% of *IDH*-mutant tumors compared to 8% tumors without the mutation (Kaminska 2019), and very high VEGF expression compared with low-grade brain tumor (Cheng 2019). HIF-1α and VEGF play pivotal roles in the development, prognosis and response to treatment of GBM. Therefore, the inhibition of HIF-1α as well as VEGF expression is a crucial strategy in GBM treatment.

IDH1 was found to be mutated in approximately 12 % of glioblastomas, and in more than 70% of WHO grade II and III astrocytomas and oligodendrogliomas and in five of six secondary glioblastomas. Hence, *IDH1* is now part of the diagnostic criteria in brain tumors and

it is a predictor of malignant transformation from lower grade glioma into glioblastoma (Nørøxe, Poulsen, & Lassen, 2016). Tumors without mutations in IDH1 often had mutations in IDH2. GBM patients with tumors that have these mutations have a better outcome than those with wild-type IDH genes (Yan et al., 2009).

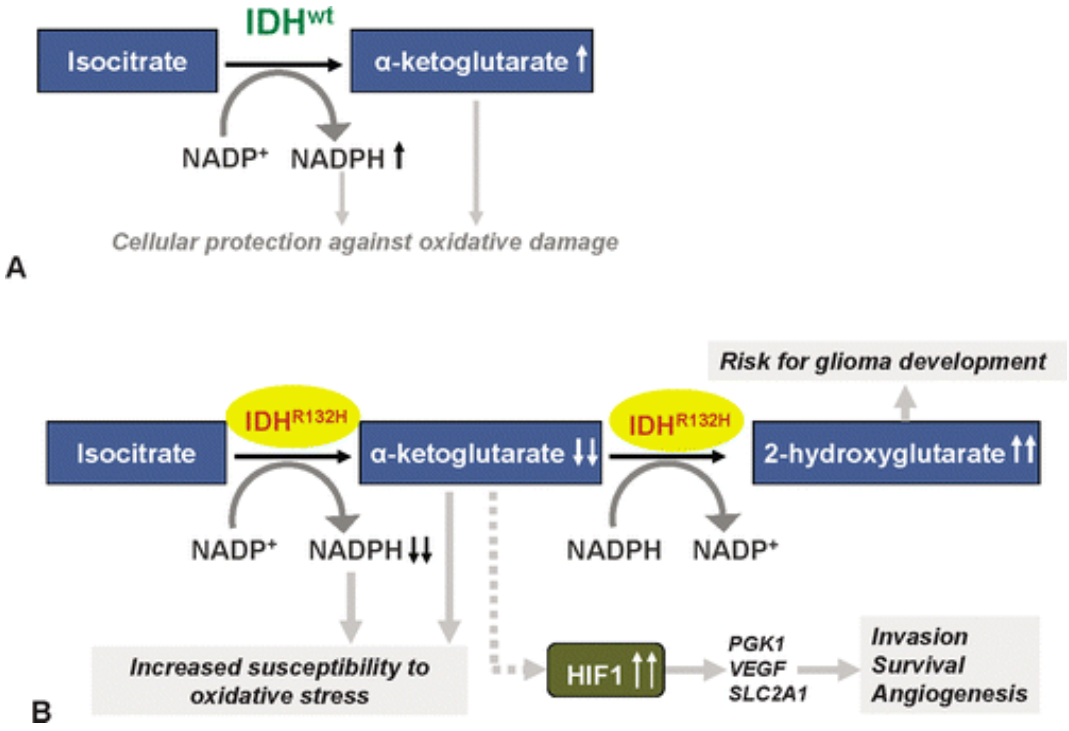

Figure 11. Putative mechanisms of isocitrate dehydrogenase (IDH) mutation in glioma tumorigenesis. A, Normal (wild-type) IDH activity. B, Mutant IDH activity (Nikiforova 2011)

D.2.b.O-6 Methylguanine DNA Methyltransferase (MGMT)

The standard drug used in treating glioblastoma as mentioned previously is the alkylating agent TMZ. TMZ transfers alkyl groups to guanine bases causing DNA damage and cell death. Some GBM cells develop resistance against TMZ. Proteomic screening of these cells revealed that presence of a specific protein determines the efficiency of the treatment and the sensitivity of the tumor cells towards TMZ. This protein is O-6 methylguanine DNA methyltransferase (MGMT) which is a DNA repair protein that removes alkyl groups from the O6 position of guanine in DNA. GBM tumors with functional MGMT exert cellular resistance to cytotoxic actions of TMZ. Methylation of *MGMT* promoter results in silenced *MGMT* that interferes with DNA

repair mechanism and thus increases TMZ cellular sensitivity and improves patients´ survival. Unmethylated *MGMT* promoter leads to active gene expression and high levels of the repair enzyme that result in chemotherapy resistance. Methylated *MGMT* promoter is found in 50% of newly diagnosed GBM, and in 75% of secondary GBM, hence it is associated with *IDH* mutation that is more common in secondary GBM (Thakkar 2014).

MGMT status is a prognostic and predictive marker in GBM tumors that is correlated with response to therapy. Tumors with methylated *MGMT* respond better to therapy including TMZ and radiotherapy, thus shows better overall survival (OS) and better progression free survival (PFS) (Arrizabalaga 2017).

D.2.c. Receptor Tyrosine Kinases

Receptor Tyrosine Kinases (RTKs) are cell surface receptors involved in cell-cell communication and are responsible of a wide range of cellular processes including cell growth, metabolism, motility, and differentiation. Abnormal RTK activation can cause many human diseases, most notably, cancers (Du 2018). The oncogenic RTK signaling is involved in cancer initiation and progression. Different studies showed that RTKs do not work in isolation but rather cooperate as networks of multiple receptors through a crosstalk known as "RTK co-activation" (Tan 2017).

Analysis of TCGA dataset revealed the first intra-tumoral heterogeneity in RTK expression in glioblastoma. These studies showed that RTKs are altered in approximately 70% of glioblastomas, of which *EGFR* is most frequently mutated (Subramanian Venkatesan 2016). Two-thirds of primary GBM harbor amplifications

and/or mutations of RTKs. The most commonly altered RTKs are the EGFR (60%) and Platelet Derived Growth Factor Receptor α (PDGFRA, 10–15%) (Chakravarty 2017).

D.2.d. Epidermal Growth Factor Receptor

EGFR is a trans-membrane tyrosine kinase receptor that modulates, upon activation, several cellular activities like growth, migration and survival. Different cancer types including GBM show enhanced activity of EGFR. Amplified EGFR in tumor leads to stimulation of cell growth, proliferation, migration, and adhesion as well as inhibition of apoptosis, all that promoting cancer progression.

About 40% of all GBM have amplified EGFR, with a higher prevalence in primary GBM (Jiang 2018, Le Rhun 2019). Amplification of EGFR in GBM is a strong predictor of poor prognosis. Several studies suggest a correlation between the presence of EGFR, p53, and the age of GBM patients . EGFR is highly expressed in older patients (>45 years) and the presence of p53 is highly expressed in those tumors (Armocida 2019). Younger patients with amplified EGFR but normal p53 showed poor prognosis. However, EGFR over-expression in older patients is associated with better prognosis. Moreover, normal or high amplification of EGFR is correlated with lower response to TMZ (Simmons 2001, Thakkar 2014).

D.2.e. Platelet-Derived Growth Factor Receptor

Platelet-Derived Growth Factor Receptor (PDGFR) is a receptor tyrosine kinase that promotes cellular events including proliferation, survival, migration, and differentiation (Ip 2018). Elevated signaling of PDGFR alpha (PDGFRA) through amplification of *PDGFR* or its ligand *PDGF* held by genomic aberrations, contributes to tumor progression in several tumor types. According to TCGA, amplification of *PDGFRA* is a very common event in GBM (12%) (Ip 2018), especially in secondary GBM (60%) (Mesti 2016). Together with EGFR, PDGFRA are the most common RTK pairs that is co-phosphorylated and activated in GBM even in the absence of amplification. Co-amplification of EGFR and PDGFRA loci at the DNA level, has been observed in approximately 5-7% of GBM (Chakravarty 2017). This event is an early driver action in gliomagenesis. Subsequently, tumor heterogeneity arises from random segregation of independent EGFR and PDGFRA in newly divided cells.

D.2.f. Glioma-CpG island Methylator Phenotype

Epigenetic alterations such as cancer specific DNA-methylation play important roles in cancer progression. The best known epigenetic abnormality is promoter specific CpG island (CGI) methylation that inhibits expression of protein coding genes, mainly tumor suppressor genes, and noncoding RNAs (ncRNA) like microRNA (miRNA) that demonstrated multiple roles in cancer pathogenesis (Kang 2019). TCGA research network identified a DNA methylation phenotype in glioblastoma called Glioma-CpG island methylator (G-CIMP), which is strongly associated with *IDH* mutation and is present in approximately 10% of secondary GBM and ~5% – 8% in primary GBM (Thakkar 2014). 2-HG produced by mutated IDH results in G-CIMP+ state. Together

with *IDH1* or *IDH2* mutations, G-CIMP phenotype leads to extensive methylation in the CpG islands of many genetic loci that in turn, down-regulates expression of selected genes. Furthermore, G-CIMP+ glioblastoma present suppression in mRNA levels for EGFR and H-Ras, a protein that regulates cell division, resulting in suppressed EGFR signaling (Li J1 2014).

D.2.g. Tumor Protein p53

Tumor protein p53 is a gatekeeping gene coding for tumor suppressor protein that consists of transcriptional activation, DNA binding, and oligomerization domains. This protein induces cell cycle arrest, apoptosis, senescence, DNA repair, or changes in metabolism in response to diverse cellular stresses. In glioblastoma, 60%-70% of secondary GBM have a mutant *p53*, while this mutation is found in only 25%-30% of primary tumors. This mutation occurs more frequent in younger GBM patients (Thakkar 2014). Total loss of function of *p53* results in impaired DNA repair and catastrophic chromosomal aberrations. Impaired or non-functional *p53* in GBM may result in relapse after radiation therapy (Yang 2020).

Another important phenomenon caused by *p53* mutation and found in a variety of tumors is chromothripsis. The latter occurs when specific genome regions are shuttered and then stitched together in a single catastrophic event. This mechanism is taken in advantage to the tumor to arise in a relatively short period of time. This incidence is found in 39% of GBM, whereas in other tumors it is only around 9% (Jovčevska 2018).

D.2.h. Losses on chromosomes

Genetic loss on chromosome 10 occurs in 80-90% of glioblastoma. It occurs either as loss of the entire chromosome or as loss of only the short or the long arm. Phosphatase and tensin (*PTEN*), is the first tumor suppressor gene identified on chromosome 10 mainly at 10q23. Mutation or deletion of *PTEN* results from loss of heterozygosity (LOH) for the *PTEN* gene on chromosome 10q23 (Thakkar 2014). This event has diagnostic, therapeutic, and prognostic significance in the management of many human cancers including 20-40% of glioblastoma. It has been proposed to be involved in early gliomagenesis and found almost exclusively in primary GBM (Abdulkareem 2013, Jovčevska 2018).

Another genetic alteration in GBM is the loss of the short arm of chromosome 1 and the long arm of chromosome 19, named 1p/19q deletions. This deletion is used to predict the response of patients to chemotherapy (Thakkar 2014).

D.2.i. Cyclin-Dependent Kinase Inhibitor 2A

Cyclin-dependent kinase inhibitor 2A **(***CDKN2A*), is a gene that codes for two proteins p16 and the p14 tumor suppressors that keep cells from dividing and growing uncontrollably. Primary GBM is associated with *p16* deletion that is most frequently inactivated by copy number deletion and DNA methylation in many cancers (Chen 2019). P16 plays a key role in cell cycle regulation by binding and inhibiting cyclin-dependent kinases (CdK-4 and -6). Moreover, p16 phosphorylates serine and threonine residues of retinoblastoma (Rb) protein. Methylation of the *p16* promoter region results in inactivation of *p16* and thus uncontrolled cell cycle. This has been reported to vary between 23% and 67% in primary tumors (Bhatia 2014).

D.2.j. DNA Polymerase Alpha-Primase

DNA polymerase α-primase complex also called replicases, is a highly conserved enzyme in eukaryotes responsible for DNA synthesis. It plays an essential role in nucleic acid metabolism including DNA replication, repair, and recombination, by using single-stranded DNA as a template for the synthesis of the complementary DNA strand (Kelman 1998). The complex comprises four distinct subunits; a catalytic subunit polymerase alpha (POLA1) (Figure 12), a regulatory subunit POLA2 and two primase subunits PRIM1 and PRIM2 (Starokadomskyy 2016). DNA polymerase alpha complex is recruited to DNA at the replicative forks during S phase of cell cycle (Han 2016). The primases initiate the DNA synthesis by oligomerising RNA:DNA primers on both leading and lagging strands that are the backbone of Okazaki fragments´ synthesis. This process is continuous on the leading strand and discontinuous on the lagging strand. Instead, the lagging strand is synthesized as a series of short fragments (Okazaki fragments) that is held and extended by the catalytic subunit POLA1 (Kelman 1998, Muzi-Falconi 2003).

Polymerases exhibit high processivity of DNA synthesis which means the ability to polymerize a huge number of nucleotides without dissociating from the DNA template. However, the amount of replicases in the cell is insufficient and the enzyme must be recycled to accomplish the replication process. Thus, polymerases act in two contradictory ways, first by tightly associating with DNA during elongation, and then rapidly ejected from DNA to associate with another DNA strand in order to synthesize the next Okazaki fragments (Kelman 1998).

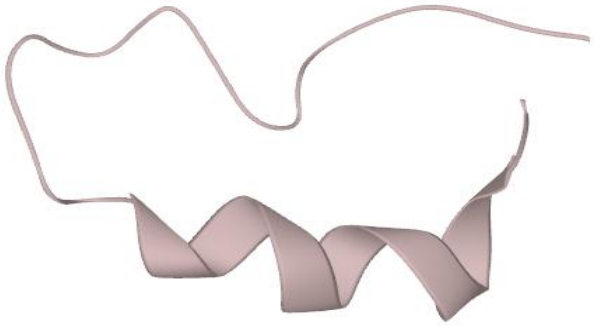

Figure 12. Secondary structure of DNA polymerase alpha catalytic subunit (POLA1), adopted from uniprot.org.

POLA1, the catalytic subunit that drives the whole machinery of the complex and initiates the replication process, is encoded by *POLA1* gene and weighs 180 kDa. It uses an RNA primer to synthesize the first ~10-20 base pairs of DNA (Han 2016). However, POLA1 has limited processivity which means it is not capable of holding the substrate throughout a consecutive reaction since it is responsible for the elongation and the creation of the Okazaki fragments. Moreover, POLA1 lacks 3´ exonuclease activity for proofreading and correcting the replication errors. Therefore, POLA1 is not well suited for efficient and continuous replication of the entire DNA strand. For these reasons, two polymerases take over for processive DNA synthesis; polymerase delta and polymerase epsilon on the lagging and leading strands, respectively.

POLA1 is found in all cells, since it is needed in very critical step for cell proliferation. According to The Human Protein Atlas, analysis of the TCGA dataset revealed an elevated RNA expression of POLA1 in glioblastoma. Antibody staining showed high protein halt of POLA1 in GBM cell lines (Atlas). Immunohistochemical staining of POLA1 in glioblastoma using mAb against POLA1 on human glioblastoma cell lines showed a percentage of POLA1-positive cells between 72 %- 77 %. *In situ*

studies on glioblastoma tissues showed 7.6 % - 45.9 % positive POLA1 staining, whereas there was no positive staining for POLA1 in normal brain tissues. These scores are correlated with the histological grade of malignancy and the proliferating potential of cells of the brain tumor (Kunishio 1990, Kunishio 1999).

D.3. Glioblastoma Subtypes:

Based on the TCGA genomic profiling, four subtypes of GBM with common histological features and distinguishable expression of signature genes were identified; proneural (PN), neural, classical, and mesenchymal (MES) (Verhaak 2010, Brennan 2013). However, further studies, refined these into three subtypes: proneural/neural, mesenchymal, and classical (Wang 2017, Teo 2019).

- **The Neural** subtype is characterized by the elevated expression of a variety of neuron markers such as neurofilament, light polypeptide (NEFL), gamma-aminobutyric acid type A receptor alpha1 subunit (GABRA1), synaptotagmin 1 (SYT1), and solute carrier family 12 member 5 (SLC12A5) (Ostrom 2016). However, neural subtype has no unique distinguishing alterations from other classes, although elevated rates of mutant proto-oncogene receptor tyrosine-protein kinase v-erb-b2 avian erythroblastic leukemia viral oncogene homolog 2 (ERBB2) were observed (Agnihotri 2014). The expression patterns of the neural subtype were found to be very similar to those of normal brain tissue specimens (Verhaak 2010, Eder 2014)
- **The proneural** subtype is often found in secondary glioblastoma (Nørøxe 2016) and was associated with younger age (Eder 2014, Ostrom 2016). It contains several proneural development genes such as *SOX* genes as well as *DCX*, *DLL3*,

ASCL1, and *TCF*. This signature is involved in developmental processes and was identified as cell cycle and proliferation signature. Moreover, the proneural signature is characterized with two major features; alterations of *PDGFRA* either amplification and/or mutation, in a high rate and point mutations in *IDH*. *PDGFRA* point mutations observed in GBM were in the Ig-domain which potentially disrupts ligand interaction (Verhaak 2010). Interestingly, proneural samples that harbor *IDH1* mutation were found to lack *PDGFR* abnormality and vice versa. Other frequent events that were also found in this subtype are *Tp53* mutations and loss of heterozygosity. Chromosome 7 amplification paired with chromosome 10 loss was found to occur in only 54% of proneural samples (Verhaak 2010, Nørøxe 2016).

G-CIMP methylation was found to be highly overrepresented in the proneural subtype and is tightly associated with IDH mutation. Proneural subtype with G-CIMP methylation have significantly better outcome with median overall survival of 150 weeks for patients with G-CIMP-positive proneural tumor compared to 42 weeks for G-CIMP-negative ones. Therefore, this subtype trends toward increased survival, whereas *MGMT* status shows no difference in response to treatment (Nørøxe 2016, Ostrom 2016).

- **The classical** subtype is characterized by *EGFR* amplification, mainly *EGFRvIII* mutation that was observed in 97% of the classical and infrequent in other subtypes. Focal 9p21.3 homozygous deletion that targets *CDKN2A* which lead to inactivation of the tumor suppressor RB pathway, loss of *PTEN* and distinct lack of *Tp53* mutations were also noticed in the subset of classical

samples sequenced even though *Tp53* is the most frequently mutated gene in glioblastoma. Neural precursor and stem cell marker such as Notch pathways, Sonic hedgehog, and Nestin, were highly expressed in the classical subtype. Amplification of chromosome 7 paired with chromosome 10 loss is found in almost 100% of the classical GBM (Verhaak 2010, Agnihotri 2014). Classical subtype is associated with better response to treatment (Daniel 2018) especially tumors with methylated *MGMT* as compared with non-*MGMT*-methylated classical tumors (Nørøxe 2016).

- **The mesenchymal** subtype displays expression of mesenchymal markers such as *CHI3L1* (also known as *YKL40*) and *MET* and mesenchymal and astrocytic markers (*CD44*, *MERTK*). Expression of these markers can cause epithelial-to-mesenchymal transition. Focal hemizygous deletions of a region at 17q11.2 that contains the tumor suppressor gene neurofibromin (*NF1)* which results in lower *NF1* expression levels. Co-mutations of *NF1* and *PTEN* were also observed in the mesenchymal phenotype, where both intersect with the serine/threonine-protein kinase (AKT) pathway, which promote survival and tumor growth. Because of high necrosis and inflammatory infiltrates in the mesenchymal subtype, genes of the tumor necrosis factor super family pathway and proinflammatory signaling NF-κB pathway such as *TRADD, RELB, TNFRSF1A* were found to be highly expressed in this subtype. *MGMT*-methylated mesenchymal tumors tend to show better response to treatment than non-*MGMT*-methylated ones (Verhaak 2010, Nørøxe 2016).

E. Retinoids:

Retinoids are fat-soluble molecules that are involved in many complex and diverse physiological processes. Retinoids comprise over 4000 natural and synthetic derivatives that share similar chemical structure with vitamin A also known as retinol. These compounds play pivotal roles mainly in epidermal development, cell differentiation, cell proliferation, apoptosis, and immune responses (Schenk 2014, Chen 2019). Retinoids, mainly retinoic acid (RA), is a critical regulatory signaling molecule involved in multiple aspects of mammalian CNS development, including the formation of the hindbrain, motor neuron axon outgrowth regional and neural patterning during development patterning and neuronal differentiation (Maden 2007, Chen 2020). Differentiation of neurons and glia occurs through the activation of the transcription of genes that encode different transcription factors, cell signaling molecules, structural proteins, enzymes and cell-surface receptors (Maden 2007). RA is also implicated in the maintenance of the differentiated state of adult neurons and disruption in RA signaling in adults leads to a malfunction in the neurons and neuronal degeneration causing several neurological diseases, including movement disorders, schizophrenia and motor neuron disease (Maden 2002). Therefore, RA could be used as a therapeutic agent for the induction of axon regeneration and the treatment of neurodegeneration.

Several studies have shown that retinoids possess antitumor effects and cause tumor regression mainly by inducing apoptosis or differentiation (Manor 2003, Shi 2017, Abdel-Samad 2018). Retinoids are used as chemotherapeutics and chemopreventive agents (Fu 2012) since they inhibit tumorigenesis by suppressing cell growth and stimulating cell differentiation (Sakoe 2010).

E.1. Signaling Pathway of Retinoids

Retinoids exert their highly pleiotropic effects through the retinoid nuclear receptors (RNRs); the retinoic acid receptors (RARs) and retinoid X receptors (RXRs). These receptors are members of the superfamily of steroid/thyroid hormone nuclear receptors that function as ligand-inducible transcription factors. There are three subtypes of each receptor complex; α, β, and γ for which there are several isoforms. In particular, there are four isoforms of RARα, five of RARβ, and two of RARγ (di Masi 2015). Furthermore, each receptor consists of six regions A/B, C, D, E, and F, whereas the most three important regions are: A/B region with a ligand-independent transcriptional activation function, C region harbors the DNA binding domain, and E region harbors the ligand binding domain. The RAR isoforms differ principally in their *N*-terminal A region, while the B to F are closely similar. This diversity in isoforms is a result of alternative splicing or of the use of different promoters upstream of the gene coding for the receptor. It allows binding of large numbers of both natural and synthetic RNRs selective ligands, including agonists, antagonists and inverse agonists (Asson-Batres 2014).

Structural data analysis has classified RNRs ligands by their actions on coregulator recruitment and dissociation. Ligand binding induces allosteric conformational changes which promote or repress receptor-coregulator interactions. Analysis revealed that coactivator recruitment occurs upon binding to an agonist, dissociation of coactivator upon binding to antagonists, whereas stabilization of receptor occurs with corepressors upon binding with inverse agonists (Asson-Batres 2014).

The retinoid receptors are activated by the natural active metabolites of retinol; all-*trans* retinoic acid (ATRA) that is also simplified as retinoic acid (RA), 13-*cis*

retinoic acid (13*c*-RA), and 9-cis-retinoic acid (9*c*-RA). ATRA and 13*c*-RA are pan-agonists that bind to all RAR isoforms with high efficiency, whereas 9-*cis*RA can bind to both RARs and RXRs and activate RAR/RXR heterodimers. After binding to its ligand, the ligand-activated RAR complex dimerizes with the same type of RAR or heterodimerizes with RXRs and act as a transcription factor controlling numerous physiological processes through the regulation of gene expression (di Masi 2015, Abdel-Samad 2019) including both repression and activation (Asson-Batres 2014).

Upon receptor dimerization, co-repressors are released and the receptor complex binds to a specific DNA regulator sequence in retinoid-responsive genes, namely the retinoic acid responsive element (RARE). Subsequently, co-activators and transcription machinery are recruited to the promoter region, including histone acetyltransferases (HATs), RNA Polymerase II, transcription factors and other mediator-containing complexes, to decompress the chromatin and initiate transcription (Asson-Batres 2014, Schenk 2014). This is called the classical model of RA pathway (Figure 13).

In the non-classical model of RA pathway, RXRs acts as a common heterodimerization partners for a number of other nuclear receptors including the thyroid hormone receptor, vitamin D receptor, liver X receptor, farnesoid X receptor, peroxisome proliferator-activated receptor γ(PPARγ), and others (Lefebvre 2010). This converts a linear signaling pathway into a very complex network resulting in diverse physiological responses including cell proliferation, cell metabolism, inflammation, blood coagulation, fatty acid transport, biosynthesis, and cell death (Abdel-Samad 2019).

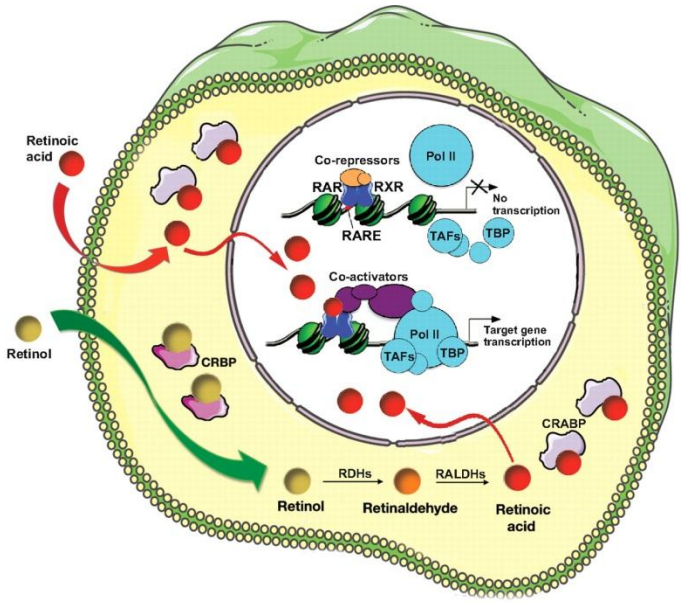

Figure 13. Retinoid signaling pathway during development, (Rhinn 2012)

ATRA also exhibits non-genomic pathway independently of the nuclear receptor action by modulating several proteins involved in signal transduction in a cell specific manner. Such actions involve activation of kinase signaling pathways via transcription factors that is located at the end of these signaling cascades leading to different transcriptional effects. For instance, in neuronal cells, ATRA activates extracellular-signal-regulated kinases (Erks) via phosphoinositide 3-kinase (PI3K) and steroid receptor coactivator (Src) kinases leading to repression of the anti-differentiative octamer-binding transcription factor 4 (Oct4). In epithelial cells and fibroblasts, ATRA binds to RARα that dimerizes and form complexes and then activate G protein alpha Q (Gaq) leading to activation of a cascade of mediators and kinases that contribute to transcriptional activation of RARα target genes (Schenk 2014).

E.2. Retinoids and Cancer

RA-induced abnormal signaling is involved in many diseases as well as in several cancers. Proper activity of RARs requires integrity of different mediators in the signaling pathways. Mutations in any of these mediators may result in defective signal transduction. Such mutations can affect transcription factors or kinases and thus lead to deficient phosphorylation and expression of RAR target genes. Several cancers such as in hepatocellular carcinoma are characterized by amplified or deregulated cytosolic kinase cascades such as Protein Kinase B (Akt) or MAPKs leading to abnormal RARα phosphorylation and thus abrogated MAPK pathway. Subsequently, the transcriptional activity of RARα is suppressed or it can as well be degraded. This aberrant signaling and RAR/RXR phosphorylation and activity is associated with tumoral growth and RA resistance (Asson-Batres 2014).

One of the most oncogenic pathways in colorectal cancer (CRC) namely the Wnt/β-catenin signaling pathway is repressed by the RXRs. RXRα is shown to interact with β-Catenin which is considered oncogenic in colon tumors, and which activity is regulated by the tumor suppressor adenomatous polyposis coli (APC). Thus studies have shown that treatment with RXR agonists leads to the degradation of β-catenin through an APC-independent mechanism (Dillard 2008). In addition, RXRs are activated in colonocytes upon treatment with the chemopreventive n-3 polyunsaturated fatty acids thus inhibiting the colonocytes proliferation (Fan 2003, Abdel-Samad 2019).

The anticancer action of retinoids is mediated by the tumor suppressor activity of RARβ. The expression of RARβ results in RA-dependent and -independent growth arrest and apoptosis (Alvarez 2007). However, *RARβ* is frequently deleted or its expression is epigenetically silenced during tumorigenesis. This highlights the need of

developing treatment strategies that overcome ATRA-resistance such as synthesizing selective RARβ ligands to restore cell differentiation and growth control (di Masi 2015).

E.3. Natural and Synthetic Retinoids

Vitamin A is an essential dietary lipid for the human body as it is required for a variety of physiological processes including embryonic development, adult growth and development, maintenance of immunity, maintenance of epithelial barriers, and vision (O'Byrne 2013). However, vitamin A cannot be synthesized by any animal species and is only obtained through diet mostly from plants as pro-vitamin β-carotene and from animal tissues as retinyl esters (REs) in the form of retinol. Vitamin A is stored as REs intracellularly in large quantities, mainly in hepatic cells. However, this form of vitamin A is biologically inactive and thus is transformed into its bioactive form retinoic acid (RA) (Schreiber 2012).

Retinoids comprises both natural (Figure 14) and synthetic (Figure 15) vitamin A analogues. They are lipophilic isoprenoids composed of a cyclic group and a linear chain with a hydrophilic end group. These compounds include retinol, retinal, retinoic acid, retinyl esters and their active derivatives and metabolites (Alizadeh 2014). All-*trans* retinoic acid (ATRA), 13-*cis* retinoic acid (13-*cis*RA) and 9-*cis* retinoic acid (9-*cis*RA) the active metabolites of retinol, are considered natural retinoids that are known to modulate cell proliferation, apoptosis, and differentiation in a cellular dependent manner. ATRA and (9-*cis*RA) have been shown to be involved in different cellular

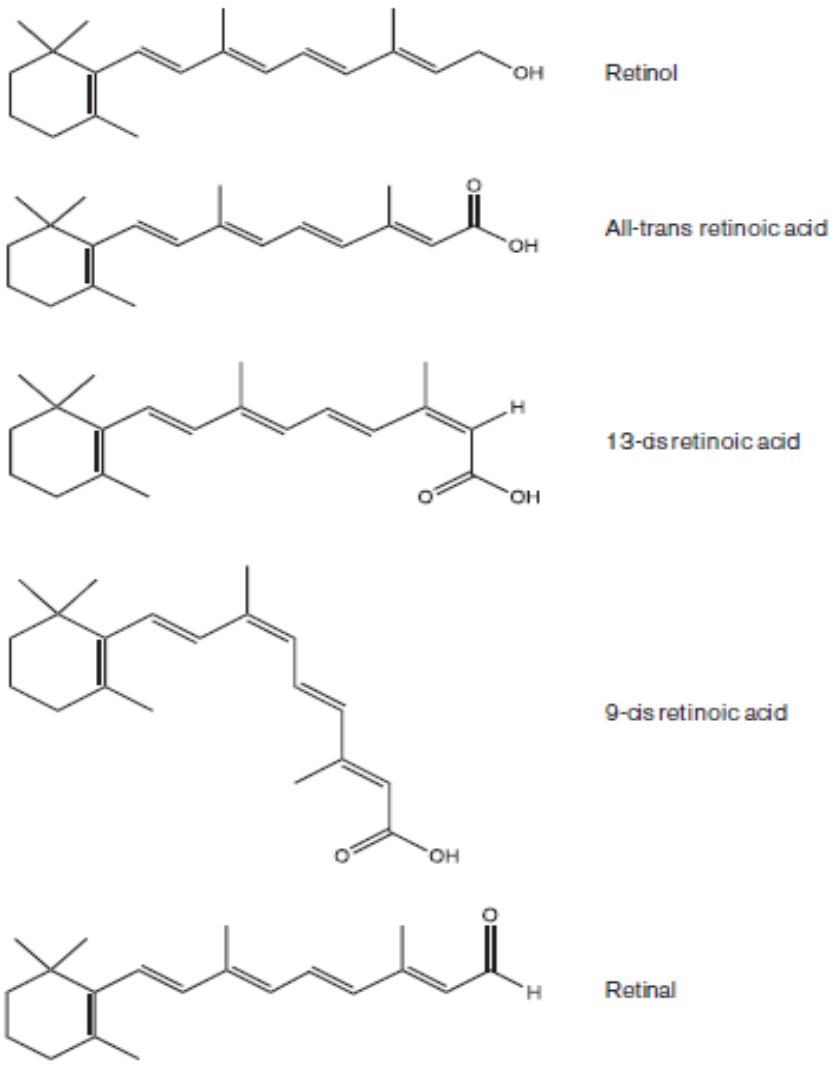

Figure 14. Natural retinoids, (Abdel-Samad 2019)

aspects such as cell differentiation, morphogenesis, proliferation, and antineoplastic (Simoni 2005). In particular, ATRA was shown to induce cell cycle arrest at the G_1 phase, inhibit cellular proliferation leading to cell death (Siddikuzzaman 2011). First, ATRA was applied as a cyto-differentiating agent in combination with other drugs in treatment regimen for patients with acute promyelocytic leukemia (APL) (Breitman 1981). APL is initiated due to the fusion of promyelocytic leukaemia (PML)/retinoic acid receptor-alpha (RAR-alpha) that is produced as a result of the unique chromosomal translocation in APL. The (PML/RARα) oncogene blocks the differentiation and increases self-renewal of leukaemic progenitor cells. The presence of this fusion oncogene is a marker of sensitivity to ATRA (Tallman 1994, de The 2010). The protein translated from this oncogene represses RARα and non-RARα target genes and disrupts PML nuclear bodies leading to immortal proliferation and inhibition of terminal differentiation. ATRA binds to RAR receptors causing degradation of PML-RARα protein through the ubiquitin-proteosome and caspase system. This results in restoration of terminal differentiation of promyelocytes. Moreover, ATRA leads to dissociation of corepressors from the repressive complex and the recruitment of coactivators to the complex. Consequently, repression of transcriptional activation of target genes is relieved resulting in restored differentiation of promyelocytes (Shen 2009).

However, the use of natural retinoids including ATRA was shown to be associated with adverse effects including teratogenicity, chemical hepatitis, increase in serum triglycerides, mucocutaneous cytotoxicity, headache, and bone toxicity (Theodosiou 2010). Moreover, the duration of complete remission induced in ATRA-treated patients is brief (3-6 months) and patients tend to relapse due to acquired

resistance to ATRA-mediated differentiation. Drug resistance may be due to attenuation or mutations in retinoid receptor signaling pathway. All these limitations often hindered the use of natural retinoids in clinical trials (Abdel-Samad 2019).

In efforts to overcome these obstacles, synthetic retinoids were developed to enhance selectivity and to reduce toxicity (Figure 15). Among the synthetic retinoids, isotretinoin, acitretin, tazarotene, and adapalene are ligands of the RAR, bexarotene is the first rexinoid (ligand of the RXR), and alitretinoin is the first panagonist (RAR+ RXR). The most promising synthetic retinoids with anti-neoplastic activities are the atypical N-(4-hydroxyphenyl) retinamide (4HPR) (Bernard 1992), 6-[3-(1-adamantyl)-4-hydroxyphenyl]-2-naphthalene carboxylic acid (CD437) (Fontana 2002), and ST1926; an analogue of CD437 (Cincinelli 2003).

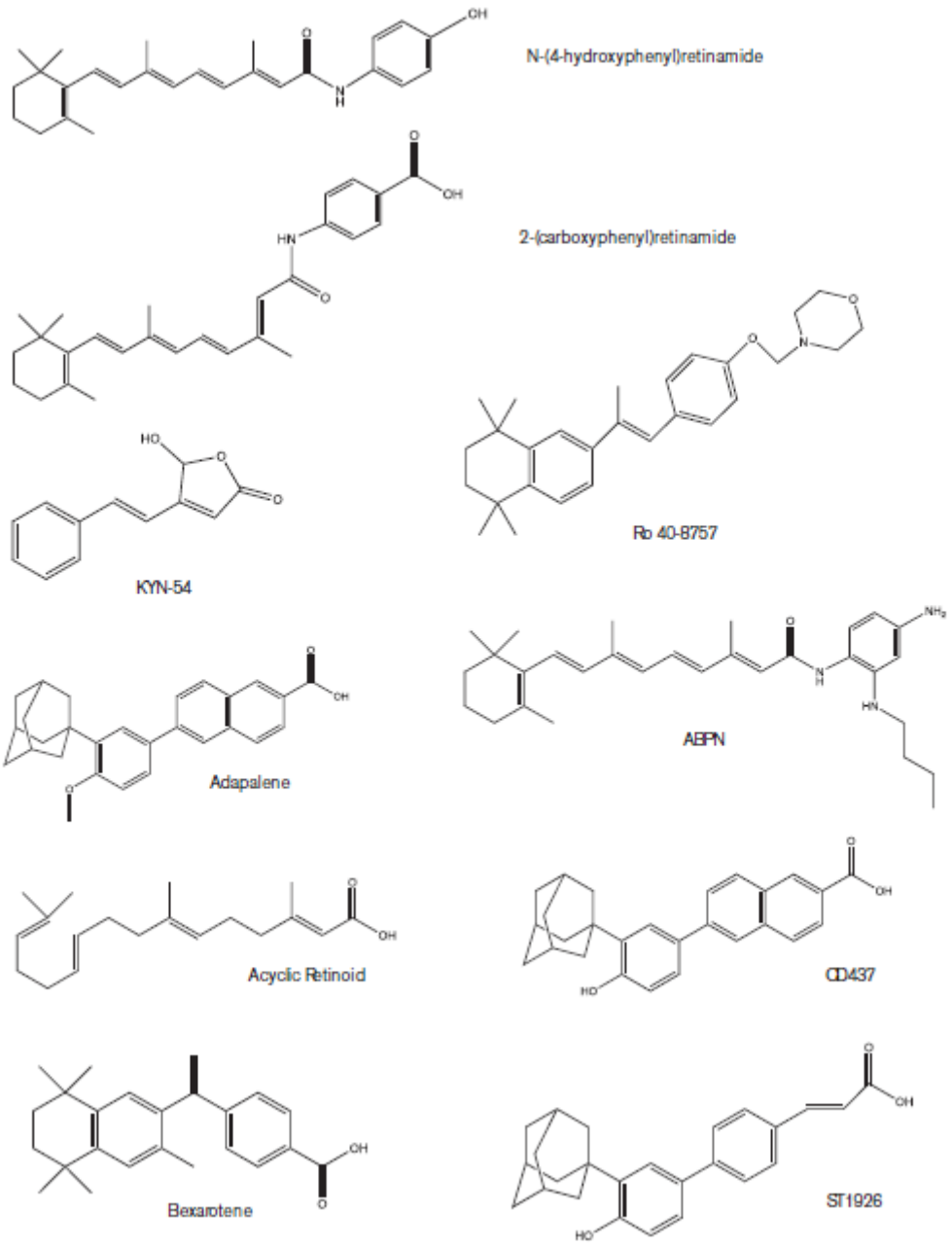

Figure 15. Synthetic retinoids, adopted from (Abdel-Samad 2019)

Atypical retinoids exert their mechanism of action through a non-classical concept of ligand-receptor interaction. They act through RARs as well as by non-receptor mediated growth regulatory or apoptogenic activities. The anti-cancer therapeutic and chemopreventive potential of atypical retinoids were already supported by preclinical and clinical data (Cincinelli 2003).

The early synthetic retinoid that gained much attention especially in breast cancer chemoprevention clinical trials was N-4-(hydroxyphenyl) retinamide (HPR or fenretinide). It has also shown to have anti-proliferative effects, inhibited the growth of RA-resistant human breast carcinoma cells, growth inhibition, and DNA fragmentation with subsequent apoptosis in both RA sensitive and refractory cell lines (Fontana 2002). HPR also reduced the proliferation of several human CRC cell lines (Abdel-Samad 2019). Furthermore, HPR was also shown to induce apoptosis in a variety of tumor types including neuroblastoma. HPR-induced apoptosis is mediated by the up-regulation of pro-apoptotic factors, followed by cytochrome c release. Caspase activation and apoptosis are the result of oxidative and endoplasmic reticulum (ER) stress. Usage of HPR has acquired considerable interest due to its mild toxicity and favorable pharmacokinetic profile in paediatric patients (Armstrong 2012). Another synthetic retinoid that is well studied in multiple cancer models including hematologic and solid tumors is 6-[3-(1-Adamantyl)-4-hydroxyphenyl]-2-naphthalene carboxylic acid, also known as CD437. It is a selective agonist to RARγ, and can bind to RARα and RARβ but with low affinity. It is active in retinoid-resistant cells and retinoid antagonists cannot block its activity (Cincinelli 2003). CD437 induced G_1 cell cycle arrest in human breast carcinoma through enhanced expression of the cyclin/cyclin dependent kinase complex inhibitor $p21^{WAF1/CIP1}$ that is expressed through a p53-independent mechanism (Fontana 2002). In addition, DNA damaging effects on CRC cell lines through inhibition of POLA1 at nanomolar concentrations have been induced upon CD437 treatment (Han 2016).

E.4. Retinoids and Glioblastoma

Vitamin A excess and supplementation have been shown to have pro-oxidant effects and are associated with increased risks of mortality resulted from cancer and other diseases. The therapeutic effect of vitamin A and retinoids in cancer remain uncertain. In fact, repeated and/or excessive exposure to endogenous RA may contribute to tumorigenesis. An imbalance in retinoid receptor expression initiated by environmental factors, mainly excessive expression of RARα and reduced expression of RARβ, leads to elevated levels of RA in glia which in turn contributes to glioma formation. Thus, treatment strategy for gliomas by combining a RARα antagonist and a RARβ agonist may be beneficial. This hypothesis suggest that RARα antagonist would be expected to inhibit RARα-induced gliomas, while the RARβ agonist would suppress tumor growth and possibly lead to regeneration of normal glia (Mawson 2012).

In vitro experiments using retinoids for treating glioblastoma-derived cell lines and primary cells revealed potential therapeutic benefits. Application of RA to human GBM cell lines or to human glioma cells xenografted in mice, inhibited proliferation and migration. Moreover, co-application of RA and cytostatic drugs induced cell cycle repression, differentiation and apoptosis (Choschzick 2014). On the other hand, ATRA induced proliferation and incomplete differentiation in brain tumor stem cells (Niu 2010), and induce moderate antiproliferative effects on human glioma cell lines upon long-term exposure at high concentrations (Schmidt 2000). In another study RA induced differentiation of glioma cells into neurons throughout a multistep mechanism mainly by acquiring several neuronal differentiation markers and decreasing the expression of several genes associated with glioma aggressiveness (Wion 2018). Therefore, data concerning the responsiveness of glioblastoma to retinoids are

contradictory most probably due to high histopathological, cellular, and molecular heterogeneity (di Masi 2015). Subsequently the need to prolong survival and overcome resistance in glioblastoma demands further research to develop effective targeted molecular therapies against this disease.

E.5. The Adamantyl Retinoid ST1926

A prominent member of synthetic retinoids family is the adamantly retinoid ST1926 or E-4-(4′-hydroxy-3′-admantyl biphenyl-4-yl) acrylic acid, a CD437 analogue (Figure 16). ST1926 is synthesized from CD437 through a three-step sequence where the naphthalene ring in CD437 is substituted by a styrene moiety in ST1926 (Cincinelli 2003). Several studies, including studies from our laboratory showed that ST1926 exerts potent antitumor activities in both *in vitro* and *in vivo* solid tumor models derived from human ovarian carcinoma, lung carcinoma, rhabdomyosarcoma, and melanoma at well-tolerated doses, independently of RARs and *p53* signaling pathways (Cincinelli 2003, Zuco 2004, Basma 2016, Abdel-Samad 2018, Karam 2018, Bahmad HF 2019). Antitumor effect of ST1926 was also demonstrated *in vitro* and *in vivo* in leukemia models for acute myeloid leukemia (AML) (Garattini 2004), adult T-cell leukemia (El Hajj 2014), and chronic myeloid leukemia (CML) (Nasr 2015) with minimal side-effects. ST1926 was shown to induce genotoxic stress and exert its cytotoxic and antiproliferative effects mainly by causing double-strand breaks (Zuco 2005, Valli 2008). Studies in AML demonstrated a proactive role of proteasome in ST1926-induced DNA damage and apoptosis (Fratelli 2013). In addition, ST1926 resulted in an immediate increase in cytosolic calcium that is directly related to apoptosis (Garattini 2004). In comparison to CD437, ST1926 displayed favorable pharmacokinetic profile,

and can be given orally while achieving micromolar concentrations in human and mouse plasma (Sala 2009, Basma 2016).

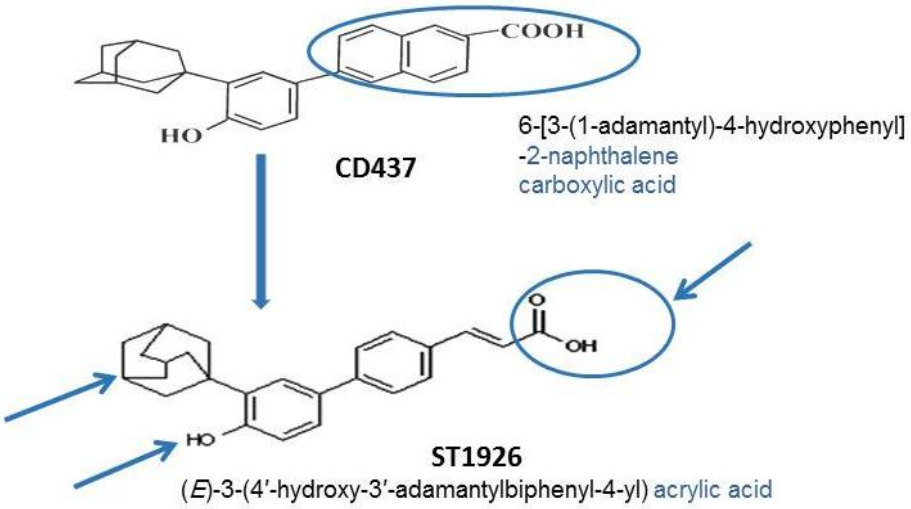

Figure 16. ST1926, a potent CD437 analogue.

Abdel Samad et. al showed in a study on a panel of human CRC cell lines that ST1926 induces growth inhibition independently of *p53* and *p21* status and reduces the tumor volume as well as the doubling time in a xenograft mouse model. They have also shown ST1926-induced growth inhibitory effects resulted in apoptosis, S-phase cell-cycle arrest, dissipation of mitochondrial potential, and early DNA damage. Similarly to CD437, ST1926 exert its anti-proliferative effect by inhibition of POLA1 activity and reducing its protein levels (Figure 17) (Abdel-Samad 2018). In a phase I clinical trials on patients with ovarian carcinoma, ST1926 showed low absorption and extensive glucuroconjugation which resulted in limited bioavailability, as micromolar concentrations dropped shortly to submicromolar levels (Sala 2009). Another study

from our laboratory aimed to develop nanoparticle formulation of ST1926 which improved its bioavailability and reduced the tumor burden even at four-fold lower the effective concentration (El-Houjeiri 2017, Abdel-Samad 2019). These findings raise the hope to consider ST1926 in glioblastoma treatment especially since POLA1 is elevated in glioblastoma tissues versus normal counterparts.

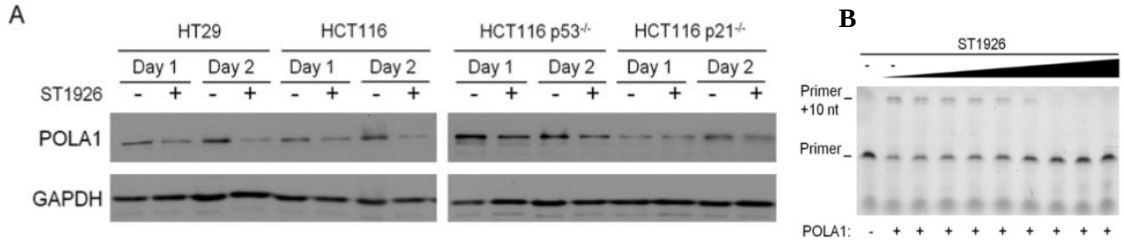

Figure 17. ST1926 reduces POLA1 protein levels in colorectal cancer cells (A) ST1926 reduces POLA1 protein levels in CRC. (B) ST1926 reduces POLA1 activity in CRC, using the *in vitro* primer extension assay (Abdel-Samad 2018).

CHAPTER II

OBJECTIVE, SPECIFIC AIMS, AND SIGNIFICANCE

GBM is the most aggressive and deadliest form of brain tumors. Despite the available therapies, GBM presents low survival rates and frequent relapses. Unfortunately, the tumor cannot be completely eliminated surgically because of its infiltrative nature. Furthermore, the restrictive nature of the BBB excludes many chemotherapies (Groothuis 2000, Wang 2014). Although systematic antiproliferative drugs and other alkylating agents have the ability to cross the BBB, their survival benefits remain low. Moreover, these compounds confer many side effects and serious toxicity problems (Lee 2017). Locally delivered drugs can circumvent the BBB and decrease side effects caused by systemic administration (Perry 2007). However, these drugs do not increase the survival rate significantly (De Bonis 2012). GBM is known for its high tumor heterogeneity which is the main cause behind resistance to many traditional cytotoxic chemotherapeutics. Therefore, there is an eminent need to develop more adapted and efficient treatments for patients with GBM. Retinoids, both natural and synthetic, have shown multiple effects in many cancer types through the regulation of cell proliferation, cell differentiation, and induction of apoptosis (Das 2010, Tang 2011). The complexity of GBM suggests that drugs such as retinoids may provide significant benefits. Indeed, the use of retinoids in GBM cells has shown inhibition of neurosphere growth, decreased clonogenicity, and reduced cancer stem cell markers (Gersey 2019). However, some limitations such as toxicity and non-specificity hindered the use of natural retinoids in clinical trials (Theodosiou 2010, Abdel-Samad 2019). Thus, synthetic retinoids offer improved selectivity to overcome these

limitations. The synthetic adamantly retinoid ST1926 has shown antitumor effects in several cancer types by inducing apoptosis and growth inhibition at sub-micromolar concentrations independently of retinoid receptor signaling pathway. Recently, we identified ST1926 as an inhibitor of POLA1 (Abdel-Samad 2018). The latter has been found to be elevated in GBM. This suggests ST1926 as a relevant and attractive drug to be used against GBM.

Based on these facts, we aim to characterize the antitumor activities and the mechanism of action of ST1926 in GBM. Accordingly, we will use *in vitro* and *in vivo* human GBM tumor models. Specifically, we will target the following aims:

- Investigate the antitumor effect of ST1926 on cell proliferation and growth.
- Examine the cell death mechanism mediated by ST1926 in GBM cells.
- Determine the cell cycle progression following ST1926 treatment.
- Profile the protein alterations affected by ST1926 treatment.
- Understand the mechanism of action of ST1926 in GBM.
- Test the impact of ST1926 administration on xenograft GBM models in mice.

Our findings may lead to novel therapeutic strategies in treating GBM with less toxicity. ST1926 may be reconsidered as an efficient treatment to suppress glioblastoma progression by targeting POLA1 in cancerous cells. With these preclinical studies, we anticipate that ST1926 may be considered as a key drug to prolong the survival rate and improve the quality of life for GBM patients.

CHAPTER III

MATERIALS AND METHODS

A. *In Vitro Human GBM Models*

A.1. Cell Culture

U87MG and U251 are the most commonly used human cell lines in GBM research (Clark 2010). U87MG is abbreviation for Uppsala 87 malignant glioma. This cell line was firstly obtained from a 44 years old female patient at Uppsala University in Sweden in 1966. However, in 2016 researchers, through genetic profiling and transcriptome analysis, discovered that the cell line distributed by the American Type Culture Collection (ATCC) is not identical with the cells obtained from the patient in Uppsala. The new version, which is used in our project, belongs to an adult male patient, whereas U251 is isolated from a 75 years old male patient. Both patients suffered from pleomorphic glioma.

Both cell lines are classified as grade IV glioblastoma/astrocytoma and are reported as *IDH*-wild type (Ichimura 2009) and harbor a methylated *MGMT* promoter (Oh 2017). U251 has a mutated *p53*, while U87MG has a wild-type *p53* gene (Giakoumettis 2018). U87MG has an epithelial morphology while U251 shows fibroblastic patterns (Figure 18). One of the major features of the U87MG genome is the large number of chromosomal abnormalities (Clark 2010). Mutational analysis of the U87MG genome revealed different classes of genetic mutations including single-nucleotide variations (SNVs), insertions/deletions (indels), and translocations (Giakoumettis 2018). Both cell lines are routinely passaged at three days intervals.

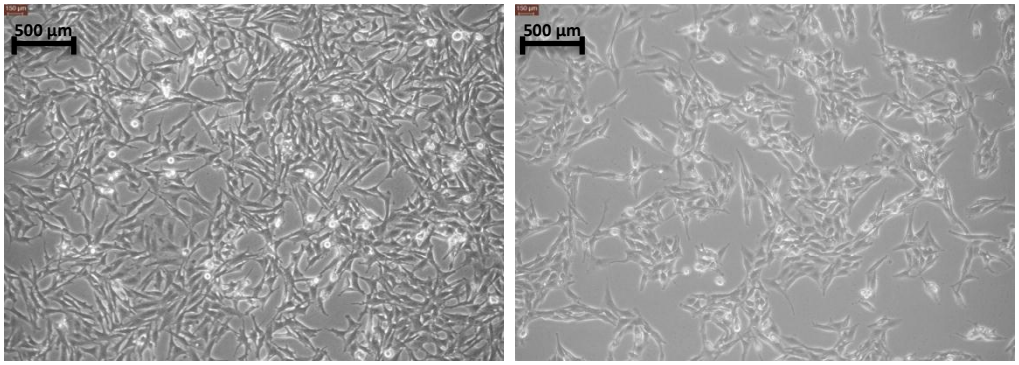

Figure 138. U251 (left) **and U87MG** (right) 48 h after seeding

The two cell lines have different biological characteristics particularly regarding cell proliferation, migration, and invasion. For instance U87MG have a higher migration and invasion capability as well as higher proliferation rate than U251 (Qi 2016). They also differ in nicotinamide nucleotide metabolic process regulation, RNA splicing, glycolysis, and purine metabolism which may account for the distinct phenotypes of these GBM cell lines (Qi 2016).

The two other GBM cell lines used in our study are U118 and A172. U118 is obtained from a human adult male patient. These cells present a wild-type *IDH* (Ichimura 2009, Krell 2019) and a wild-type *p53* (Geng 2010). A172 has a disrupted transcription of proto-oncogene *ABL1* that codes for a tyrosine receptor kinase, which is important in tumorigenesis. This results in a fusion between *ABL1* and Core-Binding Factor Subunit Beta (*CBFB*), a protein coding gene, contributing to the formation of the *ABL1-CBFB* gene fusion. However, the A172 cell line is able to survive in the absence of a functional *ABL* gene product, indicating a non-housekeeping effect of *ABL* (Heisterkamp 1990). Major GBM cell lines mutations are summarized in Table 1.

Cell lines	Origin	*CDKN2A* Deletion	*PTEN mutation*	*p53 mutation*	EGFR overexpression	*IDH mutation*	Invasiveness	Angiogenic
A172	53 Y male	Yes	Yes	No	N/A	No	N/A	N/A
U-118	47 Y male	Yes	Yes	Yes	N/A	No	N/A	N/A
U87 MG	Adult male	Yes	Yes	No	No	No	Low	High
U251	75 Y male	Yes	Yes	Yes	Yes	No	Low	High

Table 1. Gene mutations according to Sanger Institute COSMIC database (ATCC, 2019), (Ichimura 2009, Giakoumettis 2018), (N/A: not available)

A.2. Cell Growth Conditions

U87MG, U251, U118, and A172 cells were cultured in Dulbecco´s Modified Eagle´s medium/nutrient mixture F-12 Ham (DMEM-F12) (Sigma Aldrich, USA) supplemented with 10% fetal bovine serum (FBS) (Sigma Aldrich, USA), 1% of penicillin-streptomycin (Sigma Aldrich, USA), 1% non-essential amino acids (Sigma Aldrich, USA), and 1% sodium pyruvate (Sigma Aldrich, USA). Cells were incubated at 37°C in a humidified incubator (95% air, 5% CO_2) to grow. When cells reached 70 to 80% confluency, they were washed with calcium free-phosphate buffered saline (PBS) (Sigma Aldrich, USA), then trypsinized with trypsin-ethylene-diamine tetra acetic acid (EDTA) (Sigma Aldrich, USA) for 1 minute, and then incubated at 37°C up to 5 minutes. Trypsin effect is inhibited by the addition of fresh medium. Cells were transferred to new flasks in a ratio of 1:5 for the U251 and U87MG, and 1:3 for U118 and A172, for maintenance and to be expanded before experiments.

A.3. Cell Preparation for Experiments

When cells were almost confluent, they were prepared for experiments. For this aim, cell number was determined using a hemocytometer according to the following formula: cells/ml = average number of cells x dilution factor x 10^4. Cells were counted using trypan blue exclusion dye using 0.4% trypan blue solution.

A.4. Preparation of ST1926

ST1926 was obtained from Biogen Institute (Ariano Irpino, Italy) and was reconstituted in 0.1% dimethylsulfoxide (DMSO) at a concentration of 0.5 M, aliquoted, stored at −80°C, and used up to six months. To treat the cells, an aliquot of stock ST1926 (0.5 M) was diluted in pure ethanol to reach 10^{-2} M and then serially diluted in medium into different concentrations.

B. Cell Viability:

B.1. Trypan Blue Assay

A simple way to determine the anti-proliferative effect of ST2926 on GBM cells is to measure cell viability using trypan blue exclusion assay. Trypan blue is a colorimetric dye that is used to determine the amount of viable versus dead cells. Trypan blue is taken up by the dead cells which allows differentiation between blue non-viable cells and white unstained viable cells under the microscope. To perform the experiment, cells were seeded in triplicate in 96-well plates at a density of 5,000 cells/100 µl per well and were grown in DMEM-F12-Ham media in the absence or presence of ST1926. Supernatants containing the dead cells were collected and attached live cells were washed with PBS and harvested by trypsin/ EDTA then added to the supernatant. Cell pellet was resuspended in 100 µl media then 20 µl of cell suspension

was mixed with 20 µl of trypan blue (1.4 mM trypan blue, 154 mM NaCl, 500 mM EDTA, pH=8). Results represent the average of triplicates ± standard deviation (SD).

B.2. MTT Assay:

3-(4,5-dimethylthiazol-2-yl)-2,5- diphenyltetrazolium bromide (MTT) is a colorimetric assay used to assess cell metabolic activity. It is based on the ability of nicotinamide adenine dinucleotide phosphate (NADPH)-dependent cellular oxireductases, found in the mitochondria, to reduce MTT (yellow color) to its insoluble formazan (purple color) as a measurement of mitochondrial metabolic activity. For this experiment, U87MG, U251, U118, and A172 cells were seeded in triplicates in 96-well plates at a density of 5,000 cells/well. When cells were attached and reached ~ 50% confluency (~24 hours later), they were treated with different concentrations of ST1926 ranging from 0.01 µM to 100 µM diluted in 100 µl complete media, for up to three days. For each time point, 10 mg/ml thiazolyl blue tetrazolium bromide dye (MTT, Sigma-Aldrich) was added to each well (final concentration 1 mg/ml). The plates were incubated at 37°C for 3 hours, which allowed the metabolically active viable cells to convert the yellow tetrazolium salt into insoluble purple formazan crystals due to the high levels of NADH and NADPH. The resultant intracellular formazan crystals were dissolved by adding 100 µL of SDS-based solubilizing agent and left to incubate overnight. The reduced MTT optical density (OD) was measured at a wavelength of 595 nm using an ELISA microplate reader (Multiskan Ex). The percentage cell viability was expressed as percentage growth relative to control untreated cells. Results represent the average of at least three independent experiments ± standard error of the mean (SEM).

B.3. Sulforhodamine B Assay:

Sulforhodamine B (SRB) cell cytotoxicity assay is a colorimetric assay for measuring *in vitro* cytotoxicity based on cellular protein content. SRB is a bright-pink aminoxanthene dye containing two sulfonic groups that bind to basic amino-acid residues under mild acidic conditions, and dissociate under basic conditions. The assay was first purchased as a kit (Abcam, ab235935), and then we optimized an in-house protocol. This assay consists of a fixation trichloroacetic acid (TCA) solution, the SRB dye and a 10 mM Tris base solution (pH 10.5) solubilization solution.

The in-house SRB assay was performed on U87MG and U251 cells whereby cells were seeded in triplicates in 96-well plates at a density of 5,000 cells/well. After 24 hours, cells were treated with different concentrations of ST1926 (0.01 μM, 0.5 μM, and 1 μM) diluted in 100 μl complete media, for up to three days. At each time point, 25 μl of the fixation solution was added to each well. The plate was then incubated at 4°C for 1 hour. Afterwards, the supernatant was discarded and viable cells remained attached. The cells were then washed four times with 200 μl double distilled water (ddH_2O) and the plate was left to air dry and could be kept at room temperature up to one month. To perform the SRB staining, 50 μl of 0.04 % SRB dye was added to each well and incubated at room temperature for 1 hour. The wells were then washed with 200 μl 1% acetic acid 4 times. When the wells dried up, 100 μl of 10 mM Tris base solubilization solution was added and the plate was put on an orbital shaker for 10 minutes. The intensity of the pink color that reflects the amount of proteins proportional to the number of viable cells in each well was measured at a wavelength of 510 nm using the microplate Tristar reader. The percentage of cell viability was expressed as percentage

growth by comparing treated wells at indicated concentrations to untreated cells. Results represent the average of three independent experiments ± SEM.

C. *In Silico* Evaluation of *POLA1* Levels

To investigate the levels of *POLA1* in glioblastoma, we performed *in silico* analysis using Oncomine, a web base datamining platform that allows us to search several cancer microarray freely available online databases (Need to add reference or a website for Oncomine). We selected research comparing GBM tissues to normal brain counterparts that investigated *POLA1* expression levels with a P-value less than 0.05. We identified three different studies that showed elevated POLA1 mRNA levels in human GBM patient tissues in comparison to normal brain tissues (Shai 2003, Sun 2006, Murat 2008).

D. **Cell Cycle Analysis**

D.1. Seeding and Collecting Cells:

U87MG and U251 cells were seeded into 100 mm dishes at a ratio of $1x10^6$ cells/dish which were incubated overnight until desired confluency. Cells were treated with 0.5 μM of ST1926 for up to three days, then they were gently harvested to avoid debris formation: the media containing floating and dead cells was transferred into a 15 ml falcon tube. Cells were washed with 2 ml PBS and transferred to the corresponding falcon tube. Cells were then trypsinized with 1 ml trypsin/EDTA for 1 minute and incubated up to 5 minutes at 37°C. The effect of trypsin was inhibited by 2 ml medium and transferred into the falcon tube. The falcon tubes were centrifuged at 1200 rpm for 5 minutes at 4°C and the formed cell pellets were carefully washed with 1 ml of cold PBS and centrifuged again at same conditions. The supernatant was discarded, and the pellet was resuspended carefully with 1 ml ice cold PBS supplemented with 4 ml cold absolute ethanol. Samples were stored at -20°C until staining and analysis was performed within 10 days.

D.2. Cell Staining and Reading:

For staining, the fixed cells were thawed for 30 minutes at room temperature, and then centrifuged at 1200 rpm for 5 minutes. The supernatant was carefully removed with a yellow tip, and the tubes were tapped gently to dissolve the pellet. One ml ice cold PBS was added to each tube to wash the cells. Pipetting up and down was avoided in these steps. The cell pellets were then treated for 45 minutes with 100 μl of 200 μg/ml DNase-free RNase A with gentle tapping every 15 minutes to prevent pellet precipitation. Cells were centrifuged as described earlier, and the supernatant was

discarded. Cell pellets were resuspended using 300 µl ice cold PBS and transferred to polystyrene round-bottom flow tubes (BD Flacon). Cells were then stained with 15 µl of 1 mg/ml propidium iodide (PI) (Sigma Aldrich, USA) and incubated for 10 minutes in the dark. To measure cellular DNA content, fluorescence of PI, was obtained using flow cytometry (FACScan, Becton Dickinson). A total of 10,000 gated events were acquired in order to assess the proportions of cells of different stages of the cell cycle. Results represent the average of three independent experiments ± SEM.

E. **TUNEL Assay**

The terminal deoxynucleotidyl transferase dUTP nick end labeling (TUNEL) assay is a measure of apoptosis through detection of DNA double strand breaks (DSBs) which is a late apoptotic event. DNA strand breaks contain free 3'-OH termini which may be conjugated to dUTP-fluorescein through the enzymatic action of terminal deoxynucleotidyl transferase and fluorescein fluorescence can be detected by flow cytometry. To investigate whether ST1926 induces apoptosis in GBM cell lines, cells were seeded in a density of 1 x 10^6 cell/ flask in a 75 cm^2 flasks (T75). Cells were then treated with 0.5 µM ST1926 or left treated with solvent for control. Two extra control wells, one for positive and one for negative controls, were prepared to be used in the experiment. At the indicated time point, cells were collected by trypsinization, washed with 1% BSA in 1X PBS, and then fixed with 4% formaldehyde for 30 minutes at room temperature. Subsequently, cells were washed with 1X PBS and incubated with 100 µl of permeabilization solution (0.1% triton X-100 in 0.1% sodium- citrate) on ice for 2 minutes and then centrifuged at 4,000 rpm at 4°C for 10 minutes. Samples were washed once with 200 µl of 1X PBS, and pellets were re-suspended and incubated for

one hour at 37°C in an incubator in the dark in TUNEL reagents: 50 µl of labeling solution for negative control, and 50 µl of TUNEL reaction mixture for the other samples. The TUNEL reaction mixture was prepared of 5 µl enzyme + 45 µl labeling solution for each sample. Cells were then washed twice with 1X PBS, re-suspended in 1 ml 1X PBS, and transferred into polystyrene falcon round bottom tubes for flow cytometry (FACScan, Becton Dickinson) analysis. A total of 10,000 gated events were acquired in order to assess the proportions of apoptotic cells quantified with the excitation wavelength set at 470–490 nm and the emission wavelength at 505 nm. Results represent the average of three independent experiments ± SEM.

F. Protein Profiling

F.1. Western Blotting:

F.1.a. Seeding and Collecting Cells:

U87MG and U251 cells were seeded into 100 mm dishes at a ratio of $1x10^6$ cells/dish which were incubated for 24 hours until desired confluency. The cells were then treated with 0.5 µM of ST1926 for 2, 6, 24 and 48 hours. For each experiment, one control was used where cells were only treated with solvent medium for 48 hours. At each time point, the dish was put on ice and the cells were scraped using cell scraper, collected and transferred into a 15 ml falcon tube and kept on ice. To assure that all cells were collected, the dish was washed with 2 ml ice cold PBS and transferred to the corresponding tube. Samples were then centrifuged at 1,500 rpm for 5 minutes at 4°C. The supernatant was discarded, and the cells were washed with 1 ml ice cold PBS and transferred into an Eppendorf tube. The cells were then centrifuged at 3,000 rpm for 5 minutes at 4°C. Finally, the supernatant was removed, and the cell pellets were frozen at -80°C.

F.1.b. Protein Extraction:

Cell pellets were taken out from –80°C and put on ice. Lysis buffer was prepared from Nonidet™ P 40-based lysis buffer 1 % (v/v) that contains 150 mM NaCl, 25 mM Tris pH 7.4, 5% glycerol, 1 mM Glycerol (v/V), and 1 mM EDTA. To that, we added 2 mM sodium orthovanadate (Na_3VO_4), 1x protease inhibitor, 1 mM sodium pyrophosphate, and 10 mM sodium fluoride (NaF). Lysis buffer (200 µl – 300 µl) was added to cell pellets. Cells were left on ice for 30 minutes while vortexing every 10 minutes. Cell lysates were then sonicated 10 cycles for 30 seconds/cycle and then spinned at 16,000 rpm for 20 minutes at 4°C. The supernatants that contain the protein lysates were then transferred to new Eppendorf tubes. Two µl was taken from each protein lysate and mixed with 18 µl of lysis buffer for dilution (10 folds). From the new diluted protein lysates 2 µl were taken, mixed with 398 µl ddH_2O. To that, 100 µl of Bradford Protein Assay dye reagent (Bio-Rad) was added for quantification. 200 µl of each sample was transferred to a 96-well plate in duplicates and read within 1 hour by ELISA microplate reader (Multiskan Ex) at 595 nm. The average of the duplicates was considered as the protein concentration in each sample.

The quantification was compared to protein reference standard concentrations prepared from 20 µg/ml bovine serum albumin (BSA) ranged from 0 µg/ml to 10 µg/ml (Table 2).

Concentration (µg/ml)	ddH_2O (µl)	BSA (µl)	Bradford (µl)
0	400	0	100
2	350	50	100
4	300	100	100
6	250	150	100
8	200	200	100
10	150	250	100

Table 2. Preparation of protein reference standard concentrations of BSA. BSA concentrations were diluted in water. Bradford dye reagent was added for quantification within 1 hour. 200 µl of each standard concentration transferred to a 96-well plate in duplicates together with protein lysate samples and quantified by ELISA microplate reader.

***F.1.c. Gel Electrophoresis*:**

Sodium dodecyl sulfate (SDS)-polyacrylamide gels (PAGE) were prepared depending on the molecular weight of the proteins we wanted to detect, 12% - 15% for low molecular weight proteins and 8% - 10% for high molecular weight proteins. Samples were prepared for loading by mixing each sample with 4x lammeli containing 5 % β-mercaptoethanol. The samples were then heated at 95°C for 10 minutes and mixed by vortexing every 2 minutes. Protein ladder (TriColor Broad Protein Ladder-Biotech rabbit) was loaded in the first well, and the samples were then loaded in the following wells in 50 µg/30 µl per well. Gels were merged with 1x running buffer containing Tris base, glycine, SDS and ddH_2O, and were electrophoresed at 70 V until the samples crossed the stacking gels, and then increased to 100 V until the dye front reaches the bottom of the gel, approximately after one and a half hour.

F.1.d. Transfer to Nitrocellulose Membranes:

When the electrophoresis was done, gels were carefully removed and transferred to nitrocellulose membranes and arranged in a sandwich together with blotting filters and sponges in transfer cassettes. The cassettes were then loaded in the transfer apparatus and soaked in transfer buffer containing Tris base, glycine, methanol and ddH_2O (pH=8.3) solution. The apparatus was connected to the electric supply at 30 V and left for transfer overnight in cold room. For low molecular weight proteins, transfer was performed for two hours at 80 V on ice over the bench. After transfer, the membranes were blocked with 5 % fat free milk diluted in Tris-buffered saline (TBS) and Tween-20 (TBS-T also referred to as wash buffer) for 45 minutes. The membranes were then washed 3 times for 10 minutes with wash buffer containing Tween-20 as a detergent to help remove nonspecifically bound material and prepared for probing with antibodies as described in Table 3.

Antibody	Distributor	Batch number	Origin	MW (kDa)	Dilution	Diluted in	Storage (°C)
POLA1	Abcam	AB31777	Rabbit	180	1:500	5 % milk	-20
PARP	Santa Cruz	SC7150	Rabbit	116	1:1000	5 % milk	+4
γH2AX	Cell Signaling	CS-2577S	Rabbit	15	1:1000	5 % BSA	-20
Bax	Cell Signaling	CS2772S	Rabbit	23	1:500	5 % BSA	-20
BCL2	Santa Cruz	SC-7382	Rabbit	26	1:100	5 % milk	+4
GAPDH	Abnova	MAB5476	Mouse	37	1:20000	5 % milk	-20
2° mouse anti rabbit	**Santa Cruz**	**SC-2357**	**Mouse**	**---**	**1:5000**	**5 % milk**	**+4**

Table 3. Detailed information about the used antibodies.

F.1.e. Probing with Antibodies

Different antibodies were prepared by diluting in milk or BSA, in different ratios as described in Table 3. The membranes were sealed with primary antibodies and incubated overnight. The following antibodies were used: POLA1, Poly ADP-ribose polymerase PARP, BCL2-Associated X Protein (Bax), B - cell lymphoma 2 (Bcl2), and histone variant H2AX (γH2AX). Membranes were also probed with anti-glyceraldehyde-3-phosphate dehydrogenase (GAPDH) for assessment of equal protein loading (see Tables 3 and 4). The next day, the membranes were washed 3 times with wash buffer for 30 minutes (10 minutes/wash). Membranes were then incubated with secondary antibodies for 1 hour. The secondary antibody was removed, and the membranes were washed as described previously. The membranes were then covered with luminol reagent (Bio Rad) and imaged on the ChemidocTM MP Imaging System (Bio-Rad). Representative blots were shown of three independent experiments.

Antibody	Full name	Detection
POLA1	DNA polymerase alfa	DNA synthesis
PARP	Poly ADP-ribose polymerase	Caspase-3-mediated cleavage
γH2AX	Histone variant H_2AX	DNA damage
Bax/Bcl2	BCL2-Associated X Protein / B - cell lymphoma 2	Proapoptotic / Prosurvival-Antiapoptotic)
GAPDH	Glyceraldehyde-3-phosphate dehydrogenase	Housekeeping

Table 4. The full name of antibodies used in western blot with the detection marker.

F.2. Proteomics

To evaluate the differential alterations in proteins and the signaling pathways modifications in GBM after ST1926 treatment, we seeded U87MG, U251, and U118 cells (1x 10^6 cells) in 100 mm dishes and treated with 0.5 μM ST1926 up to 48 hours. After each time point (2, 24, 48 hours), cells were collected following the procedure used for western blotting. Liquid nitrogen frozen cell pellets were shipped to the University of Florida Proteomics Core Facility for proteomics analysis.

G. *In vivo* Xenograft Tumor Mouse Model

The experiment was designed to study the effect of ST1926 on tumor growth in U87MG xenografted *Cg-Prkdc*^{scid}*Il2rg*^{tm1Wjl}/SzJ (NSG) mice.

G.1. Mouse model:

The NSG mice are immunodeficient. Their genetic background (NOD/ShiLtJ) is modified to accommodate severe combined immune deficiency (*scid*) and a complete null allele of the *interleukin-2 receptor* (IL2) receptor common gamma chain (*IL2rg*^{null}). The *scid* mutation is in the catalytic subunit of a nuclear DNA-dependent serine/threonine protein kinase (DNA-PK) which is a DNA repair complex protein (*Prkdc)* and renders the mice to become B and T cell deficient. They have also deficient natural killer (NK) cells due to *IL2rg*^{null} mutation that prevents cytokine signaling through multiple receptors. These mutations allow the mice to be humanized by engraftment of human cells without any resistance due to their immunodeficiency. Thus, the immunodeficient NSG mice are suitable models to study the effect of ST1926 on human GBM *in vivo*.

G.2. Xenograft Tumor Procedure:

A total number of 20 NSG mice (both genders) were used with ages ranging between 4 to 6 weeks and with an average mouse weight of 21 gm. The mice were injected with 4 x10^6 U87MG cells/mouse. However, only 14 mice developed palpable tumors after 3 to 4 days. The mice were then distributed into two groups: control *versus* treatment as shown in Table 5.

Group	**Control**		**ST1926 treatment**	
Animals	2 females	5 males	2 females	5 males

Table 5. Groups of NSG mice used in the experiment. Only 14 mice developed palpable tumors.

The mice were treated intraperitoneally with 15 mg/kg body weight (BW) of ST1926 (0.315 mg /dose/mouse) three times per week for four weeks continuously with a total number of 12 doses as described in Table 6. The ST1926 was dissolved in DMSO and then mixed with 90 µl of 10% Cremophor EL/ethanol/PBS. A total of 100 µl per injection were administrated to treated mice. Untreated mice were injected with 100 µl of 10% DMSO dissolved in 10% Cremophor EL/ethanol/PBS. The mice were weighed once a week and tumor volumes were measured twice a week. After 4 weeks, the mice were sacrificed and the tumors were extracted, measured, and stored in 10% formaldehyde for further staining and analysis (see Table 6).

H. Image Processing

Images of control and treated cells were acquired using Leica microscope inverted with camera and fluorescence. Images were assembled using, Photo Impact X3, Microsoft PowerPoint and Word 2010.

I. Statistical Analysis

Statistical analysis was performed using Microsoft Excel 2010. Data presented are the means ± SEM of at least three independent experiments as noted in the figure legends. The significance of the data was analyzed using two-way ANOVA analysis overall, and a Student's t test for the TUNEL results. Statistical significance was reported when the P-value was < 0.05 (*, $P < 0.05$; **, $P < 0.01$; *** $P < 0.001$).

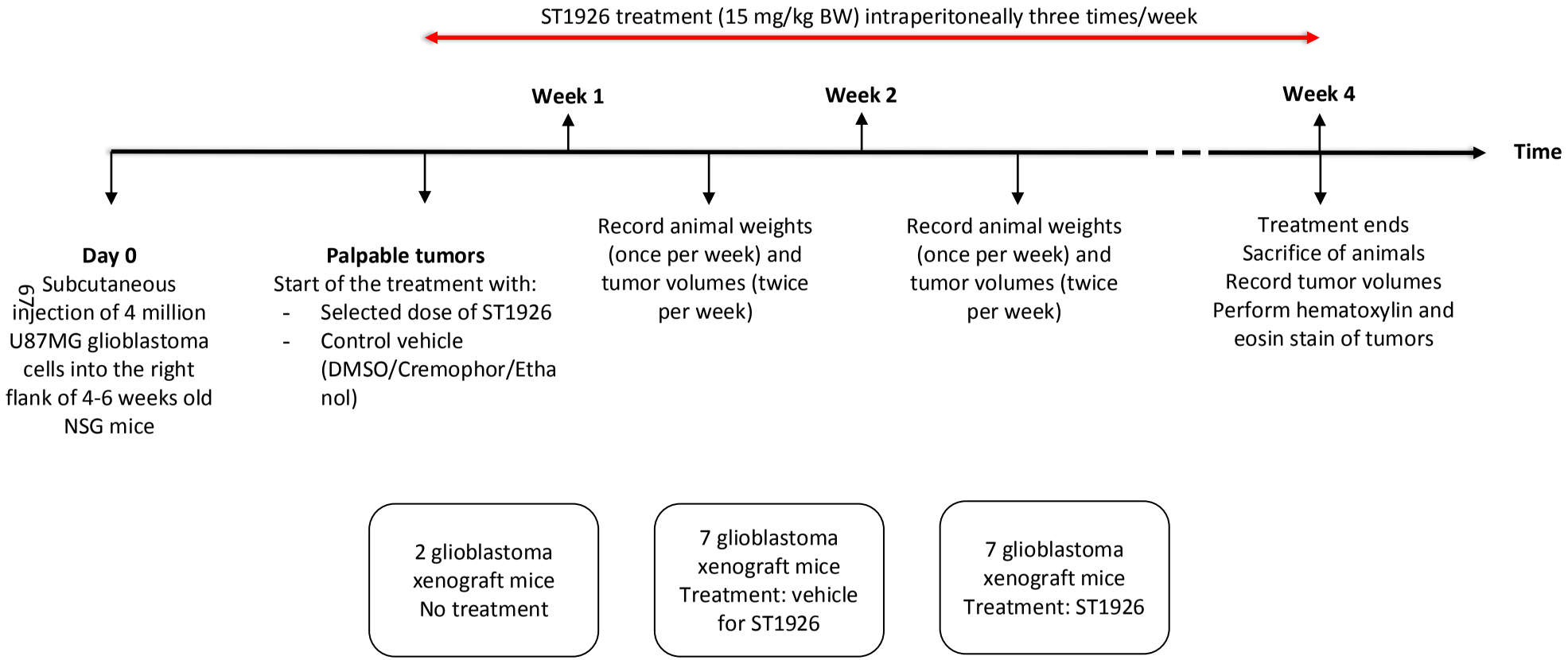

Table 6. Timeline of the in vivo experiment in NSG xenografted GBM models

CHAPTER IV

RESULTS

A. Effect of ST1926 at Various Concentrations on GBM Cell Viability

We first investigated the effect of ST1926 on the cellular growth of different GBM cell lines by the MTT assay. We observed that the viability of the U251, U87MG, U118, and A172 cells was significantly decreased after being treated with different concentrations of ST1926 (Figure 19).

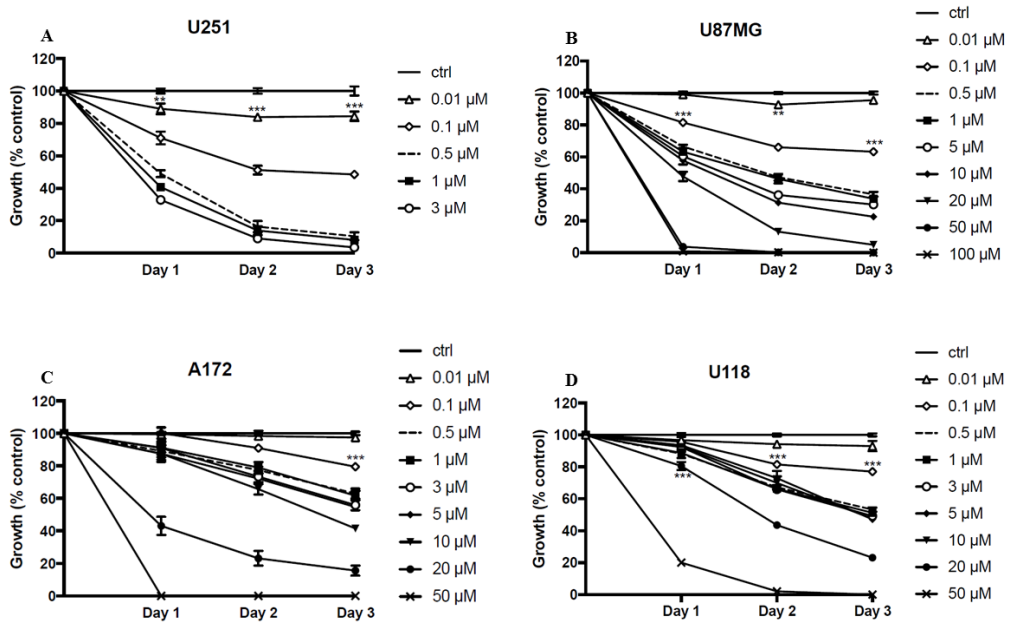

Figure 19. Growth inhibition mediated by ST1926 on human GBM cell lines. Cells were seeded at a density of 5000 cells/well in 96-well plate, treated with series of ST1926 concentrations up to three days. Cell growth assessed with MTT assay. **A:** U251. **B:** U87MG. **C:** A172. **D:** U118. Results are presented as mean ± SEM of three independent experiments, ** $P < 0.01$, *** $P < 0.001$

Interestingly, ST1926 treatment showed a time-dependent growth inhibition in all tested GBM cell lines. Sub-pharmacological concentrations of ST1926 (as low as 0.5 μM) were able to inhibit approximately 50% of cellular growth of U251 cells after 1 day of treatment (Figure 19.A) and of U87MG cells after 2 days (figure 19.B). As for the two other cell lines, higher concentrations of ST1926 were required to reach 50% viability. 20 μM suppressed cellular growth of A172 (Figure 19.A) and of U118 (Figure 19.B) by approximately 50 % after 1 and 2 days, respectively. The low IC_{50} values observed strongly suggests that ST1926 is a potent drug against different types of GBM cell lines (Table 7). Therefore, we decided to proceed with U251 and U87MG since these two cell lines respond to ST1926 treatment at pharmacologically achievable levels at 48 hours.

Cell line	**IC_{50} (μM)**	
	24 hours	**48 hours**
U251	0.5	0.1
U87MG	20	0.5
U118	>20	20
A172	20	10

Table 7. A summary of the IC_{50} of ST1926 in different GBM cell lines obtained from MTT at 24 and 48 hours.

The IC_{50} values in U251 and U87MG were further investigated by trypan blue and SRB assays to verify the obtained viability results by the mean of different viability methods. The two cell lines followed the same trend as in MTT assay. IC_{50} in U251 was verified in both trypan blue (Figure 20) and SRB (Figure 21) assays where 0.5 μM of ST1926 inhibited approximately 50 % of growth after day 1 of treatment. For U87MG, 50 % of viability was inhibited when exposed to 2 days of 0.5 μM ST1926. Moreover, these results were compatible with confluency changes of GBM cells in culture where

cells treated with 0.5 µM of ST1926 showed changes in morphology, growth inhibition, and less confluency compared to control cells (Figure 22).

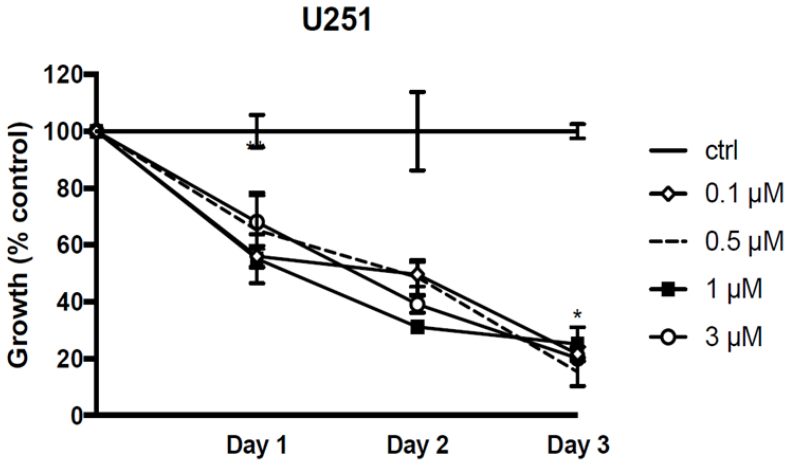

Figure 20. ST1926 effect on U251 obtained by trypan blue exclusion assay. U251 cells were seeded at a density of 5000 cells/well in 96-well plate in triplicates, then treated with series of ST1926 concentrations up to three days. Results presented as mean of one experiment ± SD, *P < 0.05.

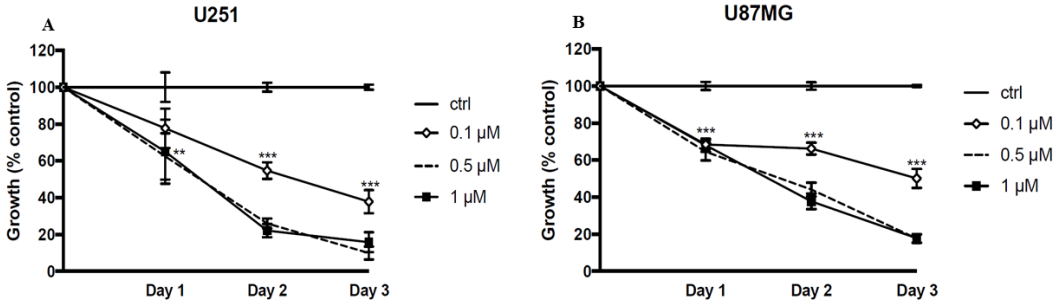

Figure 21. ST1926 effect on U251 obtained by SRB assay. U251 and U87MG cells were seeded at a density of 5000 cells/well in 96-wll plate in triplicates, then treated with series of ST1926 concentrations up to three days. **A**: U251. **B:** U87MG Results presented as mean of three independent experiments ± SEM, **P < 0.01, ***P < 0.001.

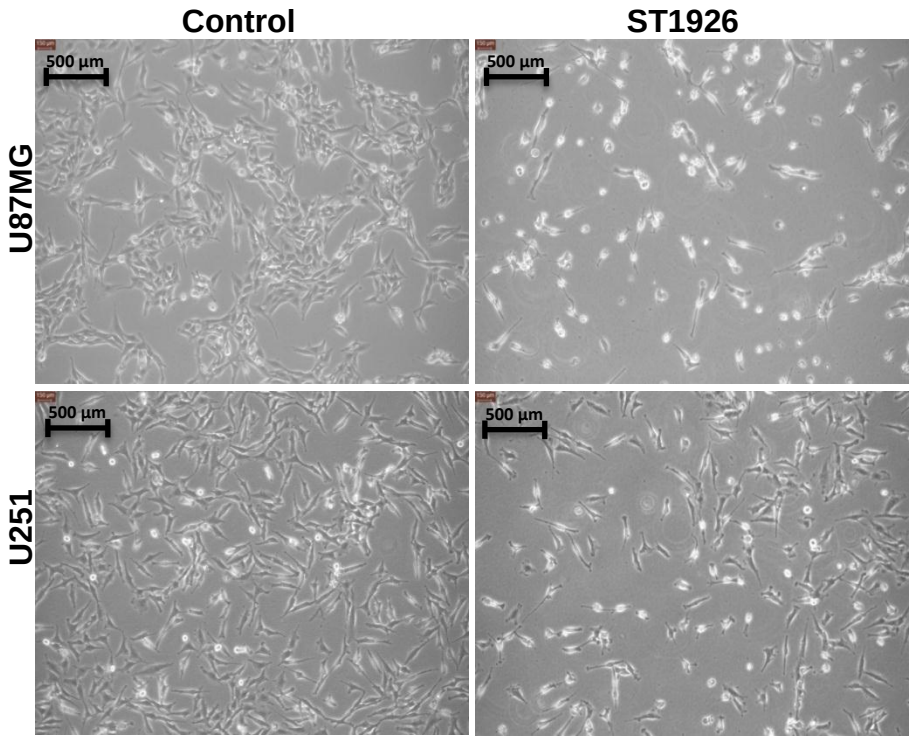

Figure 22. Morphology and confluency of cells before (left) and after (right) 0.5 µM ST1926 treatment. Approximately 50 % cellular growth inhibition (right) after 48 hours for U87MG (up) and after 24 hours for U251 (down) compared to control cells (left) cultured under the same conditions.

B. Elevated POLA1 Expression Levels in GBM

To understand the mechanism of action of ST1926 in GBM, we wanted to investigate the levels of POLA1 in GBM tissues, since previous studies from our laboratory have shown that ST1926 inhibits POLA1 in different cancer types (Abdel-Samad 2018). *In silico* analysis using Oncomine database identified three different studies comparing POLA1 in GBM patient tissues *versus* normal brain counterparts (Shai 2003, Sun 2006, Murat 2008). These studies revealed that GBM tissues have significantly higher *POLA1* expression levels in comparison with normal tissues with a p-value < 0.005 (Figure 23).

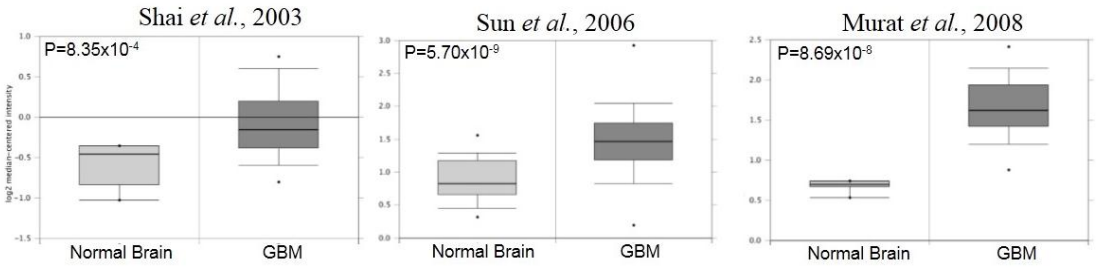

Figure 23. Elevated *POLA1* levels in GBM tissues compared to normal brain tissues. *In silico* analysis identified three different studied that showed elevated *POLA1* expression levels in GBM. Data generated from oncomine.org.

C. ST1926 treatment of GBM Cells Induces Sub-G1 Accumulation and G0/G1 Arrest

To determine the effect of ST1926 on the cell cycle of GBM *in vitro*, we analyzed cell cycle progression by examining cellular DNA content distribution. The cells were treated with 0.5 μM ST1926 up to three days and then stained with propidium iodide. DNA content that reflects the proportion of cells in each phase of the cell cycle was assessed by flow cytometry.

ST1926 resulted in cell accumulation in the sub-G1 phase (Figure 24.A, 25.A). The percentage of U251 cells in the sub-G_1 phase increased from 4% in the control to 7% upon ST1926 treatment for 1 day and reached 13 % and 17% after 2 and 3 days, respectively (Figure 24.B). In addition, ST1926 induced a significant G_0/G_1 cell cycle arrest upon treatment with 0.5 μM ST1926 for all tested time points (Figure 24.C).

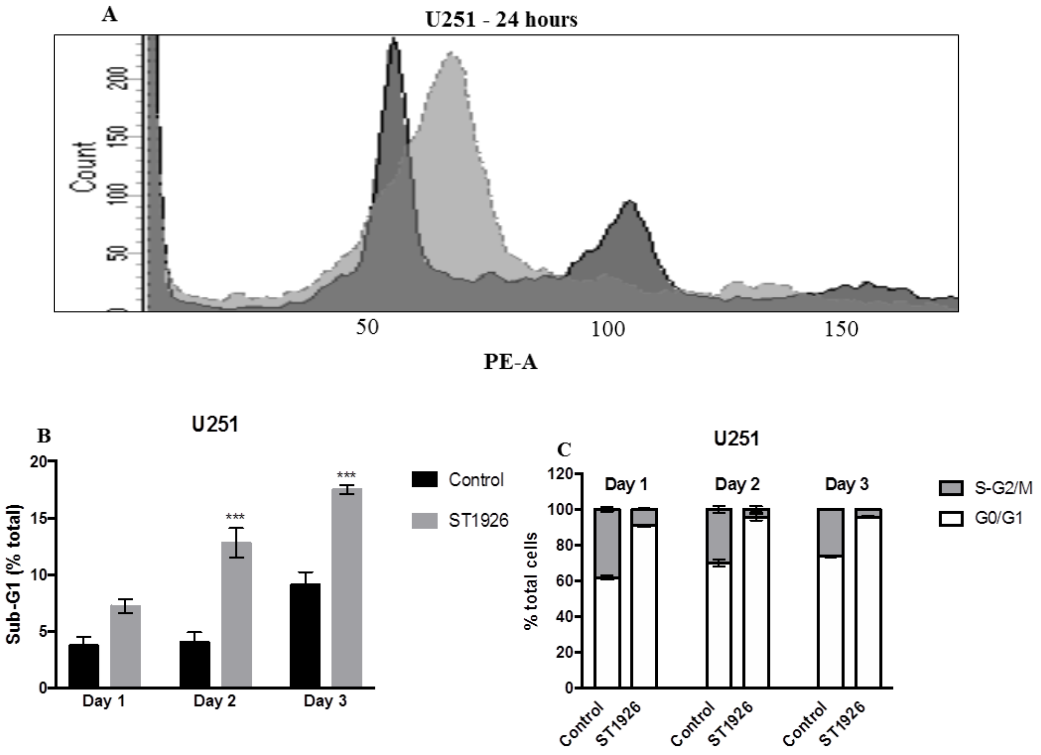

Figure 24. ST1926 treatment induces G0/G1 arrest and sub-G1 accumulation in U251. Cells were seeded at a density of 1 x 10^6 cells/dish in 100 mm culture dish, treated with 0.5 µM ST1926 up to three days. Cells were stained with propidium iodide and quantified by flow cytometry. Analysis was done using BD FACSDiva 8.0. **A:** Representative histogram of U251 cell cycle pre (dark grey) and post ST1926 treatment (light grey). **B:** Quantification of cells in sub-G1 phase up to 3 days. **C:** Quantification of total cell count in the different cell cycle phases. Results presented as mean of 3 independent experiments ± SEM, ***P < 0.001

Similarly, U87MG cell showed an increase in the sub-G1 phase upon 0.5 µM ST1926 treatment for up to three days (Figure 25.A). The percentage of U87MG cells in sub-G1 increased significantly from 10 % in control untreated cells at day 2 to 25 % and 40 % after 2 days and 3 days of ST1926 treatment, respectively (Figure 25.B). G0/G1 arrest was also observed in U87MG upon 0.5 µM ST1926 treatment for up to three days in comparison to control cells cultured under same conditions (Figure 25.C).

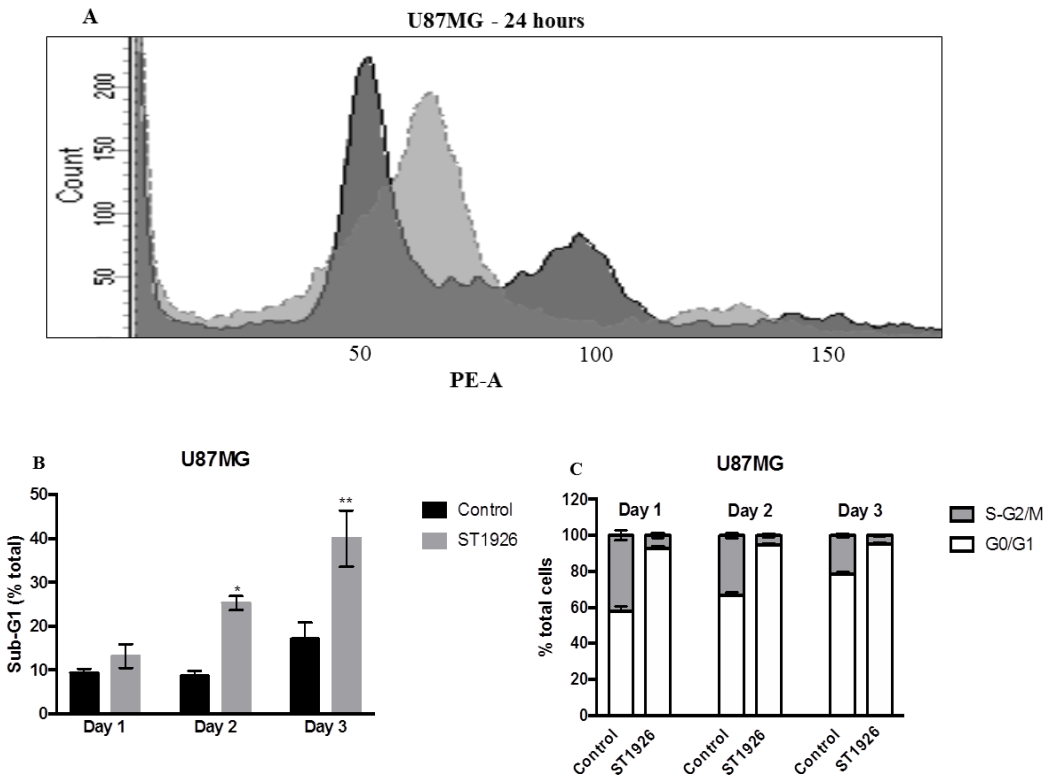

Figure 25. ST1926 induces G0/G1 arrest and sub-G1 accumulation in U87MG. Cells were seeded at a density of 1 x 10^6 cells/dish in 100 mm culture dish, treated with 0.5 μM ST1926 up to three days. Cells were stained with propidium iodide and quantified by flow cytometry. Analysis was done using BD FACSDiva 8.0. **A:** Representative histogram of U87MG cell cycle pre (dark grey) and post ST1926 treatment (light grey). **B:** Quantification of cells in sub-G1 phase up to 3 days. **C:** Quantification of total cell count in the different cell cycle phases. Results presented as mean of at 3 independent experiments ± SEM, *P < 0.05, **P < 0.01.

D. ST1926 Induces Apoptosis in GBM Cell Lines

We showed previously that ST1926 induced GBM cell accumulation in sub-G_1 phase which presumably represents apoptotic cells. To confirm apoptosis induction by ST1926 treatment, we performed a TUNEL assay to detect double stranded DNA cleavage, a hallmark of apoptosis. U251 and U87MG cells were treated with 0.5 μM ST1926. In U251, the percentage of TUNEL-positive cells increased from 3.9% in the control to 9.9 % upon treatment for 2 days. After 3 days of treatment, the percentage of

TUNEL- positive cells significantly increased from 5.9 % in the control to 80.3 % in the treated cells (Figure 26.A, B)). In U87MG cells, the percentage of TUNEL- positive cells increased from 4.8 % in the control to 25 % in the treated cells after day 2. ST1926-induced apoptosis was further observed after day 3 of treatment where the percentage of TUNEL- positive cells significantly increased from 5.6 % in the control to 37.5 % in the treated cells (Figure 26.C, D).

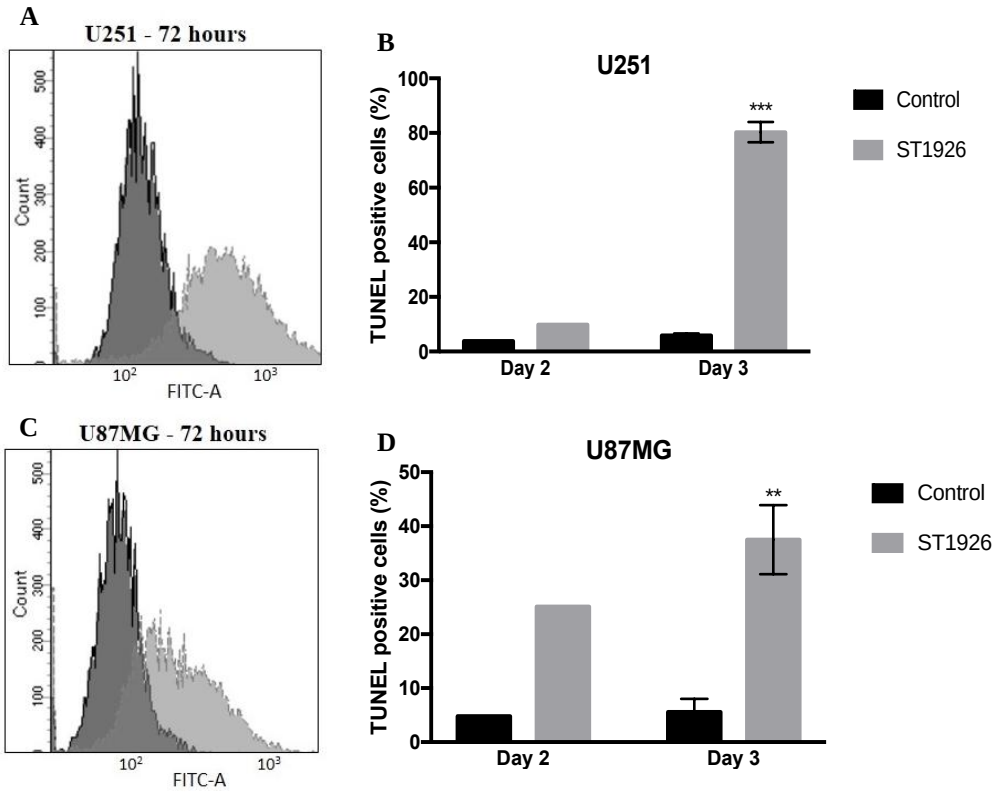

Figure 26. ST1926 induces apoptosis in U251 and U87MG. Cells were seeded at a density of 1 x 10^6 cells/flask in 75 cm^2 culture flask, treated with 0.5 µM ST1926 up to three days. Cells were stained with TUNEL reaction mixture and quantified by flow cytometry. Analysis was done using BD FACSDiva 8.0. **A, B:** U251. **C, D:** U87MG. **A, C:** Representative histogram of the shift from control cells (dark grey) into TUNEL-positive ST1926 treated cells (light grey) of U251 (A) and U87MG(C), respectively. **B, D:** Quantification of TUNEL positive cells in control and ST1926 treated U251(B) and U87MG (D) cells, respectively. Results for day 2 present as one experiment, day 3 presented as mean of three independent experiments ± SEM, **P < 0.01, ***P < 0.001

E. ST1926 Promotes PARP Cleavage Along with DNA Damage To investigate whether ST1926-induced-apoptosis in GBM cell lines is caspase-dependent, we explored caspase activation and cleavage of PARP as an indication of caspase-dependent apoptosis through western blotting. For this aim, proteins were extracted from control and ST1926 (0.5 μM) treated U251 and U87MG cells up to 48 hours. Immunoblotting against PARP (113 kD) showed an increase in PARP cleavage (death-associated fragment - 89 kD), and ultimately reached a full PARP cleavage at 48 hours in both investigated cell lines (Figure 27). We also wanted to determine the effect of ST1926 on the DNA. Therefore, we incubated the nitrocellulose membranes with γ-H2AX antibodies. We observed elevated levels of γ-H2AX in a time-dependent manner

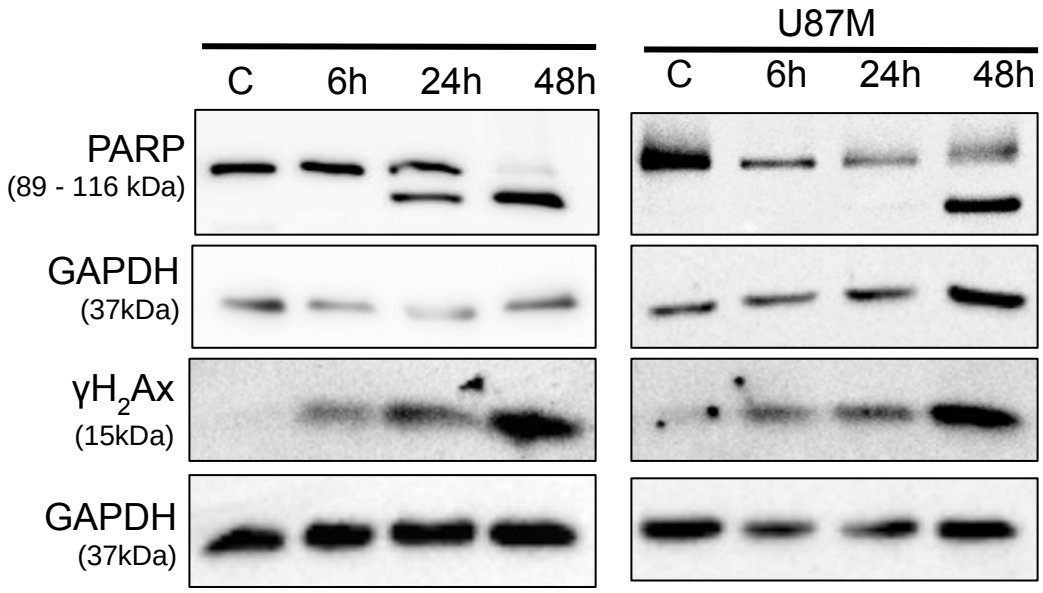

Figure 27. ST1926 promotes PARP cleavage with increased γ-H2AX levels in GBM cells. U251and U87MG cells were seeded in 100 mm culture dish at a density of 1 x 10^6 cells/plate and treated with 0.5 μM ST1926 up to 48 hours. Whole SDS lysates (150 μg/lane and 50 μg/lane) were prepared and immunoblotted against PARP and γ-H2AX antibody. Blots were re-probed with GAPDH antibody to ensure equal protein loading. Blots are representative of three independent experiments.
(Figure 27).

F. ST1926 Induces Early DNA Damage in GBM Cell Lines

To determine how early the ST1926-induced DNA damage started, we extracted proteins from U251, U87MG, and U118 cells after being treated with 0.5 μM ST1926 for 2, 6, 24, and 48 hours. Using western blot, we probed for γH2AX antibody. Results revealed that ST1926 induced a slight increase in γH2AX in all GBM cell types as early as 2 hours post-treatment (Figure 28). This indicates that ST1926 is inducing early DNA damage in GBM-treated cell lines.

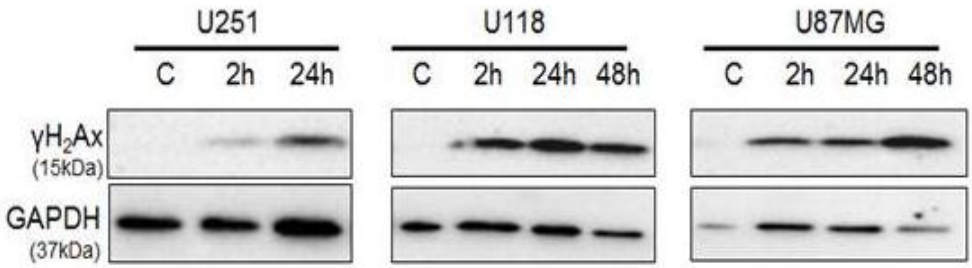

Figure 28. ST1926 causes early DNA damage in human GBM cancer cells. U251, U118, and U87MG were seeded in 100 mm culture dish at a density of 1 x 10^6 cells/plate and treated with 0.5 μM ST1926 up to 48 hours. Whole SDS lysates (30 μg/lane) were prepared and immunoblotted against γ-H2AX antibody. Blots were re-probed with GAPDH antibody to ensure equal protein loading.

G. ST1926 Decreases POLA1 Levels in GBM *in vitro*

ST1926 was shown to mediate its antitumor activities through DNA damage induction, mainly by inhibiting POLA1 activity in cancer cells, and since POLA1 levels were shown to be elevated in GBM tissues, we evaluated the effect of ST1926 on POLA1 protein levels. Therefore, U251 and U87MG cells were seeded and treated according to the procedure described earlier for western blotting. Immunoblotting against POLA1, showed decreased levels of POLA1 protein as early as 6 hours post ST1926 treatment which is a clear indication of ST1926-induced inhibition of DNA replication (Figure 29).

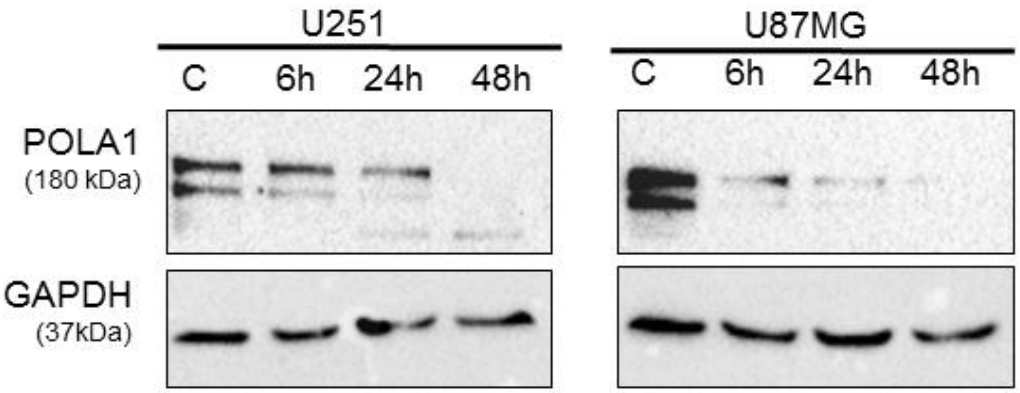

Figure 29. ST1926 reduces POLA1 protein levels in GBM cell lines. U251 and U87MG were seeded in 100 mm culture plates at a density of 1 x 10^6 cells/plate and treated with 0.5 μM ST1926 up to 48 hours. Whole SDS lysates (50 μg/lane) were prepared and immunoblotted against POLA1. Blots were re-probed with GAPDH antibody to ensure equal protein loading. Blots are representative of three independent experiments.

H. ST1926 Suppresses Tumor Growth in GBM xenografts

The potent growth suppressive and proapoptotic activities in GBM *in vitro models*, suggest that ST1926 could be a promising therapeutic approach to be considered *in vivo* in xenograft GBM models. Therefore, we evaluated the activities of ST1926 using the NSG mouse model inoculation with U87MG cells in the flank. We assessed ST1926 effect by measuring tumor volumes of mice treated with ST1926. Tumor volumes increased with time in both control and ST1926 treated mice. However, mice treated with ST1926 showed a reduction but not significant in tumor growth (Figure 30).

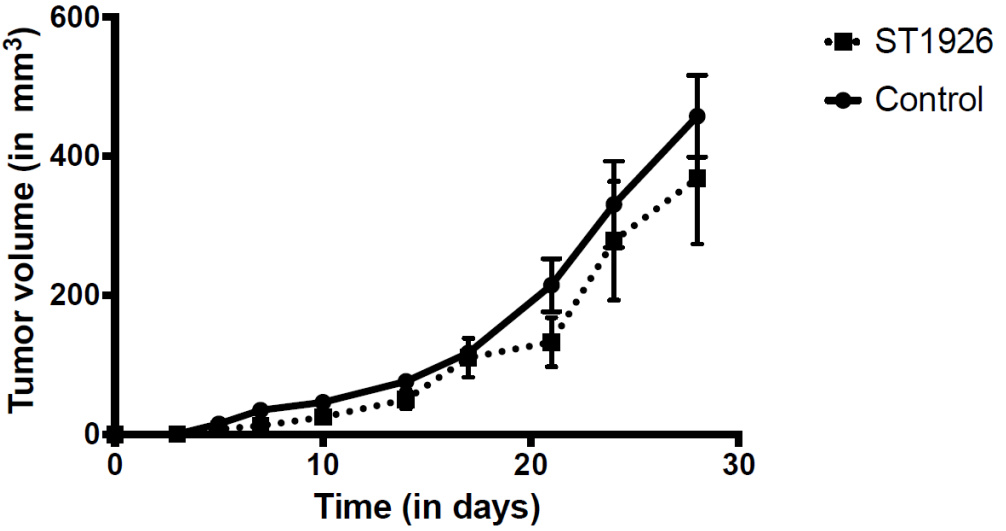

Figure 30. ST1926 delays tumor growth in GBM xenograft NSG mouse model. NSG mice were injected with 4 x 10^6 U87MG cells/mouse, treated with 15 mg/kg ST1926 intraperitoneally three times/week. Tumor volumes were measured twice a week. Mice in control group treated with the vehicle of ST1926. N=7/group

CHAPTER V

DISCUSSION

Despite relentless efforts to develop new therapies and improve the survival rates of most cancer patients of different cancer types, patients with GBM still suffer from low survival rates and poor quality of life. Due to the complexity of GBM, patients are not easily amenable to current advanced therapies resulting in aggressive recurrence, treatment-resistant relapse and rapid surrender to the tumor. Thus, devising efficient and safe therapeutic strategies is urgently needed. Retinoids, vitamin A and its natural analogues have been used as chemotherapeutics and chemopreventive agents (Fu 2012, Das 2014, Khalil 2017) since they have displayed antitumor effects mainly by suppressing cell growth and stimulating cell differentiation and cell death (Sakoe 2010). However, the use of natural retinoids in clinical trials is hindered due to their limited efficacy (Ortiz 2002) and undesirable side effects (Garattini 2014) resulting in sub-optimal clinical results. This is influenced by many factors mainly that natural retinoids are accompanied with rapid metabolism and attenuated signaling due to mutations in retinoid receptor signaling pathway which force the cancer cells to develop resistance to retinoid therapy (Tang 2011, Garattini 2014, Schenk 2014). To overcome these obstacles, there was a necessity to develop new compounds (Ortiz 2002). One of these compounds is the promising adamantyl synthetic retinoid ST1926 (Cincinelli 2003), that displayed a favorable pharmacokinetic profile in comparison to its parental CD437compound (Garattini 2004). ST1926 has shown potent anti-tumor effects in several *in vitro* and *in vivo* cancer models, including tumor growth inhibition in ovarian carcinoma (Zuco 2004, Zuco 2010), neuroblastoma (Di Francesco 2007, Di Francesco

2012), ATL (El Hajj 2014), CML (Nasr 2015), rhabdomyosarcoma (Basma 2016), AML (El-Houjeiri 2017), breast (Aouad 2017) and prostate cancers (Bahmad HF 2019) independently of RAR and *p53* signaling pathways (Cincinelli 2003).

Based on the promising anti-tumor actions of ST1926, investigating the effect of ST1926 on GBM models, may offer new insights that can be translated into novel and efficient therapeutic opportunities for patients with GBM. First, we investigated the effect of ST1926 on the viability of GBM *in vitro* models. The intra-tumor heterogeneity and the molecular traits of each cell line draw different patterns for the therapeutic decision-making (Campos 2016). Since these cell lines have different genetic backgrounds, they responded differently to ST1926. For instance, all tested cell lines have in common several molecular traits mainly wild type *IDH*. Patients with tumors that have *IDH* mutated gene have better outcome than those with wild type gene (Yan 2009), since mutant *IDH* can be used as a target for therapeutic intervention. In addition, these cell lines have different *p53* status. U251 and U118 have mutated *p53*, while U87MG and A172 have a wild type *p53* gene (Giakoumettis 2018). Tumor cells with mutated *p53* tend to survive radiation therapy and patients with such tumors relapse in a short period of time (Yang 2020). In our study, ST1926 induced cell death independently of *p53* status which was also established in CRC (Abdel-Samad 2018), Rhabdomyosarcoma (Basma 2016), ovarian carcinoma (Zuco 2004) and breast cancer (Aouad 2017). Both U87MG and U251 have methylated *MGMT* (Oh 2017), but different EGFR levels (Giakoumettis 2018). Researchers have shown that the diversity in cancer cells, in genetic and epigenetic alterations (Guo 2019), and in germline and somatic mutations (He 2013, Yan 2017) result in polymorphism in genes encoding for drug-metabolizing enzymes, the transporters, drug targets, drug binding sites, and

disease-related genes. Put together, these alterations cooperate to alter drug sensitivity (Juan-Blanco 2018) and cells response to treatment. Hence, complete understanding of genetic and epigenetic heterogeneity of GBM cells may contribute in understanding the intricate interplay between GBM cell lines used in our study and ST1926 molecule. This may reveal the mechanism of action of ST1926 in GBM cells, and explain the variability in cell response to different concentrations and exposure time to ST1926.

In a recent study by De Liu *et al*., that was published while writing this thesis, researchers tested ST1926 on several GBM cell lines including U87MG and U251, the IC_{50} was achieved at higher concentrations of ST1926 when evaluated by MTT assay (De 2020). This can be due to two possible explanations, either the cells were cultured and treated under other conditions including different cell confluencies or passages. Importantly, this latter study also tested ST1926 on normal human astrocytes, showing that ST1926 treatments at concentrations as high as 10 μM displayed no significant cytotoxicity, nor changed the morphology or induced excessive ROS production in normal human astrocytes. Hence, these findings indicate that only glioma cells were sensitive to ST1926 and not their normal counterparts (De 2020).

Previous studies from our laboratory showed that ST1926 inhibits cell growth mainly by targeting POLA1 and thus suppressing cellular proliferation (Abdel-Samad 2018). Performing *in silico* analysis revealed that *POLA1* expression levels are elevated in tissues derived from patients with GBM compared to normal brain tissues (Shai 2003, Sun 2006, Murat 2008). This indicates that POLA1 in GBM is an attractive target for ST1926.

Cell cycle analysis revealed a prominent accumulation of cells in the sub-G_1 phase which is presumably a pro-apoptotic region, as reported in other types of ST1926-

treated cancer cells (Zuco 2004, Zuco 2010, El Hajj 2014, Nasr 2015, Basma 2016, Aouad 2017, Abdel-Samad 2018, Karam 2018). In addition, it was shown that, prior to apoptosis induction, ST1926 causes G_0/G_1 cell cycle arrest. ST1926 affects the cell cycle in other cancer types differently, mainly by inducing S-phase arrest such as in breast cancer, rhabdomyosarcoma, and CRC cells (Basma 2016, Aouad 2017, Abdel-Samad 2018), or by causing G_1 arrest as in ovarian carcinoma (Zuco 2010), G_1/S arrest as in lung carcinoma (Zuco 2005) and G_2/M arrest as for neuroblastoma cells (Di Francesco 2012). The perturbation in cell cycle progression induced by ST1926, explains the reduction in cell growth and viability.

To confirm apoptosis in the tested GBM cell lines upon ST1926 treatment, we performed TUNEL assay to detect DNA DSBs as an indicator of late apoptotic event. Results showed that 0.5 µM ST1926 induced massive DNA fragmentation in U251 and U87MG. Using western blot, this was further approved by elevated levels of γH2AX and PARP cleavage upon ST1926 treatment. Knowing that γH2AX is the standard for DNA DSBs, upregulation of γH2AX expression levels as early as two hours post-ST1926 treatment, we emphasize that 0.5 µM ST1926 induces early DNA damage that triggers cell death. PARP is the key protein that first responds to DNA DSBs (Pascal 2018) and plays a major role in repairing DNA damage (Dantzer 1999, Dantzer 2000), a process required for normal cellular functioning and survival. In case of apoptosis, a highly specialized family of cystein-aspartate proteases (caspases) acts as signaling cascades. Once activated, these caspases initiate cell death by activating and cleaving several proteins that drive the process of apoptosis (Fischer 2003). PARP is one of these substrates that are cleaved and inactivated by caspases and its cleavage is considered as a hallmark of apoptosis (Kaufmann 1993, Tewari 1995). Cleavage of PARP leads to

loss of its catalytic activity and may prevent depletion of ATP which is required for apoptosis (Fischer 2003). Almost all caspases are known to modify PARP *in vitro* (Lazebnik 1994) while caspase-3 and caspase-7 are shown to cleave PARP *in vivo* (Lazebnik 1994, Margolin 1997). The cleavage mediated by these caspases yields an 85-89 kDa PARP fragment (Lazebnik 1994, Chaitanya 2010) which was observed in our study. In brain tumors, especially gliomas, caspase-3 is the one implicated in PARP cleavage (Bhaskara 2005, Bhaskara 2009). Based on these facts, we conclude that 0.5 µM ST1926 inhibits cellular growth in U251 and U87MG by inducing DNA damage that precedes a caspase-3-dependent apoptosis. This finding is consistent with similar studies that examined the effect of ST1926 in different cancer types (Aouad 2017, Abdel-Samad 2018, Karam 2018, Bahmad HF 2019). It remains to be determined by the use of caspase inhibitors whether ST1926-induced cell death is caspase-dependent.

Next, we examined the effect of ST1926 on POLA1 protein levels, since ST1926 was shown to exert its anti-tumor effect through POLA1 inhibition (Abdel-Samad 2018). POLA1 is the initiator of eukaryotic DNA replication which is pursued later on by other polymerases (Muzi-Falconi 2003). The parental molecule of ST1926, CD437 was shown to target POLA1 and thus preventing cellular proliferation (Han 2016). Similarly to CD437, ST1926 was shown to reduce the protein levels and inhibit the activity of POLA1 in a concentration-dependent manner (Abdel-Samad 2018). Since POLA1 is overexpressed in GBM, it is a pertinent molecular feature and an attractive target for ST1926. Performing western blotting revealed that 0.5 µM ST1926 reduced POLA1 levels in both U251 and U87MG in a time-dependent manner. This was complemented with reduced cell viability and induced cell death.

To test the susceptibility of GBM cells to undergo apoptosis via the extrinsic or the intrinsic pathway upon ST1926 treatment, we probed for Bcl2 proteins that bind to the outer membrane of the mitochondria and regulate the release of cytochrome c, a central event in apoptosis (Raisova 2001, Kiraz 2016). The relative amount of apoptosis-promoting and apoptosis-inhibiting signals is determined by the ratio of Bax/Bcl2 proteins. The interaction of these proteins among others determines whether a cell lives or dies (Westphal 2013) and the imbalance in Bax/Bcl2 ratio triggers apoptosis (Singh 2015). Depending on this ratio, we can assess the ability of drugs to induce apoptosis and the sensitivity of cells to respond to the treatment (Raisova 2001). Released cytochrome c enters the cytosol, binds to apoptotic proteases, and activates a caspase cascade that in turn leads to apoptosis. This is the intrinsic pathway for apoptosis (Enari 1996). Using the antibodies that were presented in the method part, we could not detect any bands for neither Bax or Bcl2, although both U251 (Liang 2019) and U87MG cells (Shi 2010) express these proteins. We are currently optimizing the blotting protocol and trying other antibodies. We are looking forward to further investigations of the anti-tumor effect of ST1926 in GBM on the angiogenesis of the tumor by evaluating the levels of VEGF and HIF-1α, two major proteins that determine the prognosis of GBM upon ST1926 treatment.

To assess ST1926 efficacy *in vivo,* U87MG cells were inoculated in the flank of NSG xenografted mouse model. Injection of 15 mg/kg of ST1926 three times a week resulted in a reduction of the tumor size. However this reduction is not statistically significant to consider the treatment regimen sufficient for treating GBM. ST1926 have shown promising effects in several solid and liquid tumor models as well as in xenograft models (Karam 2018). Treatment with ST1926 inhibited tumor growth, reduced the size

of the tumor and prolonged survival in various tumor xenograft models (El Hajj 2014, El-Houjeiri 2017, Abdel-Samad 2018, Bahmad HF 2019). The treatment regimen in these studies differs from our study either in dosage, in the duration of the experiment, or in the administration mode and period. Thus, more optimization is needed to achieve significant effects on GBM tumors, in particular daily administration. De Liu *et al.*tested another GBM cell line with different ST1926 treatment regimen *in vivo*. ST1926 also reduced KI-67, a protein that is strongly associated with tumor aggressiveness and proliferation with few side effects.

Several areas of research should be performed to test the impact of ST1926 on the invasion of GBM cell lines by performing migration assay and the involvement of RAR signaling in the mechanism of ST1926 in GBM should be explored further. We are awaiting for the proteomic analysis results which will open up new research areas to identify other mediators in the mechanism of action of ST1926 in GBM. De Liu *et al*. described another mechanism of action of ST1926 in GBM which involves the mitochondria. According to their study, ST1926 significantly impairs complex II function, thus reduces ATP production and promotes the production of reactive oxygen species which leads to apoptosis (De 2020). Together with our findings, we conclude that ST1926 is potent anti GBM drug that attacks tumor cells and mediates cell death from different aspects.

A. Future Perspectives

One of the major obstacles facing drug development against GBM is the drug delivery across the BBB. Despite its hydrophobic properties and the relatively low molecular weight (374.5 g/mol) (Dréan 2016), ST1926 possesses a hydrophilic end (carboxyl group) that may deter its passage through the BBB to ultimately reach GBM tumor inside the brain. To test whether ST1926 will cross the BBB, we plan to perform a biomimetic *in vitro* BBB model, in collaboration with the laboratory of Dr. Marwan El Sabban. GBM cells will be co-cultured with astrocytes and endothelial cells in culture wells with semipermeable membrane. This apparatus will be inserted in a well plate, in order to simulate the BBB *in vitro* (Figure 31). The endothelium with astrocytes will create a barrier between the drug and the GBM cells, where its tightness will be measured by transendothelial electrical resistance (TEER). After adding ST1926, the effect on GBM will be detected and the concentration of ST1926 passing the semipermeable membrane to the well will be determined by liquid chromatography with fluorimetric detection at 330 nm (Basma *et al.* 2015).

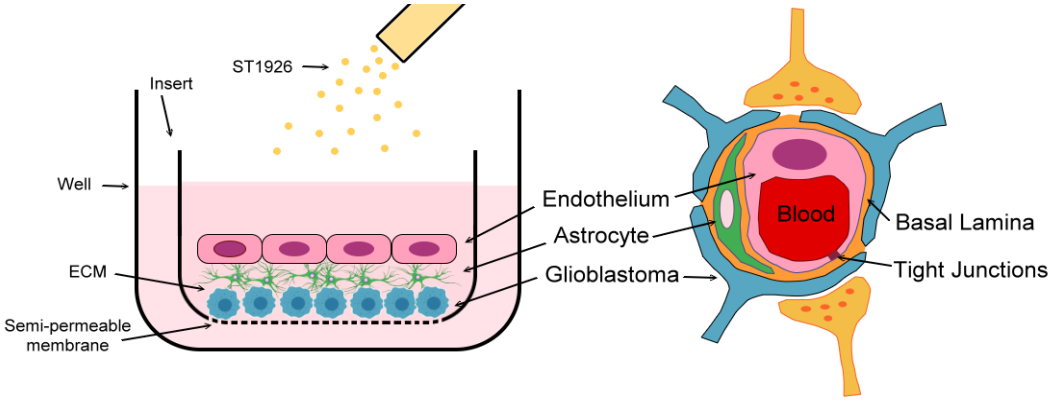

Figure 31. Schematic description of the biomimetic in vitro BBB which will be conducted in collaboration with Dr. Marwan El Sabban´s laboratory.

Recently, several new strategies are competing to improve drug delivery, mainly nanomedicine. Nanomedicine has gained widespread attention especially in cancer therapy as it enables more efficient tumor targeting, enhances bioavailability, and increases drug stability with lower toxicity (Tong 2016). In case ST1926 does not cross the BBB, we suggest nanoparticle formulation of ST1926, since it was shown to improve its bioavailability and had the ability to reduce the tumor burden at lower concentrations compared to the naked drug (El-Houjeiri 2017).

For better mimicking the GBM microenvironment, we propose to develop an orthotopic GBM mouse model in which we plan to inoculate the mouse brain with GBM cell lines at 2-3 mm to the right of the bregma and the sagittal suture, and 1 mm anterior to the coronal suture (Kratzsch 2018). The cell suspension should be injected in a speed of 3 µl over one minute in order to insure that the tumor grows in the correct location in the brain (Figure 32). When these mice start to develop tumors, ST1926 will be administrated and tumor volume and animal survival will be determined.

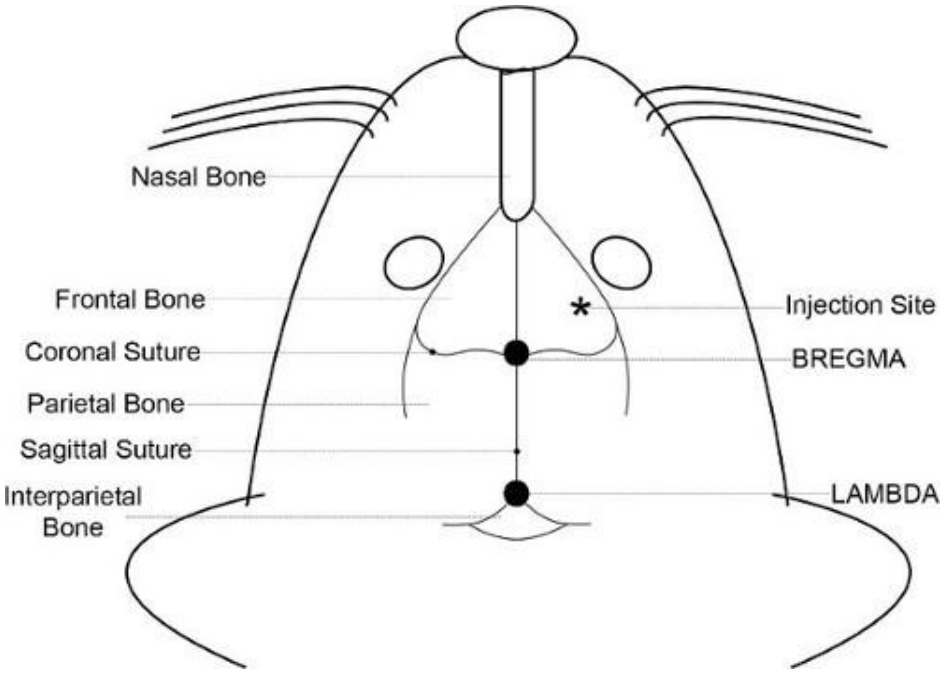

Figure 32. Scheme over the procedure of the orthotopic xenograft model. Procedure and figure adopted from: https://www.jove.com/video/52017/creating-anatomically-accurate-reproducible intracranial-xenografts

B. Limitations

Working on this project was challenging and we faced several limitations. As a new project, experiments demanded optimization and thus needed to be conducted several independent times in order to find the best protocol and to get significant results. Proteomic analysis would offer thorough information about different players in this mechanism. However, due to the current situation, samples were shipped to the USA but are still not processed yet.

On a different note, it would be more representative if we had GBM cell lines from different genders, as sexual differences would affect the response to treatment. GBM cell line with different *IDH* status would uncover if there is any role for IDH in the mechanism of action of ST1926.

C. Conclusion

In our study, we examined the anti-tumor effect of ST1926 in GBM both *in vitro* and *in vivo* and investigated its mechanism of action. We showed that ST1926 is a potent drug that inhibits cellular growth of several GBM cell lines at submicromolar concentrations with IC_{50} values of 0.5 µM, while higher concentrations did not affect their normal counterparts (De 2020). ST1926 slightly reduced tumor size in GBM xenograft models without traces of any toxicity in the mouse model. Mechanistically, ST1926 affects the DNA, induces DSB which leads to elevated γH2AX and inhibits PARP-mediated DNA repair (Figure 33. A). Furthermore, ST1926 reduces POLA1 levels, which were found to be highly expressed in GBM compared to normal brain tissues (Figure 33. B). The suggested treatment leads to G_0/G_1 cellcycle arrest and cell accumulation in the presumably apoptotic sub-G1 phase (Figure 33.C). ST1926-mediated cell death in GBM cells occurs by inducing a caspase-3 apoptosis, independently of *p53* status.

With our findings and further research, we hope to repurpose ST1926 in clinical trials for patients with GBM and provide patients with better quality of life and prolonged lifespan.

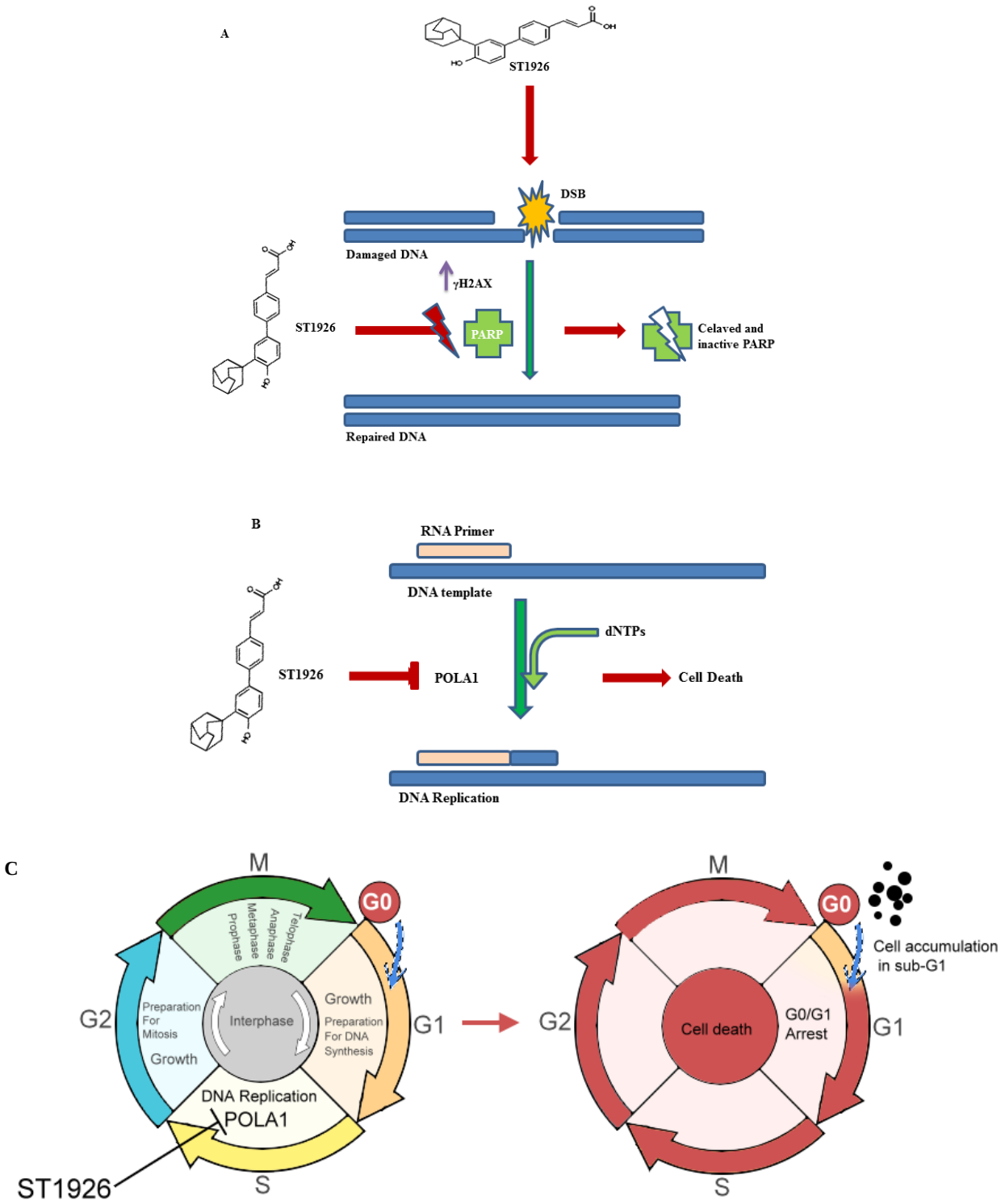

Figure 33. Summary of the mechanism of action of ST1926 in GBM. **A:** ST1926 induces DSB which leads to elevated levels of γH2AX. PARP is cleaved and inactivated in response to ST1926 treatment. **B:** ST1926 inhibits POLA1 in DNA synthesis and thus obstructs DNA replication and cell proliferation. **C:** Inhibition of POLA1 lead to G_0/G_1 cell cycle arrest and cell accumulation in the sub-G1 phase causing cell cycle arrest and apoptosis in GBM cells.

REFERENCES

1. Abbott, N. J., A. A. K. Patabendige, D. E. M. Dolman, S. R. Yusof and D. J. Begley (2010). "Structure and function of the blood–brain barrier." Neurobiology of Disease **37**(1): 13-25.
2. Abbott, N. J., L. Rönnbäck and E. Hansson (2006). "Astrocyte–endothelial interactions at the blood–brain barrier." Nature Reviews Neuroscience **7**(1): 41-53.
3. Abdel-Samad, R., P. Aouad and N. Darwiche (2019). "Natural and synthetic retinoids in preclinical colorectal cancer models." Anticancer Drugs **30**(7): e0802.
4. Abdel-Samad, R., P. Aouad, H. Gali-Muhtasib, Z. Sweidan, R. Hmadi, H. Kadara, E. L. D'Andrea, A. Fucci, C. Pisano and N. Darwiche (2018). "Mechanism of action of the atypical retinoid ST1926 in colorectal cancer: DNA damage and DNA polymerase alpha." Am J Cancer Res **8**(1): 39-55.
5. Abdulkareem, I. H., & Blair, M. (2013). "Phosphatase and tensin homologue deleted on chromosome 10." Nigerian medical journal : journal of the Nigeria Medical Association **54(2)**: 79–86.
6. Agnihotri, S., K. D. Aldape and G. Zadeh (2014). "Isocitrate dehydrogenase status and molecular subclasses of glioma and glioblastoma." Neurosurg Focus **37**(6): E13.
7. Alizadeh, F., A. Bolhassani, A. Khavari, S. Z. Bathaie, T. Naji and S. A. Bidgoli (2014). "Retinoids and their biological effects against cancer." Int Immunopharmacol **18**(1): 43-49.
8. Allen Perkins, G. L. (2016). "Primary Brain Tumors in Adults." Am Fam Physician **1;93(3)**: 211-217B.
9. Alvarez, S., P. Germain, R. Alvarez, F. Rodriguez-Barrios, H. Gronemeyer and A. R. de Lera (2007). "Structure, function and modulation of retinoic acid receptor beta, a tumor suppressor." Int J Biochem Cell Biol **39**(7-8): 1406-1415.
10. Aouad, P., M. Saikali, R. Abdel-Samad, S. Fostok, L. El-Houjeiri, C. Pisano, R. Talhouk and N. Darwiche (2017). "Antitumor activities of the synthetic retinoid ST1926 in two-dimensional and three-dimensional human breast cancer models." Anticancer Drugs **28**(7): 757-770.
11. Armocida, D., A. Pesce, A. Frati, A. Santoro and M. Salvati (2019). "EGFR amplification is a real independent prognostic impact factor between young adults and adults over 45yo with wild-type glioblastoma?" Journal of Neuro-Oncology **146**(2): 275-284.
12. Armstrong, J. L., S. Martin, N. A. Illingworth, D. Jamieson, A. Neilson, P. E. Lovat, C. P. Redfern and G. J. Veal (2012). "The impact of retinoic acid treatment on the sensitivity of neuroblastoma cells to fenretinide." Oncol Rep **27**(1): 293-298.
13. Arrizabalaga, O., L. Moreno-Cugnon, J. Auzmendi-Iriarte, P. Aldaz, I. Ibanez de Caceres, L. Garros-Regulez, V. Moncho-Amor, S. Torres-Bayona, O. Pernía, L. Pintado-Berninches, P. Carrasco-Ramirez, M. Cortes-Sempere, R. Rosas, P. Sanchez-Gomez, I. Ruiz, H. Caren, S. Pollard, I. Garcia, A.-A. Sacido, R. Lovell-Badge, C. Belda-Iniesta, N. Sampron, R. Perona and A. Matheu (2017).

"High expression of MKP1/DUSP1 counteracts glioma stem cell activity and mediates HDAC inhibitor response." Oncogenesis **6**(12).
14. Asson-Batres, M. A., C. Rochette-Egly and SpringerLink (2014). The Biochemistry of Retinoic Acid Receptors I: Structure, Activation, and Function at the Molecular Level. Dordrecht, Springer Netherlands.
15. Atlas, T. H. P. "https://v15.proteinatlas.org/ENSG00000101868-POLA1/cell/CAB012274."
16. Bahmad HF, S. H., Monzer A, Hadadeh O, Cheaito K, Abdel-Samad R, Hayar B, Pisano C, Msheik H, Liu YN, Darwiche N, Abou-Kheir W (2019). "The synthetic retinoid ST1926 attenuates prostate cancer growth and potentially targets prostate cancer stem-like cells." Mol Carcinog **58(7)**: 1208-1220.
17. Basma, H., S. E. Ghayad, G. Rammal, A. Mancinelli, M. Harajly, F. Ghamloush, L. Dweik, R. El-Eit, H. Zalzali, W. Rabeh, C. Pisano, N. Darwiche and R. Saab (2016). "The synthetic retinoid ST1926 as a novel therapeutic agent in rhabdomyosarcoma." International Journal of Cancer **138**(6): 1528-1537.
18. Bernard, B. A., J. M. Bernardon, C. Delescluse, B. Martin, M. C. Lenoir, J. Maignan, B. Charpentier, W. R. Pilgrim, U. Reichert and B. Shroot (1992). "Identification of synthetic retinoids with selectivity for human nuclear retinoic acid receptor gamma." Biochem Biophys Res Commun **186**(2): 977-983.
19. Bhaskara, V. K., S. Challa, M. Panigrahi and P. P. Babu (2009). "Differential PARP cleavage: an indication for existence of multiple forms of cell death in human gliomas." Neurol India **57**(3): 264-268.
20. Bhaskara, V. K., M. Panigrahi, S. Challa and P. P. Babu (2005). "Comparative status of activated ERK1/2 and PARP cleavage in human gliomas." Neuropathology **25**(1): 48-53.
21. Bhatia, V., M. M. Goel, A. Makker, S. Tewari, A. Yadu, P. Shilpi, S. Kumar, S. P. Agarwal and S. K. Goel (2014). "Promoter Region Hypermethylation and mRNA Expression ofMGMTandp16Genes in Tissue and Blood Samples of Human Premalignant Oral Lesions and Oral Squamous Cell Carcinoma." BioMed Research International **2014**: 1-10.
22. Breitman, T. R., S. J. Collins and B. R. Keene (1981). "Terminal differentiation of human promyelocytic leukemic cells in primary culture in response to retinoic acid." Blood **57**(6): 1000-1004.
23. Brem, S., & Abdullah, K. G. (2017). "Glioblastoma." Philadelphia, PA: Elsevier.
24. Brennan, C. W., R. G. Verhaak, A. McKenna, B. Campos, H. Noushmehr, S. R. Salama, S. Zheng, D. Chakravarty, J. Z. Sanborn, S. H. Berman, R. Beroukhim, B. Bernard, C. J. Wu, G. Genovese, I. Shmulevich, J. Barnholtz-Sloan, L. Zou, R. Vegesna, S. A. Shukla, G. Ciriello, W. K. Yung, W. Zhang, C. Sougnez, T. Mikkelsen, K. Aldape, D. D. Bigner, E. G. Van Meir, M. Prados, A. Sloan, K. L. Black, J. Eschbacher, G. Finocchiaro, W. Friedman, D. W. Andrews, A. Guha, M. Iacocca, B. P. O'Neill, G. Foltz, J. Myers, D. J. Weisenberger, R. Penny, R. Kucherlapati, C. M. Perou, D. N. Hayes, R. Gibbs, M. Marra, G. B. Mills, E. Lander, P. Spellman, R. Wilson, C. Sander, J. Weinstein, M. Meyerson, S. Gabriel, P. W. Laird, D. Haussler, G. Getz and L. Chin (2013). "The somatic genomic landscape of glioblastoma." Cell **155**(2): 462-477.
25. Cairns, R. A. and T. W. Mak (2013). "Oncogenic Isocitrate Dehydrogenase Mutations: Mechanisms, Models, and Clinical Opportunities." Cancer Discovery **3**(7): 730-741.

26. Campos, B., L. R. Olsen, T. Urup and H. S. Poulsen (2016). "A comprehensive profile of recurrent glioblastoma." Oncogene **35**(45): 5819-5825.
27. Chaitanya, G. V., A. J. Steven and P. P. Babu (2010). "PARP-1 cleavage fragments: signatures of cell-death proteases in neurodegeneration." Cell Commun Signal **8**: 31.
28. Chakravarty, D., A. M. Pedraza, J. Cotari, A. H. Liu, D. Punko, A. Kokroo, J. T. Huse, G. Altan-Bonnet and C. W. Brennan (2017). "EGFR and PDGFRA co-expression and heterodimerization in glioblastoma tumor sphere lines." Scientific Reports **7**(1).
29. Chen, H., M. Chidboy and J. F. Robinson (2020). "Retinoids and Developmental Neurotoxicity: utilizing toxicogenomics to enhance adverse outcome pathways and testing strategies." Reprod Toxicol.
30. Chen, W., S. Zhao, W. Zhu, L. Wu and X. Chen (2019). "Retinoids as an Immunity-modulator in Dermatology Disorders." Arch Immunol Ther Exp (Warsz) **67**(6): 355-365.
31. Chen, Y.-F., P.-C. Shih, H.-M. Kuo, S.-N. Yang, Y.-Y. Lin, W.-F. Chen, S.-J. Tzou, H.-T. Liu and N.-F. Chen (2020). "TP3, an antimicrobial peptide, inhibits infiltration and motility of glioblastoma cells via modulating the tumor microenvironment." Cancer Medicine.
32. Chen, Y.-J., P. Li, X. Zhang, L. Gu, J. Zhou and D. Deng (2019). "P16 methylation increases the sensitivity of cancer cells to the CDK4/6 inhibitor palbociclib." Plos One **14**(10): e0223084.
33. Cheng, S.-Y., N.-F. Chen, P.-Y. Lin, J.-H. Su, B.-H. Chen, H.-M. Kuo, C.-S. Sung, P.-J. Sung, Z.-H. Wen and W.-F. Chen (2019). "Anti-Invasion and Antiangiogenic Effects of Stellettin B through Inhibition of the Akt/Girdin Signaling Pathway and VEGF in Glioblastoma Cells." Cancers **11**(2): 220.
34. Choschzick, I., E. Hirseland, H. Cramer, S. Schultz, J. Leppert, V. Tronnier and C. Zechel (2014). "Responsiveness of stem-like human glioma cells to all-trans retinoic acid and requirement of retinoic acid receptor isotypes alpha, beta and gamma." Neuroscience **279**: 44-64.
35. Cincinelli, R., S. Dallavalle, L. Merlini, S. Penco, C. Pisano, P. Carminati, G. Giannini, L. Vesci, C. Gaetano, B. Illy, V. Zuco, R. Supino and F. Zunino (2003). "A Novel Atypical Retinoid Endowed with Proapoptotic and Antitumor Activity." Journal of Medicinal Chemistry **46**(6): 909-912.
36. Clark, M. J., N. Homer, B. D. O'Connor, Z. Chen, A. Eskin, H. Lee, B. Merriman and S. F. Nelson (2010). "U87MG decoded: the genomic sequence of a cytogenetically aberrant human cancer cell line." PLoS Genet **6**(1): e1000832.
37. Clark, O., K. Yen and I. K. Mellinghoff (2016). "Molecular Pathways: Isocitrate Dehydrogenase Mutations in Cancer." Clinical Cancer Research **22**(8): 1837-1842.
38. Daneman, R. and A. Prat (2015). "The Blood–Brain Barrier." Cold Spring Harbor Perspectives in Biology **7**(1): a020412.
39. Daniel, P. M., G. Filiz, M. J. Tymms, R. G. Ramsay, A. H. Kaye, S. S. Stylli and T. Mantamadiotis (2018). "Intratumor MAPK and PI3K signaling pathway heterogeneity in glioblastoma tissue correlates with CREB signaling and distinct target gene signatures." Experimental and Molecular Pathology **105**(1): 23-31.
40. Dantzer, F., G. de La Rubia, J. Ménissier-De Murcia, Z. Hostomsky, G. de Murcia and V. Schreiber (2000). "Base excision repair is impaired in

mammalian cells lacking Poly(ADP-ribose) polymerase-1." Biochemistry **39**(25): 7559-7569.
41. Dantzer, F., V. Schreiber, C. Niedergang, C. Trucco, E. Flatter, G. De La Rubia, J. Oliver, V. Rolli, J. Ménissier-de Murcia and G. de Murcia (1999). "Involvement of poly(ADP-ribose) polymerase in base excision repair." Biochimie **81**(1-2): 69-75.
42. Das, A., Banik, N. L., & Ray, S. K. (2010). "Glioblastoma: Molecular Mechanisms of Pathogenesis and Current Therapeutic Strategies. In S. K. Ray (Ed.), Retinoids for the treatment of glioblastoma." New York: Springer: 265–281.
43. Das, B. C., P. Thapa, R. Karki, S. Das, S. Mahapatra, T. C. Liu, I. Torregroza, D. P. Wallace, S. Kambhampati, P. Van Veldhuizen, A. Verma, S. K. Ray and T. Evans (2014). "Retinoic acid signaling pathways in development and diseases." Bioorg Med Chem **22**(2): 673-683.
44. Davis, M. (2016). "Glioblastoma: Overview of Disease and Treatment." Clinical Journal of Oncology Nursing **20**(5): S2-S8.
45. De Bonis, P., C. Anile, A. Pompucci, A. Fiorentino, M. Balducci, S. Chiesa, G. Maira and A. Mangiola (2012). "Safety and efficacy of Gliadel wafers for newly diagnosed and recurrent glioblastoma." Acta Neurochir (Wien) **154**(8): 1371-1378.
46. De, L., T. Yuan and Z. Yong (2020). "ST1926 inhibits glioma progression through regulating mitochondrial complex II." Biomed Pharmacother **128**: 110291.
47. De Nunzio, G., H. M. Fathallah-Shaykh, A. DeAtkine, E. Coffee, E. Khayat, A. K. Bag, X. Han, P. P. Warren, M. Bredel, J. Fiveash, J. Markert, N. Bouaynaya and L. B. Nabors (2019). "Diagnosing growth in low-grade gliomas with and without longitudinal volume measurements: A retrospective observational study." PLOS Medicine **16**(5): e1002810.
48. de The, H. and Z. Chen (2010). "Acute promyelocytic leukaemia: novel insights into the mechanisms of cure." Nat Rev Cancer **10**(11): 775-783.
49. Deanna Glass-Macenka, L. H., Ashley Varner, Erica Weiss, Patrick Y. Wen (2013). "Understanding Brain Tumors_Chapter 2." Cancer Support Commuinty, National Brain Tumor Society, http://braintumor.org.
50. Di Francesco, A. M., D. Meco, A. R. Torella, G. Barone, M. D'Incalci, C. Pisano, P. Carminati and R. Riccardi (2007). "The novel atypical retinoid ST1926 is active in ATRA resistant neuroblastoma cells acting by a different mechanism." Biochem Pharmacol **73**(5): 643-655.
51. Di Francesco, A. M., P. Ubezio, A. R. Torella, D. Meco, F. Pierri, G. Barone, G. Cusano, C. Pisano, M. D'Incalci and R. Riccardi (2012). "Enhanced cell cycle perturbation and apoptosis mediate the synergistic effects of ST1926 and ATRA in neuroblastoma preclinical models." Invest New Drugs **30**(4): 1319-1330.
52. di Masi, A., L. Leboffe, E. De Marinis, F. Pagano, L. Cicconi, C. Rochette-Egly, F. Lo-Coco, P. Ascenzi and C. Nervi (2015). "Retinoic acid receptors: From molecular mechanisms to cancer therapy." Molecular Aspects of Medicine **41**: 1-115.
53. Dillard, A. C. and M. A. Lane (2008). "Retinol Increases beta-catenin-RXRalpha binding leading to the increased proteasomal degradation of beta-catenin and RXRalpha." Nutr Cancer **60**(1): 97-108.

54. Dréan, A., L. Goldwirt, M. Verreault, M. Canney, C. Schmitt, J. Guehennec, J. Y. Delattre, A. Carpentier and A. Idbaih (2016). "Blood-brain barrier, cytotoxic chemotherapies and glioblastoma." Expert Rev Neurother **16**(11): 1285-1300.
55. Du, Z. and C. M. Lovly (2018). "Mechanisms of receptor tyrosine kinase activation in cancer." Molecular Cancer **17**(1).
56. Eder, K. and B. Kalman (2014). "Molecular Heterogeneity of Glioblastoma and its Clinical Relevance." Pathology & Oncology Research **20**(4): 777-787.
57. El-Houjeiri, L., W. Saad, B. Hayar, P. Aouad, N. Tawil, R. Abdel-Samad, R. Hleihel, M. Hamie, A. Mancinelli, C. Pisano, H. El Hajj and N. Darwiche (2017). "Antitumor Effect of the Atypical Retinoid ST1926 in Acute Myeloid Leukemia and Nanoparticle Formulation Prolongs Lifespan and Reduces Tumor Burden of Xenograft Mice." Mol Cancer Ther **16**(10): 2047-2057.
58. El Hajj, H., B. Khalil, B. Ghandour, R. Nasr, S. Shahine, A. Ghantous, R. Abdel-Samad, A. Sinjab, H. Hasegawa, M. Jabbour, W. W. Hall, G. Zaatari, G. Dbaibo, C. Pisano, A. Bazarbachi and N. Darwiche (2014). "Preclinical efficacy of the synthetic retinoid ST1926 for treating adult T-cell leukemia/lymphoma." Blood **124**(13): 2072-2080.
59. Ellor, S. V., T. A. Pagano-Young and N. G. Avgeropoulos (2014). "Glioblastoma: Background, Standard Treatment Paradigms, and Supportive Care Considerations." The Journal of Law, Medicine & Ethics **42**(2): 171-182.
60. Enari, M., R. V. Talanian, W. W. Wong and S. Nagata (1996). "Sequential activation of ICE-like and CPP32-like proteases during Fas-mediated apoptosis." Nature **380**(6576): 723-726.
61. Fan, Y. Y., T. E. Spencer, N. Wang, M. P. Moyer and R. S. Chapkin (2003). "Chemopreventive n-3 fatty acids activate RXRalpha in colonocytes." Carcinogenesis **24**(9): 1541-1548.
62. Fischer, U., R. U. Jänicke and K. Schulze-Osthoff (2003). "Many cuts to ruin: a comprehensive update of caspase substrates." Cell Death Differ **10**(1): 76-100.
63. Fontana, J. A. and A. K. Rishi (2002). "Classical and novel retinoids: their targets in cancer therapy." Leukemia **16**(4): 463-472.
64. Fratelli, M., J. N. Fisher, G. Paroni, A. M. Di Francesco, F. Pierri, C. Pisano, K. Godl, S. Marx, A. Tebbe, C. Valli, M. Gianni, M. Stravalaci, M. Gobbi, M. Terao and E. Garattini (2013). "New insights into the molecular mechanisms underlying sensitivity/resistance to the atypical retinoid ST1926 in acute myeloid leukaemia cells: the role of histone H2A.Z, cAMP-dependent protein kinase A and the proteasome." Eur J Cancer **49**(6): 1491-1500.
65. Fu, Y. S., Q. Wang, J. X. Ma, X. H. Yang, M. L. Wu, K. L. Zhang, Q. Y. Kong, X. Y. Chen, Y. Sun, N. N. Chen, X. H. Shu, H. Li and J. Liu (2012). "CRABP-II methylation: a critical determinant of retinoic acid resistance of medulloblastoma cells." Mol Oncol **6**(1): 48-61.
66. Garattini, E., M. Bolis, S. K. Garattini, M. Fratelli, F. Centritto, G. Paroni, M. Gianni, A. Zanetti, A. Pagani, J. N. Fisher, A. Zambelli and M. Terao (2014). "Retinoids and breast cancer: from basic studies to the clinic and back again." Cancer Treat Rev **40**(6): 739-749.
67. Garattini, E., E. Parrella, L. Diomede, M. Gianni, Y. Kalac, L. Merlini, D. Simoni, R. Zanier, F. F. Ferrara, I. Chiarucci, P. Carminati, M. Terao and C. Pisano (2004). "ST1926, a novel and orally active retinoid-related molecule

inducing apoptosis in myeloid leukemia cells: modulation of intracellular calcium homeostasis." Blood **103**(1): 194-207.
68. Geng, Y., L. Kohli, B. J. Klocke and K. A. Roth (2010). "Chloroquine-induced autophagic vacuole accumulation and cell death in glioma cells is p53 independent." Neuro Oncol **12**(5): 473-481.
69. Gersey, Z., A. D. Osiason, L. Bloom, S. Shah, J. W. Thompson, A. Bregy, N. Agarwal and R. J. Komotar (2019). "Therapeutic Targeting of the Notch Pathway in Glioblastoma Multiforme." World Neurosurg **131**: 252-263 e252.
70. Giakoumettis, D., A. Kritis and N. Foroglou (2018). "C6 cell line: the gold standard in glioma research." Hippokratia **22**(3): 105-112.
71. Giese, A., R. Bjerkvig, M. E. Berens and M. Westphal (2003). "Cost of migration: invasion of malignant gliomas and implications for treatment." J Clin Oncol **21**(8): 1624-1636.
72. Goodenberger, M. L. and R. B. Jenkins (2012). "Genetics of adult glioma." Cancer Genetics **205**(12): 613-621.
73. Graham, T. A. and A. Sottoriva (2017). "Measuring cancer evolution from the genome." The Journal of Pathology **241**(2): 183-191.
74. Groothuis, D. R. (2000). "The blood-brain and blood-tumor barriers: a review of strategies for increasing drug delivery." Neuro Oncol **2**(1): 45-59.
75. Guillamón-Vivancos, T., U. Gómez-Pinedo and J. Matías-Guiu (2015). "Astrocytes in neurodegenerative diseases (I): function and molecular description." Neurología (English Edition) **30**(2): 119-129.
76. Guo, M., Y. Peng, A. Gao, C. Du and J. G. Herman (2019). "Epigenetic heterogeneity in cancer." Biomark Res **7**: 23.
77. Hahn, W. C., Counter, C.M, Lundberg, A.S, Beijersbgern, R.L, Brooks, M.W, Weinberg, R.A (1999). "Creation of human tumor cells with defined genetic elements." Nature **400**: 464-468.
78. Han, T., M. Goralski, E. Capota, S. B. Padrick, J. Kim, Y. Xie and D. Nijhawan (2016). "The antitumor toxin CD437 is a direct inhibitor of DNA polymerase α." Nature Chemical Biology **12**(7): 511-515.
79. Hanahan, D. and R. A. Weinberg (2000). "The Hallmarks of Cancer." Cell **Volume 100**(Issue 1): Pages 57-70.
80. Hanahan, D. and Robert A. Weinberg (2011). "Hallmarks of Cancer: The Next Generation." Cell **144**(5): 646-674.
81. He, N., N. Kim and S. Yoon (2013). "Somatic mutation patterns and compound response in cancers." BMB Rep **46**(2): 97-102.
82. Heisterkamp, N., C. Morris, L. Sender, E. Knoppel, L. Uribe, M. Y. Cui and J. Groffen (1990). "Rearrangement of the human ABL oncogene in a glioblastoma." Cancer Res **50**(11): 3429-3434.
83. Ichimura, K., D. M. Pearson, S. Kocialkowski, L. M. Bäcklund, R. Chan, D. T. Jones and V. P. Collins (2009). "IDH1 mutations are present in the majority of common adult gliomas but rare in primary glioblastomas." Neuro Oncol **11**(4): 341-347.
84. Ip, C. K. M., P. K. S. Ng, K. J. Jeong, S. H. Shao, Z. Ju, P. G. Leonard, X. Hua, C. P. Vellano, R. Woessner, N. Sahni, K. L. Scott and G. B. Mills (2018). "Neomorphic PDGFRA extracellular domain driver mutations are resistant to PDGFRA targeted therapies." Nature Communications **9**(1).

85. Jaime Gállego Pérez-Larraya, J. H. (2014). "Chapter 77 - Brain metastases." Handbook of Clinical Neurology, Elsevier **Volume 121**: Pages 1143-1157.
86. Jiang, H., H. Gao, J. Kong, B. Song, P. Wang, B. Shi, H. Wang and Z. Li (2018). "Selective Targeting of Glioblastoma with EGFRvIII/EGFR Bitargeted Chimeric Antigen Receptor T Cell." Cancer Immunology Research **6**(11): 1314-1326.
87. Jovčevska, I. (2018). "Sequencing the next generation of glioblastomas." Critical Reviews in Clinical Laboratory Sciences **55**(4): 264-282.
88. Juan-Blanco, T., M. Duran-Frigola and P. Aloy (2018). "Rationalizing Drug Response in Cancer Cell Lines." J Mol Biol **430**(18 Pt A): 3016-3027.
89. Kaminska, B., B. Czapski, R. Guzik, S. Król and B. Gielniewski (2019). "Consequences of IDH1/2 Mutations in Gliomas and an Assessment of Inhibitors Targeting Mutated IDH Proteins." Molecules **24**(5): 968.
90. Kang, E. M., A. A. Yin, Y. L. He, W. J. Chen, A. Etcheverry, M. Aubry, J. Barnholtz-Sloan, J. Mosser, W. Zhang and X. Zhang (2019). "A five-CpG signature of microRNA methylation in non-G-CIMP glioblastoma." CNS Neuroscience & Therapeutics **25**(9): 937-950.
91. Karam, L., B. Houshaymi, R. Abdel-Samad, M. Jaafar, I. Halloum, C. Pisano, F. Neipel, N. Darwiche and R. Abou Merhi (2018). "Antitumor activity of the synthetic retinoid ST1926 on primary effusion lymphoma in vitro and in vivo models." Oncol Rep **39**(2): 721-730.
92. Kaufmann, S. H., S. Desnoyers, Y. Ottaviano, N. E. Davidson and G. G. Poirier (1993). "Specific proteolytic cleavage of poly(ADP-ribose) polymerase: an early marker of chemotherapy-induced apoptosis." Cancer Res **53**(17): 3976-3985.
93. Kelman, Z., J. Hurwitz and M. O'Donnell (1998). "Processivity of DNA polymerases: two mechanisms, one goal." Structure **6**(2): 121-125.
94. Khalil, S., T. Bardawil, C. Stephan, N. Darwiche, O. Abbas, A. G. Kibbi, G. Nemer and M. Kurban (2017). "Retinoids: a journey from the molecular structures and mechanisms of action to clinical uses in dermatology and adverse effects." J Dermatolog Treat **28**(8): 684-696.
95. Kinzler, K. W. V., **B** (1996). "Lessons from hereditary colorectal cancer." Cell **87**: 159-170.
96. Kiraz, Y., A. Adan, M. Kartal Yandim and Y. Baran (2016). "Major apoptotic mechanisms and genes involved in apoptosis." Tumour Biol **37**(7): 8471-8486.
97. Kratzsch, T., S. A. Kuhn, A. Joedicke, U. K. Hanisch, P. Vajkoczy, J. Hoffmann and I. Fichtner (2018). "Treatment with 5-azacitidine delay growth of glioblastoma xenografts: a potential new treatment approach for glioblastomas." Journal of Cancer Research and Clinical Oncology **144**(5): 809-819.
98. Krell, A., M. Wolter, N. Stojcheva, C. Hertler, F. Liesenberg, M. Zapatka, M. Weller, B. Malzkorn and G. Reifenberger (2019). "MiR-16-5p is frequently down-regulated in astrocytic gliomas and modulates glioma cell proliferation, apoptosis and response to cytotoxic therapy." Neuropathol Appl Neurobiol **45**(5): 441-458.
99. Kunishio, K., K. Matsumoto, H. Higashi, H. Adachi, T. Tamiya, T. Furuta and T. Ohmoto (1999). "Proliferative potential of malignant glioma cells before and after interstitial brachytherapy." Neurol Med Chir (Tokyo) **39**(5): 341-349.
100. Kunishio, K., N. Mishima, T. Matsuhisa, K. Tsuno, N. Matsumi, T. Satoh, K. Matsumoto, T. Furuta, A. Nishimoto and T. Shiraishi (1990).

"Immunohistochemical demonstration of DNA polymerase alpha in human brain-tumor cells." J Neurosurg **72**(2): 268-272.
101. Lau, D., S. T. Magill and M. K. Aghi (2014). "Molecularly targeted therapies for recurrent glioblastoma: current and future targets." Neurosurgical Focus **37**(6): E15.
102. Laws, E. R., Jr. and K. Thapar (1993). "Brain tumors." CA Cancer J Clin **43**(5): 263-271.
103. Lazebnik, Y. A., S. H. Kaufmann, S. Desnoyers, G. G. Poirier and W. C. Earnshaw (1994). "Cleavage of poly(ADP-ribose) polymerase by a proteinase with properties like ICE." Nature **371**(6495): 346-347.
104. Le Rhun, E., M. Preusser, P. Roth, D. A. Reardon, M. van den Bent, P. Wen, G. Reifenberger and M. Weller (2019). "Molecular targeted therapy of glioblastoma." Cancer Treatment Reviews **80**: 101896.
105. Lee, C. Y. (2017). "Strategies of temozolomide in future glioblastoma treatment." Onco Targets Ther **10**: 265-270.
106. Lefebvre, P., Y. Benomar and B. Staels (2010). "Retinoid X receptors: common heterodimerization partners with distinct functions." Trends in Endocrinology & Metabolism **21**(11): 676-683.
107. Li J1, T. Z., Goyal A2, Gonda D2, Akers J2, Adhikari B2, Patel K2, Vandenberg S3, Yan W4, Bao Z4, Carter BS2, Wang R5, Mao Y6, Jiang T4, Chen CC (2014). "Epigenetic suppression of EGFR signaling in G-CIMP+ glioblastoma." Oncotarget **Vol. 5**(No. 17): 7342-7356.
108. Liang, J., N. Liu and H. Xin (2019). "Knockdown long non-coding RNA PEG10 inhibits proliferation, migration and invasion of glioma cell line U251 by regulating miR-506." General physiology and biophysics **38**(04): 295-304.
109. Louis, D. N., Ohgaki, H., Wiestler, O. D., Cavenee, W. K., Burger, P. C., Jouvet, A., Scheithauer, B. W., & Kleihues (2007). "The 2007 WHO Classifcation of Tumours in CNS." Acta neuropathologica **114(2)**: 97–109.
110. Madala, H., S. Punganuru, V. Arutla, S. Misra, T. Thomas and K. Srivenugopal (2018). "Beyond Brooding on Oncometabolic Havoc in IDH-Mutant Gliomas and AML: Current and Future Therapeutic Strategies." Cancers **10**(2): 49.
111. Maden, M. (2002). "Retinoid signalling in the development of the central nervous system." Nat Rev Neurosci **3**(11): 843-853.
112. Maden, M. (2007). "Retinoic acid in the development, regeneration and maintenance of the nervous system." Nat Rev Neurosci **8**(10): 755-765.
113. Manor, D., E. N. Shmidt, A. Budhu, A. Flesken-Nikitin, M. Zgola, R. Page, A. Y. Nikitin and N. Noy (2003). "Mammary carcinoma suppression by cellular retinoic acid binding protein-II." Cancer Res **63**(15): 4426-4433.
114. Margolin, N., S. A. Raybuck, K. P. Wilson, W. Chen, T. Fox, Y. Gu and D. J. Livingston (1997). "Substrate and inhibitor specificity of interleukin-1 beta-converting enzyme and related caspases." J Biol Chem **272**(11): 7223-7228.
115. Mawson, A. (2012). "Retinoids in the treatment of glioma: a new perspective." Cancer Management and Research: 233.
116. McCormick, F. (1999). "Signaling networks that cause cancer." Trends in Cell Biology **Volume 9**(Issue 12): Pages M53-M56.
117. Medikonda, R., G. Dunn, M. Rahman, P. Fecci and M. Lim (2020). "A review of glioblastoma immunotherapy." Journal of Neuro-Oncology.

118. Mesti, T. and J. Ocvirk (2016). "Malignant gliomas: old and new systemic treatment approaches." **50**(2): 129.
119. Murat, A., E. Migliavacca, T. Gorlia, W. L. Lambiv, T. Shay, M. F. Hamou, N. de Tribolet, L. Regli, W. Wick, M. C. Kouwenhoven, J. A. Hainfellner, F. L. Heppner, P. Y. Dietrich, Y. Zimmer, J. G. Cairncross, R. C. Janzer, E. Domany, M. Delorenzi, R. Stupp and M. E. Hegi (2008). "Stem cell-related "self-renewal" signature and high epidermal growth factor receptor expression associated with resistance to concomitant chemoradiotherapy in glioblastoma." J Clin Oncol **26**(18): 3015-3024.
120. Muzi-Falconi, M., M. Giannattasio, M. Foiani and P. Plevani (2003). "The DNA polymerase alpha-primase complex: multiple functions and interactions." ScientificWorldJournal **3**: 21-33.
121. Nasr, R. R., R. A. Hmadi, R. M. El-Eit, A. N. Iskandarani, M. N. Jabbour, G. S. Zaatari, F. X. Mahon, C. C. Pisano and N. D. Darwiche (2015). "ST1926, an orally active synthetic retinoid, induces apoptosis in chronic myeloid leukemia cells and prolongs survival in a murine model." Int J Cancer **137**(3): 698-709.
122. Niederhuber, E, J. armitage, O, J. doroshow, J. kastan, B, M. tepper and J. E (2020). Abeloff's Clinical Oncology E-Book. US, Elsevier.
123. Nikiforova, M. N. and R. L. Hamilton (2011). "Molecular diagnostics of gliomas." Arch Pathol Lab Med **135**(5): 558-568.
124. Niu, C. S., M. W. Li, Y. F. Ni, J. M. Chen, J. M. Mei, J. Li and X. M. Fu (2010). "Effect of all-trans retinoic acid on the proliferation and differentiation of brain tumor stem cells." J Exp Clin Cancer Res **29**: 113.
125. Nørøxe, D. S., H. S. Poulsen and U. Lassen (2016). "Hallmarks of glioblastoma: a systematic review." ESMO Open **1**(6): e000144.
126. O'Byrne, S. M. and W. S. Blaner (2013). "Retinol and retinyl esters: biochemistry and physiology." J Lipid Res **54**(7): 1731-1743.
127. Oh, S. J., J. I. Yang, O. Kim, E. J. Ahn, W. D. Kang, J. H. Lee, K. S. Moon, K. H. Lee and D. Cho (2017). "Human U87 glioblastoma cells with stemness features display enhanced sensitivity to natural killer cell cytotoxicity through altered expression of NKG2D ligand." Cancer Cell Int **17**: 22.
128. Ohgaki, H. and P. Kleihues (2007). "Genetic Pathways to Primary and Secondary Glioblastoma." The American Journal of Pathology **170**(5): 1445-1453.
129. Ortiz, M. A., Y. Bayon, F. J. Lopez-Hernandez and F. J. Piedrafita (2002). "Retinoids in combination therapies for the treatment of cancer: mechanisms and perspectives." Drug Resist Updat **5**(3-4): 162-175.
130. Oscar-Berman, M., B. Shagrin, D. L. Evert and C. Epstein (1997). "Impairments of brain and behavior: the neurological effects of alcohol." Alcohol Health Res World **21**(1): 65-75.
131. Ostrom, Q. T., P. Liao, L. C. Stetson and J. S. Barnholtz-Sloan (2016). "Epidemiology of Glioblastoma and Trends in Glioblastoma Survivorship." 11-19.
132. Pascal, J. M. (2018). "The comings and goings of PARP-1 in response to DNA damage." DNA Repair (Amst) **71**: 177-182.

133. Perry, J., A. Chambers, K. Spithoff and N. Laperriere (2007). "Gliadel wafers in the treatment of malignant glioma: a systematic review." Curr Oncol **14**(5): 189-194.
134. Pozo, L., J. J. Sanchez-Carrillo, A. Martinez, A. Blanes and S. J. Diaz-Cano (2007). "Differential kinetic features by tumour topography in cutaneous small-cell neuroendocrine (Merkel cell) carcinomas." Journal of the European Academy of Dermatology and Venereology **0**(0): 070802021952008-???
135. Qi, S. and Y. Liu (2016). "Differences in protein expression between the u251 and u87 cell lines." Turkish Neurosurgery.
136. Raisova, M., A. M. Hossini, J. Eberle, C. Riebeling, T. Wieder, I. Sturm, P. T. Daniel, C. E. Orfanos and C. C. Geilen (2001). "The Bax/Bcl-2 ratio determines the susceptibility of human melanoma cells to CD95/Fas-mediated apoptosis." J Invest Dermatol **117**(2): 333-340.
137. Rea, P. (2016). "Essential Clinically Applied Anatomy of the Peripheral Nervous System in the Head and Neck, Chapter 1 - Overview of the Nervous System." Academic Press: Pages 1-20.
138. Regine Schneider-Stock, A. G., Khuloud Bajbouj, MelodySaikali, Nadine Darwiche (2012). "Epigenetic mechanisms of plant-derived anticancer drugs." Frontiers in Bioscience, Landmark **17**: 129-173.
139. Reitman, Z. J. and H. Yan (2010). "Isocitrate Dehydrogenase 1 and 2 Mutations in Cancer: Alterations at a Crossroads of Cellular Metabolism." JNCI Journal of the National Cancer Institute **102**(13): 932-941.
140. Rhinn, M. and P. Dollé (2012). "Retinoic acid signalling during development." Development **139**(5): 843-858.
141. Roy P, S. B. (2016). "Cancer and cure: A critical analysis." Indian J Cancer **53**: 441-442.
142. Sakoe, Y., K. Sakoe, K. Kirito, K. Ozawa and N. Komatsu (2010). "FOXO3A as a key molecule for all-trans retinoic acid-induced granulocytic differentiation and apoptosis in acute promyelocytic leukemia." Blood **115**(18): 3787-3795.
143. Sala, F., M. Zucchetti, R. Bagnati, M. D'Incalci, S. Pace, F. Capocasa and E. Marangon (2009). "Development and validation of a liquid chromatography-tandem mass spectrometry method for the determination of ST1926, a novel oral antitumor agent, adamantyl retinoid derivative, in plasma of patients in a Phase I study." J Chromatogr B Analyt Technol Biomed Life Sci **877**(27): 3118-3126.
144. Saladin, K. S. (2020). "Anatomy & physiology: the unity of form and function." **9th edition**.
145. Schenk, T., S. Stengel and A. Zelent (2014). "Unlocking the potential of retinoic acid in anticancer therapy." Br J Cancer **111**(11): 2039-2045.
146. Schmidt, F., P. Groscurth, J. Dichgans and M. Weller (2000). "Human malignant glioma cell lines are refractory to retinoic acid-mediated differentiation and sensitization to apoptosis." Cell Physiol Biochem **10**(3): 159-168.
147. Schreiber, R., U. Taschler, K. Preiss-Landl, N. Wongsiriroj, R. Zimmermann and A. Lass (2012). "Retinyl ester hydrolases and their roles in vitamin A homeostasis." Biochim Biophys Acta **1821**(1): 113-123.

148. Shai, R., T. Shi, T. J. Kremen, S. Horvath, L. M. Liau, T. F. Cloughesy, P. S. Mischel and S. F. Nelson (2003). "Gene expression profiling identifies molecular subtypes of gliomas." Oncogene **22**(31): 4918-4923.
149. Shen, Z.-X. (2009). "Molecular target therapy – towards curative regimen: a 20-year experience in the treatment of acute promyelocytic leukemia (APL) in the Shanghai Institute of Hematology." Journal of Hematology & Oncology **2**(1): A1.
150. Shi, D., G. Mi, S. Bhattacharya, S. Nayar and T. Webster (2016). "Optimizing superparamagnetic iron oxide nanoparticles as drug carriers using an in vitro blood–brain barrier model." International Journal of Nanomedicine **Volume 11**: 5371-5379.
151. Shi, L., J. Chen, J. Yang, T. Pan, S. Zhang and Z. Wang (2010). "MiR-21 protected human glioblastoma U87MG cells from chemotherapeutic drug temozolomide induced apoptosis by decreasing Bax/Bcl-2 ratio and caspase-3 activity." Brain Res **1352**: 255-264.
152. Shi, L., H. Li and Y. Zhan (2017). "All-trans retinoic acid enhances temozolomide-induced autophagy in human glioma cells U251 via targeting Keap1/Nrf2/ARE signaling pathway." Oncology Letters **14**(3): 2709-2714.
153. Siddikuzzaman, C. Guruvayoorappan and V. M. Berlin Grace (2011). "All trans retinoic acid and cancer." Immunopharmacol Immunotoxicol **33**(2): 241-249.
154. Simmons, M. L., K. R. Lamborn, M. Takahashi, P. Chen, M. A. Israel, M. S. Berger, T. Godfrey, J. Nigro, M. Prados, S. Chang, F. G. Barker, 2nd and K. Aldape (2001). "Analysis of complex relationships between age, p53, epidermal growth factor receptor, and survival in glioblastoma patients." Cancer Res **61**(3): 1122-1128.
155. Simoni, D., G. Giannini, M. Roberti, R. Rondanin, R. Baruchello, M. Rossi, G. Grisolia, F. P. Invidiata, S. Aiello, S. Marino, S. Cavallini, A. Siniscalchi, N. Gebbia, L. Crosta, S. Grimaudo, V. Abbadessa, A. Di Cristina and M. Tolomeo (2005). "Studies on the apoptotic activity of natural and synthetic retinoids: discovery of a new class of synthetic terphenyls that potently support cell growth and inhibit apoptosis in neuronal and HL-60 cells." J Med Chem **48**(13): 4293-4299.
156. Singh, L., N. Pushker, N. Saini, S. Sen, A. Sharma, S. Bakhshi, B. Chawla and S. Kashyap (2015). "Expression of pro-apoptotic Bax and anti-apoptotic Bcl-2 proteins in human retinoblastoma." Clin Exp Ophthalmol **43**(3): 259-267.
157. Starokadomskyy, P., T. Gemelli, J. J. Rios, C. Xing, R. C. Wang, H. Li, V. Pokatayev, I. Dozmorov, S. Khan, N. Miyata, G. Fraile, P. Raj, Z. Xu, Z. Xu, L. Ma, Z. Lin, H. Wang, Y. Yang, D. Ben-Amitai, N. Orenstein, H. Mussaffi, E. Baselga, G. Tadini, E. Grunebaum, A. Sarajlija, K. Krzewski, E. K. Wakeland, N. Yan, M. T. de la Morena, A. R. Zinn and E. Burstein (2016). "DNA polymerase-alpha regulates the activation of type I interferons through cytosolic RNA:DNA synthesis." Nat Immunol **17**(5): 495-504.
158. Subramanian Venkatesan, M. L. L., Clemens MF Dirven, Sieger Leenstra (2016). "Genetic biomarkers of drug response for small-molecule therapeutics targeting the RTK/Ras/PI3K, p53 or Rb pathway in glioblastoma." CNS Oncology **5(2)**: 77–90.

159. Sun, L., A. M. Hui, Q. Su, A. Vortmeyer, Y. Kotliarov, S. Pastorino, A. Passaniti, J. Menon, J. Walling, R. Bailey, M. Rosenblum, T. Mikkelsen and H. A. Fine (2006). "Neuronal and glioma-derived stem cell factor induces angiogenesis within the brain." Cancer Cell **9**(4): 287-300.
160. Tallman, M. S. (1994). "All-trans-retinoic acid in acute promyelocytic leukemia and its potential in other hematologic malignancies." Semin Hematol **31**(4 Suppl 5): 38-48.
161. Tan, A.-C., S. Vyse and P. H. Huang (2017). "Exploiting receptor tyrosine kinase co-activation for cancer therapy." Drug Discovery Today **22**(1): 72-84.
162. Tang, X. H. and L. J. Gudas (2011). "Retinoids, retinoic acid receptors, and cancer." Annu Rev Pathol **6**: 345-364.
163. Teo, W.-Y., K. Sekar, P. Seshachalam, J. Shen, W.-Y. Chow, C. C. Lau, H. Yang, J. Park, S.-G. Kang, X. Li, D.-H. Nam and K. M. Hui (2019). "Relevance of a TCGA-derived Glioblastoma Subtype Gene-Classifier among Patient Populations." Scientific Reports **9**(1).
164. Tewari, M., L. T. Quan, K. O'Rourke, S. Desnoyers, Z. Zeng, D. R. Beidler, G. G. Poirier, G. S. Salvesen and V. M. Dixit (1995). "Yama/CPP32 beta, a mammalian homolog of CED-3, is a CrmA-inhibitable protease that cleaves the death substrate poly(ADP-ribose) polymerase." Cell **81**(5): 801-809.
165. Thakkar, J. P., T. A. Dolecek, C. Horbinski, Q. T. Ostrom, D. D. Lightner, J. S. Barnholtz-Sloan and J. L. Villano (2014). "Epidemiologic and Molecular Prognostic Review of Glioblastoma." Cancer Epidemiology Biomarkers & Prevention **23**(10): 1985-1996.
166. Theodosiou, M., V. Laudet and M. Schubert (2010). "From carrot to clinic: an overview of the retinoic acid signaling pathway." Cell Mol Life Sci **67**(9): 1423-1445.
167. Tong, R. and D. S. Kohane (2016). "New Strategies in Cancer Nanomedicine." Annu Rev Pharmacol Toxicol **56**: 41-57.
168. Tonya Hines, C., Mayfield Clinic, Cincinnati, Ohio (2018). "Anatomy of the Brain, https://mayfieldclinic.com/pe-anatbrain.htm."
169. Upadhyay, V. A., A. M. Brunner and A. T. Fathi (2017). "Isocitrate dehydrogenase (IDH) inhibition as treatment of myeloid malignancies: Progress and future directions." Pharmacology & Therapeutics **177**: 123-128.
170. Valli, C., G. Paroni, A. M. Di Francesco, R. Riccardi, M. Tavecchio, E. Erba, A. Boldetti, M. Gianni, M. Fratelli, C. Pisano, L. Merlini, A. Antoccia, C. Cenciarelli, M. Terao and E. Garattini (2008). "Atypical retinoids ST1926 and CD437 are S-phase-specific agents causing DNA double-strand breaks: significance for the cytotoxic and antiproliferative activity." Mol Cancer Ther **7**(9): 2941-2954.
171. Verhaak, R. G. W., K. A. Hoadley, E. Purdom, V. Wang, Y. Qi, M. D. Wilkerson, C. R. Miller, L. Ding, T. Golub, J. P. Mesirov, G. Alexe, M. Lawrence, M. O'Kelly, P. Tamayo, B. A. Weir, S. Gabriel, W. Winckler, S. Gupta, L. Jakkula, H. S. Feiler, J. G. Hodgson, C. D. James, J. N. Sarkaria, C. Brennan, A. Kahn, P. T. Spellman, R. K. Wilson, T. P. Speed, J. W. Gray, M. Meyerson, G. Getz, C. M. Perou and D. N. Hayes (2010). "Integrated Genomic Analysis Identifies Clinically Relevant Subtypes of Glioblastoma Characterized

by Abnormalities in PDGFRA, IDH1, EGFR, and NF1." Cancer Cell **17**(1): 98-110.
172. Wang, Q., B. Hu, X. Hu, H. Kim, M. Squatrito, L. Scarpace, A. C. deCarvalho, S. Lyu, P. Li, Y. Li, F. Barthel, H. J. Cho, Y.-H. Lin, N. Satani, E. Martinez-Ledesma, S. Zheng, E. Chang, C.-E. G. Sauvé, A. Olar, Z. D. Lan, G. Finocchiaro, J. J. Phillips, M. S. Berger, K. R. Gabrusiewicz, G. Wang, E. Eskilsson, J. Hu, T. Mikkelsen, R. A. DePinho, F. Muller, A. B. Heimberger, E. P. Sulman, D.-H. Nam and R. G. W. Verhaak (2017). "Tumor Evolution of Glioma-Intrinsic Gene Expression Subtypes Associates with Immunological Changes in the Microenvironment." Cancer Cell **32**(1): 42-56.e46.
173. Wang, Z., H. Sun and J. S. Yakisich (2014). "Overcoming the blood-brain barrier for chemotherapy: limitations, challenges and rising problems." Anticancer Agents Med Chem **14**(8): 1085-1093.
174. Westphal, D., R. M. Kluck and G. Dewson (2013). "Building blocks of the apoptotic pore: how Bax and Bak are activated and oligomerize during apoptosis." Cell Death & Differentiation **21**(2): 196-205.
175. WHO (2018). "https://www.who.int/news-room/fact-sheets/detail/cancer."
176. Wion, D., M. Dreyfus, M. El-Atifi, M. Court, M. Bidart, C. Coutton, C. Leclech, B. Ballester, E. Garcion, A. Bouamrani and F. Berger (2018). "Reprogramming glioma cell cultures with retinoic acid: Additional arguments for reappraising the potential of retinoic acid in the context of personalized glioma therapy." Glioma **1**(2): 66.
177. Xu, W., H. Yang, Y. Liu, Y. Yang, P. Wang, S.-H. Kim, S. Ito, C. Yang, P. Wang, M.-T. Xiao, L.-x. Liu, W.-q. Jiang, J. Liu, J.-y. Zhang, B. Wang, S. Frye, Y. Zhang, Y.-h. Xu, Q.-y. Lei, K.-L. Guan, S.-m. Zhao and Y. Xiong (2011). "Oncometabolite 2-Hydroxyglutarate Is a Competitive Inhibitor of α-Ketoglutarate-Dependent Dioxygenases." Cancer Cell **19**(1): 17-30.
178. Yan, C., N. Pattabiraman, J. Goecks, P. Lam, A. Nayak, Y. Pan, J. Torcivia-Rodriguez, A. Voskanian, Q. Wan and R. Mazumder (2017). "Impact of germline and somatic missense variations on drug binding sites." The Pharmacogenomics Journal **17**(2): 128-136.
179. Yan, H., D. W. Parsons, G. Jin, R. McLendon, B. A. Rasheed, W. Yuan, I. Kos, I. Batinic-Haberle, S. Jones, G. J. Riggins, H. Friedman, A. Friedman, D. Reardon, J. Herndon, K. W. Kinzler, V. E. Velculescu, B. Vogelstein and D. D. Bigner (2009). "IDH1andIDH2Mutations in Gliomas." New England Journal of Medicine **360**(8): 765-773.
180. Yang, F., Y. Zou, Q. Gong, J. Chen, W. D. Li and Q. Huang (2020). "From astrocytoma to glioblastoma: a clonal evolution study." FEBS Open Bio.
181. Zhao, J., A. X. Chen, R. D. Gartrell, A. M. Silverman, L. Aparicio, T. Chu, D. Bordbar, D. Shan, J. Samanamud, A. Mahajan, I. Filip, R. Orenbuch, M. Goetz, J. T. Yamaguchi, M. Cloney, C. Horbinski, R. V. Lukas, J. Raizer, A. I. Rae, J. Yuan, P. Canoll, J. N. Bruce, Y. M. Saenger, P. Sims, F. M. Iwamoto, A. M. Sonabend and R. Rabadan (2019). "Immune and genomic correlates of response to anti-PD-1 immunotherapy in glioblastoma." Nature Medicine **25**(3): 462-469.
182. Zhao, S., Y. Lin, W. Xu, W. Jiang, Z. Zha, P. Wang, W. Yu, Z. Li, L. Gong, Y. Peng, J. Ding, Q. Lei, K. L. Guan and Y. Xiong (2009). "Glioma-

Derived Mutations in IDH1 Dominantly Inhibit IDH1 Catalytic Activity and Induce HIF-1 " Science **324**(5924): 261-265.
183. Zuco, V., V. Benedetti, M. De Cesare and F. Zunino (2010). "Sensitization of ovarian carcinoma cells to the atypical retinoid ST1926 by the histone deacetylase inhibitor, RC307: enhanced DNA damage response." Int J Cancer **126**(5): 1246-1255.
184. Zuco, V., C. Zanchi, G. Cassinelli, C. Lanzi, R. Supino, C. Pisano, R. Zanier, V. Giordano, E. Garattini and F. Zunino (2004). "Induction of apoptosis and stress response in ovarian carcinoma cell lines treated with ST1926, an atypical retinoid." Cell Death Differ **11**(3): 280-289.
185. Zuco, V., C. Zanchi, C. Lanzi, G. L. Beretta, R. Supino, C. Pisano, M. Barbarino, R. Zanier, F. Bucci, C. Aulicino, P. Carminati and F. Zunino (2005). "Development of resistance to the atypical retinoid, ST1926, in the lung carcinoma cell line H460 is associated with reduced formation of DNA strand breaks and a defective DNA damage response." Neoplasia **7**(7): 667-677.